



**HAL**  
open science

# Effect of the incorporation of silica nanoparticles on the stability and rheological behavior of xanthan gum formulations for use in enhanced oil recovery

Dayan Lizbeth Buitrago-Rincón

## ► To cite this version:

Dayan Lizbeth Buitrago-Rincón. Effect of the incorporation of silica nanoparticles on the stability and rheological behavior of xanthan gum formulations for use in enhanced oil recovery. Chemical and Process Engineering. Université de Lorraine; Universidad Industrial de Santander (Bucaramanga, Colombie), 2023. English. NNT : 2023LORR0407 . tel-04848977

**HAL Id: tel-04848977**

**<https://hal.univ-lorraine.fr/tel-04848977v1>**

Submitted on 19 Dec 2024

**HAL** is a multi-disciplinary open access archive for the deposit and dissemination of scientific research documents, whether they are published or not. The documents may come from teaching and research institutions in France or abroad, or from public or private research centers.

L'archive ouverte pluridisciplinaire **HAL**, est destinée au dépôt et à la diffusion de documents scientifiques de niveau recherche, publiés ou non, émanant des établissements d'enseignement et de recherche français ou étrangers, des laboratoires publics ou privés.



**UNIVERSITÉ  
DE LORRAINE**

**BIBLIOTHÈQUES  
UNIVERSITAIRES**

## AVERTISSEMENT

Ce document est le fruit d'un long travail approuvé par le jury de soutenance et mis à disposition de l'ensemble de la communauté universitaire élargie.

Il est soumis à la propriété intellectuelle de l'auteur. Ceci implique une obligation de citation et de référencement lors de l'utilisation de ce document.

D'autre part, toute contrefaçon, plagiat, reproduction illicite encourt une poursuite pénale.

Contact bibliothèque : [ddoc-theses-contact@univ-lorraine.fr](mailto:ddoc-theses-contact@univ-lorraine.fr)  
*(Cette adresse ne permet pas de contacter les auteurs)*

## LIENS

Code de la Propriété Intellectuelle. articles L 122. 4

Code de la Propriété Intellectuelle. articles L 335.2- L 335.10

[http://www.cfcopies.com/V2/leg/leg\\_droi.php](http://www.cfcopies.com/V2/leg/leg_droi.php)

<http://www.culture.gouv.fr/culture/infos-pratiques/droits/protection.htm>



**UNIVERSITÉ  
DE LORRAINE**

**École Doctorale SIMPPÉ  
Laboratoire Réactions et Génie  
des Procédés - LRGP**

**UNIVERSIDAD INDUSTRIAL DE SANTANDER**

**Thèse**

**Présentée et soutenue publiquement le 6 décembre 2023  
pour l'obtention du titre de**

**DOCTEUR DE L'UNIVERSITÉ DE LORRAINE**

**Mention : Génie des procédés, des produits et des molécules**

par **Dayan Lizeth BUITRAGO RINCON**

Sous la direction de Cécile LEMAITRE, Julio Andrés PEDRAZA  
AVELLA et Véronique SADTLER

**Effect of the incorporation of silica nanoparticles on the stability  
and rheological behavior of xanthan gum formulations for use in  
enhanced oil recovery**

**Membres du jury :**

Directrice de thèse :	Mme Cécile LEMAITRE	Maître de conférences, ENSIC, Nancy
Codirecteur de thèse :	M. Julio Andrés PEDRAZA AVELLA	Professeur, Universidad Industrial de Santander, Colombia
Codirectrice de thèse :	Mme Véronique SADTLER	Professeure, ENSIC, Nancy
Co-encadrant :	M. Ronald Alfonso MERCADO OJEDA	Professeur, Universidad Industrial de Santander, Colombia
Président de jury :	M. Gustavo Emilio RAMIREZ CABALLERO	Professeur, Universidad Industrial de Santander, Colombia
Rapporteur :	M. Romain CASTELLANI	Professeur, Mines Paris (Cemef) Université PSL
Rapporteuse :	Mme Lina Marcela HOYOS PALACIO	Professeure, Universidad Pontificia Bolivariana, UPB, Colombia
Examinatrice :	Mme Yuly Fernanda LÓPEZ CONTRERAS	Professeure, Universidad Industrial de Santander, Colombia
Examineur :	M. Emiliano ARIZA LEON	Professeur, Universidad Industrial de Santander, Colombia
Examineur :	M. Philippe MARCHAL	Ingénieur de recherche, LRGP, Nancy

### **Acknowledgments**

I would like to express my sincere gratitude to Dra. Cécile Lemaître, Dra. Véronique Sadtler, Dr. Julio Andrés Pedraza Avella and Dr. Ronald Alfonso Mercado Ojeda. My supervisors always encouraged me to go further. I am profoundly grateful for their unwavering support, invaluable opportunities provided, and the privilege of working within their research groups. Cécile and Véronique, definitely you are my best role models for scientists. Thank you for so much learning, kindness, and empathy. Julio and Ronald, thanks to see in me a future in research, for your patience and tireless support.

I acknowledge to Grupo de Investigación en Fenómenos Interfaciales, Reología y Simulación de Transporte (FIRST) and Génie Chimique des Milieux Rhéologiquement Complexes (GEMICO), for the financial and administrative support provided during the development of this thesis. I would like to thank all the members of these groups.

I especially want to thank Dr. Philippe Marchal and Dr. Thibault Roques-Carmes for their invaluable technical guidance and critical feedback throughout the project. My time in Nancy was very fruitful for my thesis and life.

I express my gratitude to Dr. Lazhar Benyahia, Dr. Alain Durand, Dr. Khalid Ferji, Dr. Guillaume Pickaert, Dra. Carole Arnal-Herault, Dr. Arlex Chavez, Msc. Samuel F. Muñoz-Navarro, and Msc. María Sandoval for their invaluable contributions to the development of this research and their technical support in conducting conclusive tests. A sincere thanks to Professor Crisostomo Barajas Ferreira for your valuable cooperation.

This research was possible thanks to Vicerrectoría de Investigación y Extensión (VIE) at Universidad Industrial de Santander (UIS) and Sous-Direction des Études Doctorales at Université de Lorraine (UL), through the agreement of cooperation between both universities. Nidia Jaimes y Sabrina Divoux was an extensive and intricate process, and you persevered throughout. Thank you very much.

I thank to all external laboratories involved in this research: Laboratorio Rayos X (UIS), Laboratorio de Ciencias de Superficies (UIS), Laboratorio de Microscopía (UIS), Laboratoire de Chimie Physique Macromoléculaire LCPM (UL), Laboratoire des Molécules et Matériaux du Mans, Laboratorio Recobro Mejorado (UIS) and Laboratorio de Minerales, Biohidrometalurgia y Ambiente (UIS).

Special thanks to my lifelong friends, who have consistently encouraged me to persevere on this journey; you are my extended family.

Last but certainly not least, my deepest gratitude goes to my beloved family. Infinite thanks for your extraordinary love, unconditional encouragement, and support. None of these would have been possible without you, *los amo*.

***Thank you so much, Muchas gracias, Merci beaucoup.***

**Table of Contents**

	Page
<b>Introduction</b> _____	<b>11</b>
<b>Chapter I. Rheological Behavior and Preparation Methods of Nanofluids</b> _____	<b>28</b>
Abstract _____	28
Introduction _____	29
Materials and methods _____	30
<i>Preparation of xanthan gum solutions and nanoparticles suspensions</i> _____	30
<i>Sonication Treatment and DLS Tests</i> _____	31
<i>Rheology measurement</i> _____	32
<i>Nanofluids preparation</i> _____	33
Results and Discussion _____	34
<i>Xanthan Gum and Nanoparticles</i> _____	34
<i>Xanthan Gum</i> _____	34
<i>Silica Nanoparticles</i> _____	35
Characterization of the polymer solutions _____	36
<i>Sonication Treatment</i> _____	38
<i>Influence of NaCl and Dilution curve of xanthan gum</i> _____	39
<i>Characterization of nanoparticle suspensions</i> _____	41
<i>Nanofluids preparation</i> _____	43
Conclusions _____	45

**Chapter II. Evolution of Viscosity over Time** \_\_\_\_\_ **47**

Abstract \_\_\_\_\_ 47

Introduction \_\_\_\_\_ 48

Materials and methods \_\_\_\_\_ 51

*Materials* \_\_\_\_\_ 51*Nanofluids Preparation and Influence of Temperature during Preparation* \_\_\_\_ 51*Rheological Characterization* \_\_\_\_\_ 52*Aging Tests* \_\_\_\_\_ 54*Confocal Microscopy* \_\_\_\_\_ 55*Zeta-Potential Measurements* \_\_\_\_\_ 55*Thermal Analysis* \_\_\_\_\_ 56

Results and Discussion \_\_\_\_\_ 56

*Influence of Temperature during Nanofluids Preparation* \_\_\_\_\_ 56*Aging Tests—Stability* \_\_\_\_\_ 58*Intrinsic and Relative Viscosity* \_\_\_\_\_ 62*Confocal Microscopy* \_\_\_\_\_ 64*Zeta Potential* \_\_\_\_\_ 66*Thermal Analysis* \_\_\_\_\_ 67

Conclusions \_\_\_\_\_ 68

**Chapter III. Oil Recovery Efficiency in Core Flooding Tests** \_\_\_\_\_ **70**

Abstract \_\_\_\_\_ 70

Introduction \_\_\_\_\_ 71

Materials and methods	75
<i>Materials</i>	76
<i>Fluids Preparation</i>	76
<i>Viscosity Behavior</i>	77
<i>Interfacial Tension</i>	77
<i>Core Flooding Experiments</i>	77
<i>Core Preparation</i>	78
<i>Reservoir Saturation Conditions.</i>	79
<i>Flooding Process.</i>	80
Results and Discussion	80
<i>Viscosity Behavior</i>	80
<i>Interfacial Tension</i>	82
<i>Core Flooding Results</i>	83
Conclusions	88
<b>Conclusions</b>	<b>90</b>
<b>References</b>	<b>100</b>
<b>Appendix</b>	<b>106</b>

**List of Figures**

<b>Figure I.1</b> Infrared spectrum xanthan gum _____	34
<b>Figure I.2</b> XPS of xanthan gum and silica nanoparticles _____	35
<b>Figure I.3</b> X-Ray diffraction silica nanoparticles _____	35
<b>Figure I.4</b> SEM / EDX silica nanoparticles _____	36
<b>Figure I.5</b> Evolution of polymer solution viscosity during hydration _____	37
<b>Figure I.6</b> Effect of sonication on viscosity for xanthan gum solutions _____	38
<b>Figure I.7</b> Polymer solutions after sonication _____	39
<b>Figure I.8</b> Effect of NaCl on the rheology for xanthan gum solutions _____	39
<b>Figure I.9</b> Dilution curve of xanthan gum with 3% NaCl. _____	41
<b>Figure I.10</b> Viscosity and particle size of Np-SiO <sub>2</sub> suspensions as function of sonication duration _____	43
<b>Figure I.11</b> Methods: Nanofluids viscosity as a function of the shear rate _____	44
<b>Figure II.1</b> Chemical structure of xanthan gum _____	49
<b>Figure II.2</b> Viscosity as a function of time – Short aging (30 days) _____	59
<b>Figure II.3</b> Viscosity as a function of time – Long aging (7 months) _____	60
<b>Figure II.4</b> Viscosity nanofluid against polymer solution after 7 months _____	61
<b>Figure II.5</b> Intrinsic viscosity ( $\mu$ ) as a function of time _____	63
<b>Figure II.6</b> Relative viscosity $\mu_{rel}$ as a XG concentration _____	64
<b>Figure II.7</b> Confocal microscopy images _____	65
<b>Figure III.1</b> Polymers molecular structure _____	73
<b>Figure III.2</b> Core flooding experimental setup. _____	78

**Figure III.3** Viscosity of solutions with and without NaCl as a function of shear rate. \_\_\_\_ 81

**Figure III.4** Displacement efficiency (%) as a function of porous volume injected. \_\_\_\_\_ 84

**Figure III.5** Viscosity as a function of time at a shear rate of  $7.3 \text{ s}^{-1}$ . \_\_\_\_\_ 86

**List of Tables**

	<b>Page</b>
<b>Table I.1.</b> <i>Preparation methods of the nanofluids</i> _____	33
<b>Table I.2.</b> <i>Viscosity of nanoparticles suspensions</i> _____	42
<b>Table II.1.</b> <i>Relative viscosity increases due to preparation temperature</i> _____	57
<b>Table II.2.</b> <i>Zeta potential</i> _____	66
<b>Table III.1.</b> <i>Interfacial tension</i> _____	83
<b>Table III.2.</b> <i>Core flood experiments</i> _____	85

**List of Appendix**

<b>Appendix A.1.</b> Xanthan gum technical data sheet _____	106
<b>Appendix A.2.</b> Silica Nanoparticles technical data sheet _____	108
<b>Appendix A.3.</b> Sodium chloride technical sheet. _____	109
<b>Appendix A.4.</b> Mineral Oil. _____	110
<b>Appendix A.5.</b> Effect of Silica Nanoparticles in Xanthan Gum Solutions: _____	111
Rheological Behavior and Preparation Methods of Nanofluids _____	112
<b>Appendix A.6.</b> Effect of Silica Nanoparticles in Xanthan Gum Solutions: Evolution of Viscosity over Time _____	113
<b>Appendix A.7.</b> Differential Scanning Calorimetry (DSC) measurements _____	114
<b>Appendix A.8.</b> Thermogravimetric analysis _____	118

## Resumen

**Título:** Efecto de la incorporación de nanopartículas de sílice en la estabilidad y comportamiento reológico de formulaciones con goma de xantana para uso en recobro mejorado de petróleo.

**Autor:** Dayan Lizeth Buitrago Rincón \*\*

**Palabras claves:** goma de xantana, nanopartículas de sílice, dispersiones, reología, recobro mejorado de petróleo.

**Descripción:** Con el aumento de la demanda global de energía y los desafíos que enfrenta la producción convencional de petróleo, la búsqueda de métodos efectivos de Recuperación Mejorada de Petróleo (EOR, por sus siglas en inglés) se intensifica. Este estudio explora el potencial de las nanopartículas de sílice hidrofílicas (Np-SiO<sub>2</sub>) para mejorar la viscosidad y la estabilidad reológica de soluciones de Goma de Xantana (XG), presentando una alternativa prometedora para aplicaciones en EOR.

La investigación está diseñada para explorar la influencia de las Np-SiO<sub>2</sub> en las soluciones de XG, centrándose en tres aspectos clave: el impacto en la viscosidad, el comportamiento reológico bajo tensiones externas y fuerzas iónicas (Na<sup>+</sup> y Cl<sup>-</sup>), y la caracterización fisicoquímica de XG y las nanopartículas de sílice. La metodología abarca un análisis detallado de las propiedades y la naturaleza tanto de XG como de las Np-SiO<sub>2</sub>, el establecimiento de un proceso estandarizado para la formulación de nanofluidos, y la evaluación de la estabilidad y macroestructura de los nanofluidos mediante viscosimetría capilar, medidas de potencial Z y microscopía confocal. El estudio también monitorizará la evolución de la viscosidad con el tiempo. Además, se llevarán a cabo pruebas de coreflooding para comparar nanofluidos de XG con soluciones de poliácridamida hidrolizada (HPAM), centrándose en las interacciones roca-fluido y la tensión interfacial. A través de este enfoque integral, la investigación tiene como objetivo proporcionar conocimientos valiosos sobre las posibles aplicaciones de las Np-SiO<sub>2</sub> para mejorar el rendimiento y la estabilidad de las soluciones de XG, especialmente en el contexto de procesos de EOR.

---

\* Tesis de doctorado

\*\* Universidad Industrial de Santander. Facultad de Ingenierías Fisicoquímicas. Escuela de Ingeniería Química. Director: Dr. Julio Andrés Pedraza Avella. Codirector: Dr. Ronald Alfonso Mercado Ojeda  
Université de Lorraine. Laboratoire Réactions et Génie des Procédés (LRGP). Directora: Dr. Cécile Lemaitre. Codirectora: Dr. Véronique Sadtler.

### Abstract

**Title:** Effect of the incorporation of silica nanoparticles on the stability and rheological behavior of xanthan gum formulations for use in enhanced oil recovery \*

**Author:** Dayan Lizeth Buitrago Rincón \*\*

**Keywords:** xanthan gum; silica nanoparticles; dispersions; rheology; Enhanced oil recovery.

**Description:** With global energy demands on the rise and conventional oil production facing challenges, the search for effective Enhanced Oil Recovery (EOR) methods intensifies. This study explores the potential of hydrophilic silica nanoparticles to enhance the viscosity and rheological stability of xanthan gum (XG) solutions, presenting a promising alternative for EOR applications.

This research is designed to explore the influence of hydrophilic silica nanoparticles on xanthan gum (XG) solutions, with a focus on three key aspects: viscosity impact, rheological behavior under external stresses and ionic forces ( $\text{Na}^+$  and  $\text{Cl}^-$ ), and the physicochemical characterization of XG and silica nanoparticles. The methodology encompasses a detailed analysis of the properties and nature of both XG and silica nanoparticles, the establishment of a standardized process for nanofluid formulation, and the assessment of nanofluid stability and macrostructure using capillary viscometry, Z potential measurements, and confocal microscopy. The study will also monitor the evolution of viscosity over time. Additionally, core flooding tests will be conducted to compare XG nanofluids with Hydrolyzed Polyacrylamide (HPAM) solutions, focusing on rock-fluid interactions and interfacial tension. Through this comprehensive approach, the research aims to provide valuable insights into the potential applications of hydrophilic silica nanoparticles in enhancing the performance and stability of XG solutions, particularly in the context of Enhanced Oil Recovery (EOR) processes.

---

\* Ph.D. thesis

\*\* Universidad Industrial de Santander. Faculty of Physicochemical Engineering. Department of Chemical Engineering. Advisor: Dr. Julio Andrés Pedraza Avella Co-Advisor: Dr. Ronald Alfonso Mercado Ojeda  
Université de Lorraine. Laboratoire Réactions et Génie des Procédés (LRGP). Advisor: Dr. Cécile Lemaitre Co-Advisor: Dr. Véronique Sadtler.

## Résumé

**Titre :** Effet de l'incorporation de nanoparticules de silice sur la stabilité et le comportement rhéologique des formulations de gomme xanthane pour une utilisation dans la récupération assistée du pétrole\*

**Auteur :** Dayan Lizeth Buitrago Rincón \*\*

**Mots-clés :** gomme xanthane ; nanoparticules de silice ; dispersions ; rhéologie ; Récupération assistée du pétrole.

**Description :** Avec la demande énergétique mondiale en hausse et la production de pétrole conventionnel confrontée à des défis, la recherche de méthodes efficaces de Récupération Assistée du Pétrole (RAP) s'intensifie. Cette étude explore le potentiel des nanoparticules de silice hydrophiles pour améliorer la viscosité et la stabilité rhéologique des solutions de gomme xanthane (GX), présentant ainsi une alternative prometteuse pour les applications de RAP.

Cette recherche est conçue pour explorer l'influence des nanoparticules de silice hydrophiles sur les solutions de gomme xanthane (GX), en se concentrant sur trois aspects clés : l'impact sur la viscosité, le comportement rhéologique sous contraintes externes et forces ioniques ( $\text{Na}^+$  et  $\text{Cl}^-$ ), et la caractérisation physico-chimique de la GX et des nanoparticules de silice. La méthodologie comprend une analyse détaillée des propriétés et de la nature de la GX et des nanoparticules de silice, l'établissement d'un processus normalisé pour la formulation de nanofluides, et l'évaluation de la stabilité des nanofluides et de leur macrostructure à l'aide de la viscosimétrie capillaire, des mesures de potentiel Z, et de la microscopie confocale. L'étude suivra également l'évolution de la viscosité dans le temps. De plus, des essais de déplacement de noyau seront menés pour comparer les nanofluides de GX avec les solutions de Polyacrylamide Hydrolysée (HPAM), en se concentrant sur les interactions roche-fluides et la tension interfaciale. Grâce à cette approche globale, la recherche vise à fournir des informations précieuses sur les applications potentielles des nanoparticules de silice hydrophiles dans l'amélioration des performances et de la stabilité des solutions de GX, en particulier dans le contexte des processus de RAP.

---

\* Ph.D. thesis

\*\* Universidad Industrial de Santander. Faculty of Physicochemical Engineering. Department of Chemical Engineering. Advisor: Dr. Julio Andrés Pedraza Avella Co-Advisor: Dr. Ronald Alfonso Mercado Ojeda  
Université de Lorraine. Laboratoire Réactions et Génie des Procédés (LRGP). Advisor: Dr. Cécile Lemaitre Co-Advisor: Dr. Véronique Sadtler.

### **Introduction Résumé**

La demande mondiale croissante en énergie, associée au déclin des champs de production pétrolière et à la maturation des champs existants, a suscité un intérêt considérable pour la recherche et le développement de technologies de Récupération Assistée du Pétrole (RAP). Traditionnellement, la production primaire de pétrole dépendait de la pression inhérente dans les réservoirs. Cependant, cette pression diminue avec le temps, ce qui rend nécessaire l'utilisation de techniques de récupération secondaire impliquant l'injection d'eau ou de gaz pour maintenir la pression de l'écoulement de pétrole (Irima, 2014). Cependant, lorsque ces méthodes ne suffisent pas, des stratégies de récupération tertiaire, y compris la RAP, sont impératives. Les méthodes de récupération tertiaire impliquent l'utilisation de sources d'énergie externes et l'incorporation d'additifs pour déplacer le pétrole piégé dans les roches poreuses en raison des forces capillaires et visqueuses (Floerger, s.d. ; Ghoumrassi-Barr & Aliouche, 2016 ; Seright, 2009).

À l'échelle mondiale, le facteur de récupération est d'environ 36 % et celui de la Colombie est d'environ 20 %. Cette disparité souligne l'urgence d'adopter des approches de RAP en Colombie pour combler cet écart (Ecopetrol 2020). Notamment, les méthodes de Récupération Assistée du Pétrole par voie Chimique (RAPC), impliquant des polymères, des agents tensioactifs, des alcalis, et d'autres encore, ont attiré l'attention. L'injection de solutions polymères a donné des résultats opérationnels positifs, avec des augmentations du facteur de récupération allant de 5 % à 15 % par rapport à l'injection d'eau (récupération secondaire) (Ecopetrol, 2020 ; Ghoumrassi-Barr & Aliouche, 2016).

Les polymères hydrosolubles jouent un rôle crucial dans l'augmentation de la viscosité de l'eau injectée, souvent multipliée par des facteurs de 10 à 50. Cette augmentation de viscosité renforce le rapport de mobilité entre le fluide de déplacement (solution polymère) et le fluide

déplacé (pétrole brut) pendant les processus de RAP, ce qui se traduit par des taux de récupération du pétrole accrus (Irima, 2014 ; Seright, 2009 ; Shahzad, 2015 ; Sveistrup, 2015). Cependant, au-delà de l'augmentation de la viscosité, la stabilité des solutions polymères est primordiale, assurant une viscosité constante et une intégrité structurale du polymère dans le temps, surtout dans des conditions de réservoir variables incluant les fluctuations de température, les dynamiques de pression, les variations de la force ionique (en raison des minéraux dissous), et les contraintes mécaniques (forces de cisaillement) lors de l'injection et du transport à travers les milieux poreux (Jimenez, 2009 ; Shahzad, 2015).

Plusieurs facteurs influent sur l'évaluation et la sélection des polymères pour la Récupération Assistée du Pétrole (RAP). Parmi ceux-ci figurent la nécessité d'une solution polymère présentant une large gamme de viscosité qui facilite le balayage efficace du pétrole brut. Tout aussi important est le maintien d'un profil rhéologique constant lors de l'injection et à l'intérieur du réservoir, même dans des conditions de transport difficiles, notamment des températures élevées, une salinité élevée, une pression élevée, une dureté élevée, une teneur élevée en minéraux, et des contraintes de déformation. Le polyacrylamide partiellement hydrolysé (HPAM) est actuellement l'un des polymères les plus largement utilisés pour les applications de RAP (Sheng, 2011). Ses mérites comprennent sa capacité à supporter d'intenses contraintes mécaniques de cisaillement et son adaptabilité aux structures chimiques, permettant des modifications qui intensifient la résistance aux conditions de formation spécifiques (par exemple, les copolymères tels que HPAM-AMPS et les polyacrylamides sulfonés) (Floerger, s.d. ; Shahzad, 2015). Cependant, le HPAM présente des inconvénients notables, tels que le coût élevé associé à sa synthèse et à ses modifications structurelles, ainsi que sa susceptibilité inhérente à la salinité, à

la dureté, à la présence d'agents tensioactifs ou d'autres produits chimiques, et ses implications environnementales potentielles (Floerger, s.d. ; Sheng, 2011).

Par conséquent, il y a eu une tendance à explorer des alternatives d'origine biologique avec un équilibre technique-économique favorable, comme le montre la gomme xanthane (GX). En plus d'être rentable (5:1), la gomme xanthane présente un comportement à haute viscosité lorsqu'elle est confrontée à des forces ioniques telles que le sel ou la dureté. Cette résilience découle de sa ramification structurelle (polymère ramifié), qui est compatible avec la plupart des agents tensioactifs et autres additifs couramment utilisés dans les formulations de récupération tertiaire (Ghoumrassi-Barr et al., 2015). Cependant, la détermination de la composition structurale de la gomme xanthane est difficile. Sur des durées prolongées d'exposition à des conditions défavorables, notamment la température, la salinité et les contraintes de déformation, la gomme xanthane subit des changements de conformation, c'est-à-dire des mouvements de rotation ou de couplage au sein de la molécule. Ces changements conduisent à l'affaiblissement et finalement à la rupture des liaisons intermoléculaires (groupes carboxyles COOH dans sa structure latérale-eau) et intramoléculaires (liaisons au sein de la même molécule, CCOH) (Michael Houryieh, 2006). Ce processus favorise la perte de viscosité et la précipitation du polymère (dégradation). Malgré ces limites, le potentiel intrinsèque de la gomme xanthane en tant que biopolymère et ses attributs environnementaux positifs nécessitent des recherches visant à modifier et à sauvegarder son utilité en tant qu'additif réussi dans les méthodologies de récupération tertiaire.

Dans la recherche de stratégies qui renforcent ou maintiennent les liaisons intermoléculaires et intramoléculaires dans une solution polymère, l'intégration de nanoparticules émerge comme une amélioration prospective pour les traitements biopolymériques, tels que la gomme xanthane (Jordan, 2014 ; Pi, 2016). À mesure que la taille des particules diminue, leur

impact devient plus prononcé : les nanoparticules à l'échelle nanométrique (allant de 1 à 100 nm) présentent des rapports surface-volume accrus. La diminution de la liaison des atomes de surface conduit à une coordination incomplète, entraînant une augmentation discernable de l'énergie libre de surface (Adel, 2015 ; Bracho García, 2013 ; Ogolo, 2012).

Leurs dimensions nano, associées à la composition chimique de la nano-surface, permettent la sélection de nanoparticules qui atténuent les faiblesses observées dans les solutions de xanthane. En conséquence, les nanoparticules de silice se sont révélées être une avenue prometteuse. Leur compatibilité avec le réservoir, principalement avec les composants sableux prédominants, les rend attrayantes. Cela est complété par les propriétés distinctives de leurs surfaces, caractérisées par des groupes siloxane (Si-O-Si) et des silanols (Si-OH). Cette chimie de surface unique favorise en outre une affinité pour l'eau, leur conférant une nature hydrophile compatible avec la structure de la GX (Ibrahim, 2015 ; Min-Ho, 1999 ; Pi, 2016).

Les résultats de recherches récentes ont suggéré que l'incorporation de nanoparticules de silice pourrait entraîner une réduction des transitions conformationnelles de la gomme xanthane, renforçant ainsi les liaisons à la fois entre et à l'intérieur des molécules (Saravanan, 2016 ; Yousefvanda, 2015). Ce phénomène peut être rationalisé par la formation de liaisons chimiques entre les groupes hydroxyle (-OH) à la surface des nanoparticules de silice et les molécules de xanthane, agissant comme des points d'ancrage qui relient la nanoparticule et la macromolécule (Pi, 2016 ; Yousefvanda, 2015). Cette interaction introduit de nouvelles structures polymères réticulées, tridimensionnelles et plus rigides. Soumises à des températures élevées, à des forces ioniques et à des contraintes de déformation ou d'allongement, ces structures présentent des profils rhéologiques améliorés grâce à une transition conformationnelle retardée (Jordan et al., 2014). D'autres études ont suggéré que la présence de nanoparticules dans les systèmes aqueux pourrait

potentiellement améliorer la mobilité des fluides dans les réservoirs. Cependant, les mécanismes précis et les critères régissant leur efficacité restent énigmatiques (Camesano, 2001 ; Pi, 2016 ; Saravanan, 2016). Actuellement, l'intégration de nanoparticules est considérée comme une technique innovante en raison de son potentiel et de la rareté d'informations complètes pour en établir la viabilité technique et économique. Par conséquent, une compréhension plus profonde des interactions nanoparticule-biopolymère, à la fois de manière isolée et en tandem avec la présence d'ions dans les solutions et les réponses aux contraintes thermo-mécaniques, est impérative.

En revanche, un nombre limité de projets se sont concentrés sur la préparation de fluides utilisant de la saumure, ce qui confère des avantages opérationnels aux solutions contenant de la gomme xanthane, réputée pour sa supériorité face au sel par rapport aux polymères synthétiques. L'incorporation de nanoparticules de silice vise à amplifier les performances, notamment la stabilité rhéologique, de ces fluides. D'un point de vue opérationnel, diriger la recherche vers la réalisation de ces scénarios permettrait non seulement d'améliorer la stabilité des fluides contre des déformations substantielles ou des fluctuations de température, mais également d'établir une alternative techniquement, économiquement et environnementalement compétitive aux polymères synthétiques plus coûteux.

L'objectif principal de cette étude était d'étudier l'impact des nanoparticules de silice hydrophiles sur la viscosité des solutions de gomme xanthane. De plus, l'étude visait à analyser de manière exhaustive la persistance du comportement rhéologique de ces fluides sous l'influence de contraintes thermo-mécaniques et de l'introduction de forces ioniques ( $\text{Na}^+$  et  $\text{Cl}^-$ ) sur une période prolongée. Les tests expérimentaux visaient à émuler certaines conditions représentatives des processus de récupération assistée du pétrole. L'interaction entre les nanoparticules de silice et la gomme xanthane est hypothétiquement facilitée par des liaisons physiques faibles telles que les

liaisons hydrogène ou les forces dipôle-dipôle, qui servent de points d'ancrage. Cette interaction entraîne un mouvement transitionnel retardé du polymère, préservant ainsi les attributs visqueux du fluide sur des plages opérationnelles plus larges.

Les composants utilisés dans cette étude provenaient de sources commerciales : la gomme xanthane a été fournie par Sukin Industries, une entreprise colombienne spécialisée dans les matériaux polymères (voir annexe A.1). Les nanoparticules de silice (Np-SiO<sub>2</sub>) utilisées étaient de l'Aerosil 300 fumée, achetée chez Evonik Industries (voir annexe A.2). Le chlorure de sodium a été fourni par Sigma-Aldrich (voir annexe A.3). Le polymère synthétique, connu sous le nom de Polyacrylamide Hydrolysée (HPAM) FLOPAAM 3230 S, a été utilisé. Enfin, l'huile synthétique utilisée dans l'expérimentation était de l'huile minérale USP, provenant de Chemical Elements LTDA (voir annexe A.4).

Dans le premier chapitre, une caractérisation détaillée des nanoparticules et du biopolymère a été réalisée, identifiant la nature des matériaux, leurs propriétés physico-chimiques, et les groupes fonctionnels permettant leur éventuelle liaison. Ensuite, un processus de formulation et de préparation de nanofluides a été standardisé, où son interaction a été exposée à la stabilité de la solution générée, puis la macrostructure (nanoparticule polymère) a été évaluée contre différents tests corroborant la résistance de la liaison entre la nanoparticule et le polymère, montrant son application possible aux processus de récupération chimique à l'échelle du laboratoire. L'objectif de ce chapitre était de déterminer la meilleure méthode pour la préparation de nanofluides.

Dans le deuxième chapitre, l'évolution de la viscosité des nanofluides et des solutions de GX dans le temps a été établie. L'effet des nanoparticules sur les formulations a été mesuré au fil du temps par le biais de tests de stabilité. De plus, des tests de viscosimétrie capillaire, de potentiel Z et de microscopie confocale ont été présentés, ce qui nous a permis de déterminer l'interaction

entre la GX et les nanoparticules. Ce chapitre inclut également des évaluations TGA et DSC dans les formulations.

Le chapitre III, dernier chapitre, présente des tests de déplacement de noyau, montrant les résultats du déplacement linéaire de la solution polymère de GX et du nanofluide. Une comparaison avec une solution de HPAM a été établie. De plus, les résultats des interactions roche-fluides (saturation, perméabilité, swirr) et des tests de tension interfaciale ont été présentés. Enfin, les résultats des pourcentages de récupération incrémentiels de RAP ont été estimés pour les formulations comparatives.

Les résultats liés à l'interaction entre la gomme xanthane et les nanoparticules de silice représentent une voie prometteuse pour améliorer notre compréhension du comportement des fluides biopolymères et de leurs applications potentielles dans la Récupération Assistée du Pétrole (RAP). Cette étude s'est concentrée sur l'influence des nanoparticules de silice hydrophiles sur la viscosité et la stabilité rhéologique des solutions de gomme xanthane, offrant ainsi une opportunité d'élargir leur champ d'application en tant que substituts aux traitements polymères synthétiques. Cette alternative devient cruciale compte tenu des préoccupations environnementales et sanitaires ainsi que des coûts importants associés aux traitements existants.

Actuellement, un nombre limité d'applications industrielles ont examiné les dynamiques d'interaction entre la gomme xanthane et les nanoparticules de silice. Étonnamment, malgré le potentiel évident de cette interaction, peu de recherches ont été dirigées vers le développement de nanofluides comprenant de la gomme xanthane et des nanoparticules de silice pour la récupération assistée du pétrole (RAP). Par conséquent, il est nécessaire de mener des recherches approfondies sur cette technologie. Son importance dépasse la simple promesse et a le potentiel d'avoir un impact positif substantiel tant sur la durabilité environnementale que sur la viabilité économique.

## Introduction

The escalating global energy demand, coupled with declining oil production fields and maturation of existing ones, has attracted significant interest to the research and development of technologies for Enhanced Oil Recovery (EOR). Traditionally, primary oil production has depended on the inherent pressure within reservoirs. However, this pressure wanes over time, prompting the need for secondary recovery techniques involving water or gas injection to maintain oil flow pressure (Irima, 2014). However, when these methods fall short, tertiary recovery strategies, including EOR, are imperative. Tertiary recovery methods entail harnessing external energy sources and incorporating additives to move the oil trapped in porous rocks owing to capillary and viscous forces (Floerger, n.d.; Ghomrassi-Barr & Aliouche, 2016; Seright, 2009).

Globally, the recovery factor is approximately 36% and that of Colombia is around 20%. This disparity underscores the urgency of adopting EOR approaches in Colombia to bridge this gap (Ecopetrol 2020). Notably, Chemical Enhanced Oil Recovery (CEOR) methods, involving polymers, surfactants, alkalis, and more, have garnered attention. Injecting polymer solutions has yielded operational success, with recovery factor increments ranging from 5% to 15% compared to water injection (secondary recovery) (Ecopetrol, 2020; Ghomrassi-Barr & Aliouche, 2016).

Water-soluble polymers play a pivotal role in increasing the viscosity of the injected water, often amplifying it by factors of 10 to 50. This viscosity enhancement bolsters the mobility ratio between the displacing fluid (polymer solution) and the displaced fluid (crude oil) during the EOR processes, resulting in increased oil recovery rates (Irima, 2014; Seright, 2009; Shahzad, 2015; Sveistrup, 2015). However, beyond mere viscosity augmentation, the stability of polymer solutions takes center stage, ensuring consistent viscosity and structural integrity of the polymer

over time, especially under varying reservoir conditions including temperature fluctuations, pressure dynamics, ionic strength variations (due to dissolved minerals), and mechanical stresses (shearing forces) during injection and transport through porous media (Jimenez, 2009; Shahzad, 2015).

Several factors affect the assessment and selection of polymers for Enhanced Oil Recovery (EOR). Among these is the requirement for a polymer solution with a broad viscosity range that facilitates the efficient sweeping of crude oil. Equally important is the maintenance of a consistent rheological profile during injection and within the reservoir, even under challenging transport conditions, including high temperatures, salinity, pressure, hardness, mineral content, and deformation stress. Partially hydrolyzed polyacrylamide (HPAM) is currently one of the most extensively employed polymers for EOR applications (Sheng, 2011). Its merits include its capacity to withstand intense mechanical shear stresses and its adaptability to chemical structures, enabling modifications that intensify the resistance to specific formation conditions (e.g., copolymers such as HPAM-AMPS and sulfonated polyacrylamides) (Floerger, n.d.; Shahzad, 2015). However, HPAM has notable drawbacks, such as the high cost associated with its synthesis and structural alterations, along with its inherent susceptibility to salinity, hardness, the presence of surfactants or other chemicals, and potential environmental implications (Floerger, n.d.; Sheng, 2011).

Consequently, there has been a push towards exploring bio-based alternatives with a favorable technical-economic balance, exemplified by xanthan gum (XG). In addition to being cost-effective (5:1), xanthan gum exhibits high viscosity behavior when confronted with ionic forces such as salt or hardness. This resilience stems from its structural ramification (branched polymer), which is compatible with most surfactants and other additives commonly used in tertiary recovery formulations (Ghoumrassi-Barr et al., 2015). However, determining the structural

composition of xanthan gum is challenging. Over extended durations of exposure to adverse conditions, including temperature, salinity, and deformation stress, xanthan gum undergoes conformational shifts, that is, rotational or coupling movements within the molecule. These changes lead to the weakening and eventual breaking of intermolecular (COOH carboxyl groups in its lateral structure-water) and intramolecular (bonds within the same molecule, CCOH) connections (Michael Khouryieh, 2006). This process promotes the loss of viscosity and polymer precipitation (degradation). Despite these limitations, the innate potential of xanthan gum as a biopolymer and its positive environmental attributes, necessitates research aimed at modifying and salvaging its utility as a successful additive in tertiary recovery methodologies.

In the pursuit of strategies that bolster or sustain the intermolecular and intramolecular bonds in a polymer solution, the integration of nanoparticles has emerged as a prospective enhancement for biopolymeric treatments, such as xanthan gum (Jordan, 2014; Pi, 2016). As the particle size diminishes, their impact becomes more pronounced: nanoparticles at the nanoscale (ranging from 1 to 100 nm) exhibit heightened surface-area-to-volume ratios. The reduced binding of surface atoms leads to incomplete coordination, resulting in a discernible increase in the surface free energy (Adel, 2015; Bracho García, 2013; Ogolo, 2012).

Their nano dimensions, coupled with the chemical composition of the nano-surface, permit the selection of nanoparticles that mitigate the weaknesses observed in xanthan solutions. Consequently, silica nanoparticles have emerged as a promising avenue. Their compatibility with the reservoir, primarily the predominant sand components, makes them attractive choices. This is complemented by the distinctive properties of their surfaces, which are characterized by siloxane groups (Si-O-Si) and silanols (Si-OH). This unique surface chemistry further engenders an affinity

for water, endowing them with a hydrophilic nature that is compatible with the XG structure (Ibrahim, 2015; Min-Ho, 1999; Pi, 2016).

Recent research findings have proposed that the incorporation of silica nanoparticles may lead to a reduction in the conformational transitions of xanthan gum, thereby reinforcing the bonds both between and within molecules (Saravanan, 2016; Yousefvanda, 2015). This phenomenon can be rationalized by the formation of chemical bonds between the hydroxyl groups (-OH) on the surface of silica nanoparticles and xanthan molecules, acting as anchor points that connect the nanoparticle and the macromolecule (Pi, 2016; Yousefvanda, 2015). This interaction introduces novel crosslinked, three-dimensional, and more rigid polymeric structures. When subjected to high temperatures, ionic forces, and deformation or elongation stresses, these structures exhibit enhanced rheological profiles owing to a delayed conformational transition (Jordan, et al, 2014).

Other studies have suggested that the presence of nanoparticles in aqueous systems could potentially enhance the fluid mobility within reservoirs. However, the precise mechanisms and criteria governing their effectiveness remain enigmatic (Camesano, 2001; Pi, 2016; Saravanan, 2016). Currently, nanoparticle integration is considered an innovative technique due to its potential and the scarcity of comprehensive information to ascertain its technical and economic viability. Consequently, a more profound understanding of nanoparticle-biopolymer interactions, both in isolation and in tandem with ion presence in solutions and responses to thermo-mechanical stresses, is imperative.

Conversely, a limited number of projects have focused on fluid preparation using brine, which confers operational advantages to solutions featuring xanthan gum, lauded for its superior resistance to salt in comparison to synthetic polymers. The incorporation of silica nanoparticles aims to amplify the performance, particularly the rheological stability, of these fluids. From an

operational standpoint, directing research toward achieving these scenarios would not only enhance fluid stability against substantial deformations or temperature fluctuations, but also establish a technically, economically, and environmentally competitive alternative to pricier synthetic polymers.

The principal objective of this study was to investigate the impact of hydrophilic silica nanoparticles on the viscosity of xanthan gum solutions. Additionally, the investigation aimed to comprehensively analyze the endurance of the rheological behavior of these fluids under the influence of thermo-mechanical stresses and the introduction of ionic forces ( $\text{Na}^+$  and  $\text{Cl}^-$ ) over an extended period. The experimental tests aimed to emulate some representative enhanced oil recovery process conditions. The interaction between silica nanoparticles and xanthan gum is hypothesized to be facilitated by feeble physical bonds like hydrogen bridges or dipole-dipole forces, which serve as anchor points. This interaction leads to a delayed polymer's transitional movement, consequently preserving the fluid's viscous attributes across wider operational ranges.

The components employed in this investigation were commercially sourced: The xanthan gum was provided by Sukin Industries, a Colombian enterprise specializing in polymeric materials (see appendix A.1). The silica nanoparticles ( $\text{Np-SiO}_2$ ) used were fumed Aerosil 300, procured from Evonik Industries (see appendix A.2). Sodium chloride was supplied by Sigma-Aldrich (see appendix A.3). The synthetic polymer, known as Hydrolyzed Polyacrylamide (HPAM) FLOPAAM 3230 S, obtained from SNF Floerger, was employed. Finally, the synthetic oil used in the experimentation was USP mineral oil, sourced from Chemical Elements LTDA (see appendix A.4).

In the first chapter, a detailed characterization of both the nanoparticles and biopolymer was carried out, identifying the nature of the materials, their physicochemical properties, and the

functional groups that allow their possible link. Following this, a nanofluid formulation and preparation process was standardized, where its interaction was exposed to the stability of the generated solution and subsequently, the macrostructure (nanoparticle polymer) was evaluated against different tests that corroborate the bond strength between the nanoparticle and polymer, showing its possible application to chemical recovery processes on a laboratory scale. The objective of this chapter was to determine the best method for the preparation of nanofluids.

In the second chapter, the evolution of the viscosity of nanofluids and XG solutions over time was established. The effect of nanoparticles on the formulations was measured over time through stability tests. Additionally, capillary viscometry, Z potential, and confocal microscopy tests were presented, which allowed us to determine the interaction between XG and nanoparticles. This chapter also includes TGA and DSC assessments in the formulations.

Chapter III, the final chapter, presents core flooding tests, showing the results of the linear displacement of the polymeric XG solution and nanofluid. A comparison with an HPAM solution was established. Additionally, the results of rock-fluid interactions (saturation, permeability, swirl) and interfacial tension tests were presented. Finally, the results of incremental EOR recovery percentages were estimated for the comparative formulations.

Findings related to the interaction between xanthan gum and silica nanoparticles represent a promising pathway for enhancing our understanding of biopolymeric fluid behavior and its potential applications in Enhanced Oil Recovery (EOR). This study focused on the influence of hydrophilic silica nanoparticles on the viscosity and rheological stability of xanthan gum solutions, providing an opportunity to broaden their scope as substitutes for synthetic polymeric treatments. This alternative becomes crucial considering environmental and health concerns as well as the significant costs associated with existing treatments.

Currently, a limited number of industrial applications have investigated the interaction dynamics between xanthan gum and silica nanoparticles. Surprisingly, despite the evident potential of this interaction, limited research has been directed towards the development of nanofluids comprising xanthan gum and silica nanoparticles for enhanced oil recovery (EOR). Consequently, there is a need for extensive research into this technology. Its importance transcends mere promise and has the potential to have a substantial positive impact on both environmental sustainability and economic viability.

## Chapter I

### Rheological Behavior and Preparation Methods of Nanofluids

#### Abstract

The objective of this chapter is to study different methods for the preparation of nanofluids composed of hydrocolloid xanthan gum (XG) and hydrophilic silica nanoparticles (Np-SiO<sub>2</sub>) dispersed in water. First, the research materials were characterized: xanthan gum and silica nanoparticles. For xanthan gum, infrared spectroscopy, and X-Ray photoelectron spectrometry (XPS) techniques were used, while X-Ray photoelectron spectrometry (XPS), X-Ray diffraction and Scanning electron microscopy with energy dispersive X-ray spectroscopy (SEM/EDX) tests were performed for the nanoparticles.

In order to define the preparation method of the nanofluids, it was initially verified whether the order of addition of the components affected the resulting fluid viscosity. Additionally, the solubilization time required by the polymer to ensure its complete hydration was evaluated.

Next, the influence of the preparation method on the rheological response of the formulation was then analyzed: the rheological behavior of the XG solutions and Np-SiO<sub>2</sub> suspensions was first characterized individually, for different concentrations. The effect of the presence of salt (NaCl) was then evaluated. Also, the technique used to disperse the components was evaluated using sonication for both the polymer and the nanoparticles. From these results the polymer dilution curves, delimiting the dilute and semi-dilute regimes were obtained.

Finally, different preparation methods of the nanofluids were then considered, testing various factors like the hydration time of the polymer, the sonication time, and the order of aggregation of the components (XG/ Np-SiO<sub>2</sub>). In addition to viscosity profile at constant

temperature and variable shear rate test, dynamic light scattering (DLS) was used, providing a trend in the stability of the viscous profile of nanofluids. The simplest method providing a correct dispersion of the Np-SiO<sub>2</sub> as well as the increase of the viscous profile was then selected. This study provides a better understanding of the interactions between XG and Np-SiO<sub>2</sub> in solution.

This chapter resulted in a publication in the Journal Chemical Engineering Transactions: Buitrago-Rincon D. et al. "Effect of silica nanoparticles in xanthan gum solutions: Rheological behavior and preparation methods of nanofluids". Chemical Engineering Transactions ISSN: 2283-9216, AIDIC v.86 fasc. p.1171 - 1176 ,2021. DOI: 10.3303/CET2186196. (see appendix A.5).

## Introduction

The addition of polymer in a solvent causes an increase of the viscosity, due to inter and intramolecular forces within the polymer and with the surrounding solvent molecules. The intensity of the viscosity increases both depends on the nature of the polymer and the nature of the solvent. Xanthan gum (XG) is an extracellular biopolymer (Sheng, 2011) which exhibits a shear thinning rheological behavior when put in solution: the viscosity of XG solutions decreases with increasing shear rate.

The presence of charged functional groups in its side chain (carboxyl groups (-COOH)) makes it an anionic polysaccharide (Camesano et al., 2001). The structure of XG undergoes conformational changes (rotation/coupling of the molecule) when it is in an aqueous solution and is exposed to conditions of temperature, salinity, and deformation stress (Pi et al., 2016). The intermolecular (COOH - water) and intramolecular (COOH – COOH) bonds existing

in the system, tend to weaken and then break, causing a viscosity loss and/or polymer precipitation (degradation) (Sheng, 2011). This phenomenon can be explained by the conformational structure of the polymer. Indeed, XG exhibits two conformations: an ordered conformation and a disordered conformation (Carmona et al., 2015). The viscosity variations in xanthan solutions are caused by the transition from one conformation to another (ordered/disordered) (Moorhouse et al., 1977).

In the search for strategies to reinforce or maintain the inter / intra-molecular bonds that affect the viscosity and stability of XG solutions, the use of nanoparticles (Np-SiO<sub>2</sub>) is considered a possible improvement (Abidin et al., 2012). The surface of Np-SiO<sub>2</sub> allows an interaction with the carboxyl groups present in the xanthan structure (-COOH), leading the polymer chains to link with the Np-SiO<sub>2</sub>. Recent studies have suggested a limitation of the conformational transition of xanthan through the addition of Np-SiO<sub>2</sub> (Jordan et al., 2014). The interaction of the polymer with the Np-SiO<sub>2</sub> allows new cross-linked, three-dimensional, and more rigid polymeric structures, which delay their conformational transition (Pi et al., 2016). However, it is necessary to establish the optimal conditions for the preparation of these nanofluids, composed of XG and Np-SiO<sub>2</sub> dispersed in water. The present study describes and develops different methods for the elaboration of low viscosity nanofluids, evaluated through the viscosity profile as the response variable.

## **Materials and methods**

### ***Preparation of xanthan gum solutions and nanoparticles suspensions***

The commercial XG was obtained from Sukin Industries. The silica nanoparticles, purchased from Evonik Industries, were fumed Aerosil 300 amorphous hydrophilic silica NP (specific surface =  $300 \pm 30 \text{ m}^2 / \text{g}$ ), with primary units of 12nm. The sodium chloride was supplied

by Sigma Aldrich (purity  $\geq 99.5\%$  and 58.44 daltons molecular weight).

The materials were characterized by infrared spectroscopy, and X-Ray photoelectron spectrometry (XPS) for xanthan gum, while scanning electron microscopy with energy dispersive, X-Ray diffraction, and X-ray spectroscopy (SEM/EDX) tests were performed for the nanoparticles.

The polymer solutions were prepared with two different solvents. The first solvent was deionized water, in which polymer powder was incorporated at different concentrations (150, 300, 600, 1200, 2400 and 4800 ppm). The second solvent was brine, previously prepared at several concentrations of NaCl (0, 0.1, 0.5, 1 and 3 wt%), in which the polymer powder was incorporated at a concentration of 600 ppm, to evaluate the influence of ionic forces on the viscous behavior of the fluid. All solutions were left under magnetic stirring at room temperature, and bactericide was added to the solvent at a fixed concentration (80 ppm) before incorporating the polymer. In order to ensure that the polymer was fully hydrated, two different hydration times were tested: 24 and 48 h. The viscosity profiles after these two durations were compared.

Similarly, nanoparticle suspensions were prepared with the same two solvents, before their viscosity curve was determined. On the one hand, nanoparticles were dispersed at different concentrations (100, 200, and 300 ppm) in deionized water. On the other hand, NaCl brines were prepared with different concentrations (0, 0.1, 0.5, 1 and 3 wt%). All the suspensions were left under magnetic stirring for 1 h at room temperature.

### ***Sonication Treatment and DLS Tests***

The impact of a sonication treatment on the fluid's rheology was evaluated, both for XG solutions (150, 300, 600, and 1200 ppm) and for nanosuspensions (100, and 300 ppm) without the

presence of ionic charge (NaCl). The formulations were sonicated for different durations (0, 3, 6, 9, and 30 min) using a Fisher Scientific 550 Sonic Dismembrator ultrasonic processor. The amplifier frequency was set at 40 Hz and the amplitude at 20%, which corresponds to a power of approximately 300 W.

An ice-water bath was used to control the temperature of the dispersions in the cell. After each sonication treatment, the viscosity of the formulations was measured by rheological tests and by qualitative observations to detect the possible appearance of precipitates or agglomerates in the fluid. Additionally, for nanoparticle suspensions, size (agglomerate) measurements were performed through Dynamic Light Scattering (DLS) after each sonication treatment.

### ***Rheology measurement***

The rheological characterization at each stage of this chapter was performed using a Rheometric Scientific RFS II rheometer equipped with a rotating helical ribbon of 17.95 mm radius in a tank of 27.5 mm internal radius and 42 mm inner height. This helical geometry is adapted to low viscosity fluids since it generates higher torques than classical geometry, like plate/plate cells. The tests were executed at a constant temperature (25°C) and for variable shear rate (0.1 - 100 (s<sup>-1</sup>)), with sensitivities of 1 Pa. s for the viscosity and 0.002 N.m for the torque.

The effect of salinity on the rheological behavior of the generated formulations (Np-SiO<sub>2</sub> suspensions and polymer solutions) was evaluated. The dilution curve of the polymer in brine was established at the arbitrary shear rates of 6.3 s<sup>-1</sup> and 10 s<sup>-1</sup> at temperature 25°C. The viscosity curves of the dispersions obtained with the different methods was then determined.

***Nanofluids preparation***

Four different methods were considered to prepare the nanofluids (XG and Np-SiO<sub>2</sub> in water), by varying the hydration time of the polymer, the order of addition of the components, the sonication time applied to the nanoparticle suspensions, and the time of interaction between the components,

**Table I.1.** *Preparation methods of the nanofluids*

M <sup>1</sup>	T <sup>2</sup>	Step 1	Step 2	Step 3	Step 4
1	20 °C	Addition of XG and NPSiO <sub>2</sub> in water at the same time	Magnetic stirring for 24 h	-	-
2	20 °C	Addition of XG in water and magnetic stirring for 24 h	Addition of NP-SiO <sub>2</sub> powder to the XG solution	Magnetic stirring for 24 h	-
3	20 °C	Addition of NP-SiO <sub>2</sub> in water and magnetic stirring for 1 h	Sonication of NP-SiO <sub>2</sub> suspension for 30 min	Addition of XG to the NP-SiO <sub>2</sub> Suspension	Magnetic stirring for 24 h
4	20 °C	Addition of XG in water and magnetic stirring for 24 h	Addition of NP-SiO <sub>2</sub> in water and magnetic stirring (1 h). Sonication of NP- SiO <sub>2</sub> suspensions for 30 min	Mixing of the XG solution and NP-SiO <sub>2</sub> suspension (under sonication)	Magnetic stirring for 24 h

*Note.* 1. Preparation method.

2. Fluid preparation temperature

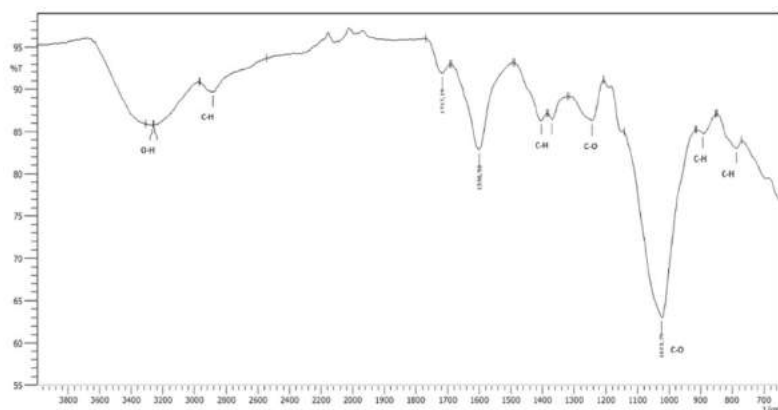
Table I.1. In this part of the study, the concentrations of Np-SiO<sub>2</sub> and XG were kept constant (300 ppm and 600 ppm respectively), as well as the temperature and pressure of the process.

## Results and Discussion

### *Xanthan Gum and Nanoparticles*

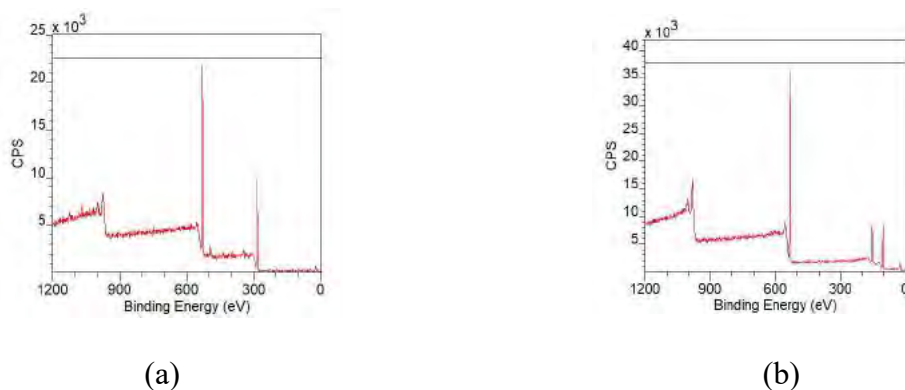
**Xanthan Gum.** Initially, the product was characterized with infrared spectroscopy to determine the presence of functional groups in the structure, Figure I.1. The presence of carbonyl groups and OH groups in the polymer structure is checked.

**Figure I.1** *Infrared spectrum xanthan gum*

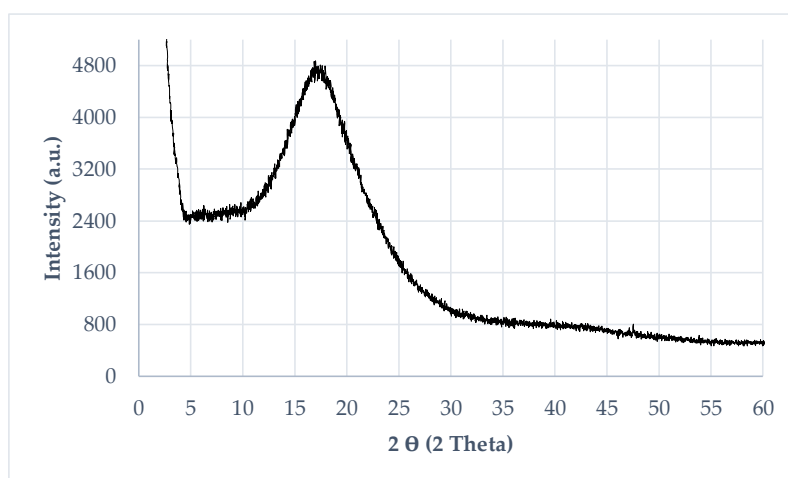


*Note.* Absorbance (or transmittance) on the vertical axis vs. frequency.

X-Ray photoelectron spectrometry (XPS) was used for the surface characterization of XG, Figure I.2(a). Surface atomic percentage (1s) of 63.14% carbon (C), 36.29% oxygen (O) and 0.57% sodium (Na) was determined.

**Figure I.2** XPS of (a) xanthan gum and (b) silica nanoparticles

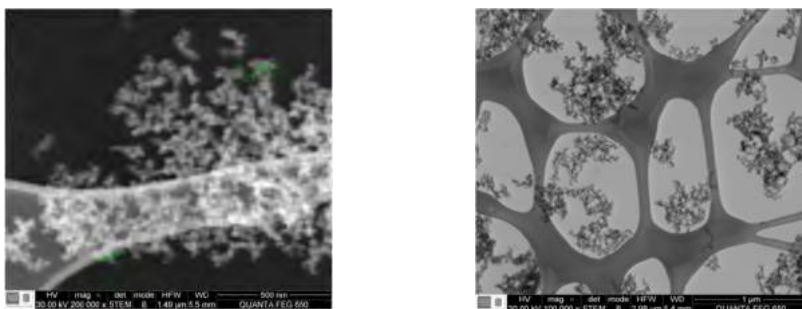
**Silica Nanoparticles.** The silica nanoparticles (Np-SiO<sub>2</sub>) were fumed Aerosil 300 amorphous hydrophilic ( $300 \pm 30 \text{ m}^2/\text{g}$ ) from Evonik Industries, appendix A.2. X-Ray photoelectron spectrometry (XPS) was used for the surface characterization, Figure I.2 (b). The composition of the nanoparticles was verified with superficial atomic percentage, yielding 55.24% oxygen (1s) and 44.76% silicon (2p).

**Figure I.3** X-Ray diffraction silica nanoparticles

The morphology of the nanoparticles was also confirmed by X-ray diffraction analysis (XRD) tests. The crystallographic structure is not determined, corresponding to amorphous silica, Figure I.3.

Micrographs were taken using scanning electron microscopy with energy dispersive X-ray spectroscopy (SEM/EDX), Figure I.4. SEM analysis shows that particle size varies from 7.21 – 10.15 nm in diameter, with an average diameter of 8 nm and a spherical geometry.

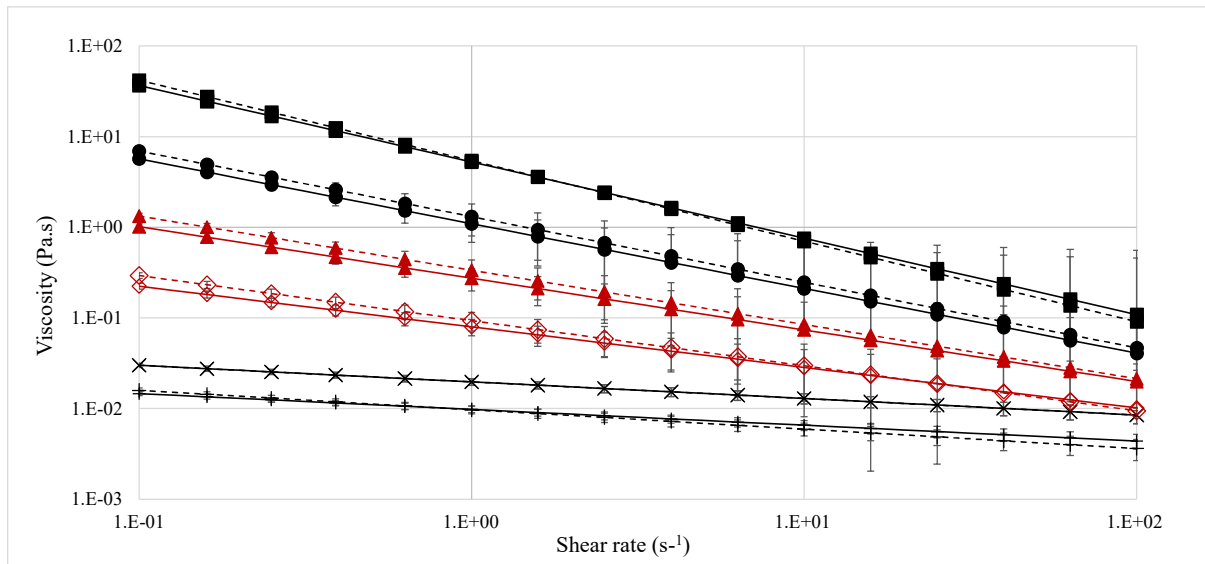
**Figure I.4** SEM / EDX silica nanoparticles



*Note.* SEM- EDX micrographies, Np-SiO<sub>2</sub> 200 000 x (left) Np-SiO<sub>2</sub> 100 000 x (right).

### ***Characterization of the polymer solutions***

The effect of the mixing time applied to the polymer solutions was evaluated for 4 concentrations to ensure complete hydration of the polymer. XG formulations from 150 ppm to 4800 ppm were prepared. An initial rheogram was measured at 24 h of hydration and a second rheogram at 48 h of hydration with magnetic stirring at room temperature. Figure I.5. shows a despicable variation in the viscosity curves for the 2 established hydration times. Therefore, it is determined that 24 h is sufficient time to ensure the complete hydration of the polymer up to a maximum concentration of 4800 ppm.

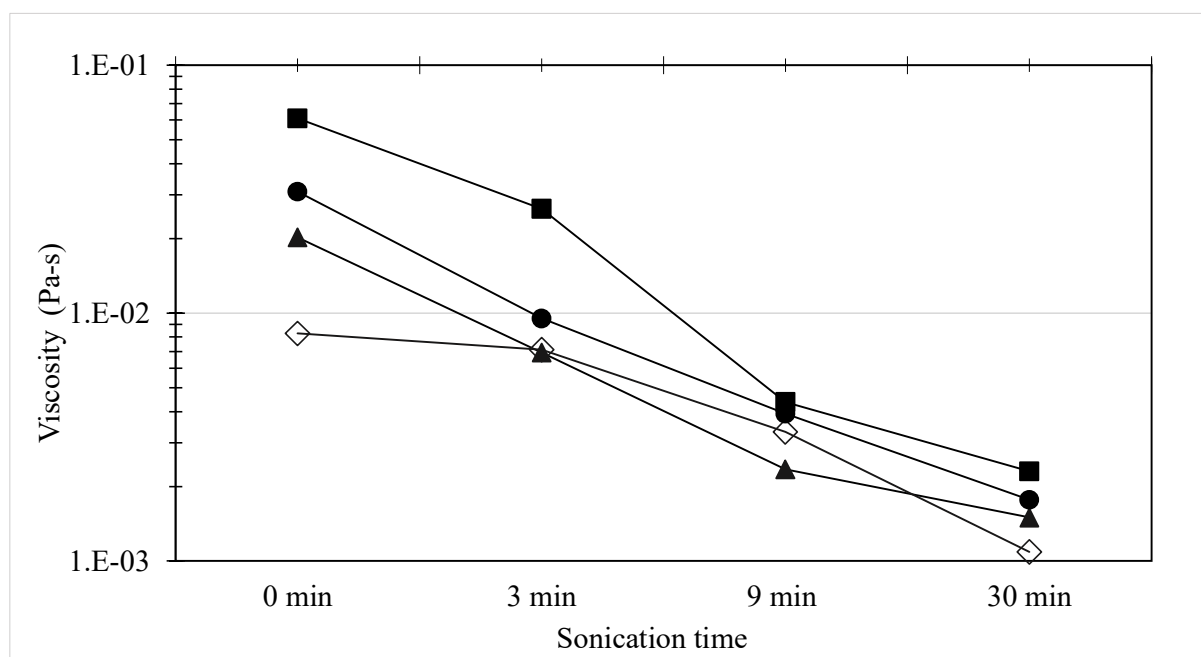
**Figure I.5** Evolution of polymer solution viscosity during hydration

*Note.* Viscosity of polymer solution in water as a function of shear rate at 24 h and 48 h. Measurements performed at  $T = 60\text{ }^{\circ}\text{C}$ . XG 4800 ppm 24 h (—■); XG 4800 ppm 48 h (- -■); XG 2400 ppm 24 h (-●); XG 2400 ppm 48 h (- -●); XG 1200 ppm 24 h (-▲); XG 1200 ppm 48 h (- -▲); XG 600 ppm 24 h (-◇); XG 600 ppm 48 h (- -◇); XG 300 ppm 24 h (-×); XG 300 ppm 48 h (- -×); XG 150 ppm 24 h (-+); XG 150 ppm 48 h (- -+).

A Newtonian behavior is observed for polymer concentrations of 150 ppm and 300 ppm XG, while polymer solutions showed a shear-thinning behavior for concentrations above 600 ppm, Figure I.5. As expected, it was observed that viscosity increases with polymer concentration.

**Sonication Treatment** . Ultrasonic energy was applied to the polymer solutions for different durations (Figure I.6). For all considered polymer concentrations, a viscosity reduction of around 50-69% was measured after the first 3 min and 87-96% after 30 min, at a shear rate of  $10 \text{ s}^{-1}$ . This indicates a degradation of the polymer due to sonication, even for the shortest sonication time. This is attributed to the implosion of microbubbles generated by cavitation under high pressure and high temperature acoustic waves, leading to the breakdown of the polymer molecules. Sonication promotes depolymerization and reduces the polymer molecular weight, with accelerated cleavages in the middle of the polymer chain (Saleh et al., 2017).

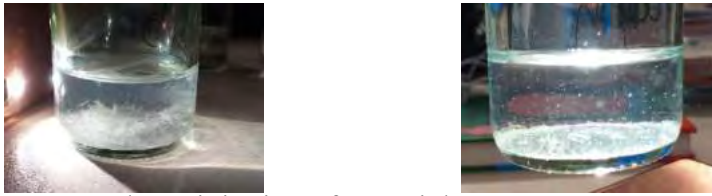
**Figure I.6** Effect of sonication on viscosity for xanthan gum solutions



*Note.* Viscosity of polymer solution in water at  $10 \text{ s}^{-1}$  shear rate, as a function sonication time. Measurements performed at  $T = 25 \text{ }^\circ\text{C}$ . XG 1200 ppm (—■); XG 600 (—●); XG 300 ppm (—▲); XG 150 ppm (—◇).

Figure I.7 shows the photographic record of the polymeric formulations after sonication. Heterogeneous fluids with polymer agglomerates are observed. These qualitative results corroborate the impossibility of applying sonication to XG polymeric solutions for the preparation of nanofluids.

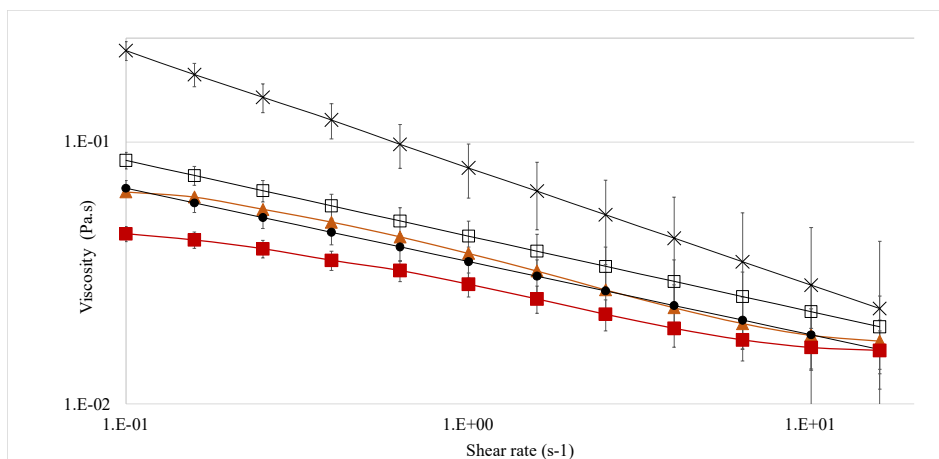
**Figure I.7** *Polymer solutions after sonication*



*Note.* Agglomerate and precipitation of material.

***Influence of NaCl and Dilution curve of xanthan gum.*** The influence of NaCl at five different concentrations on 600 ppm XG solutions was evaluated through rheograms (Figure I.8). It appears that an increase of the NaCl concentration leads to a viscosity decrease.

**Figure I.8** *Effect of NaCl on the rheology for xanthan gum solutions*



*Note.* Viscosity of polymer solutions (600 ppm XG) with different NaCl concentrations as a function of the shear rate. Measurements performed at  $T = 25\text{ }^{\circ}\text{C}$ . Water (X); 0.1% NaCl ( $\blacktriangle$ ); 0.5% NaCl ( $\square$ ), 1% NaCl ( $-\bullet$ ); 3% NaCl ( $-\blacksquare$ ).

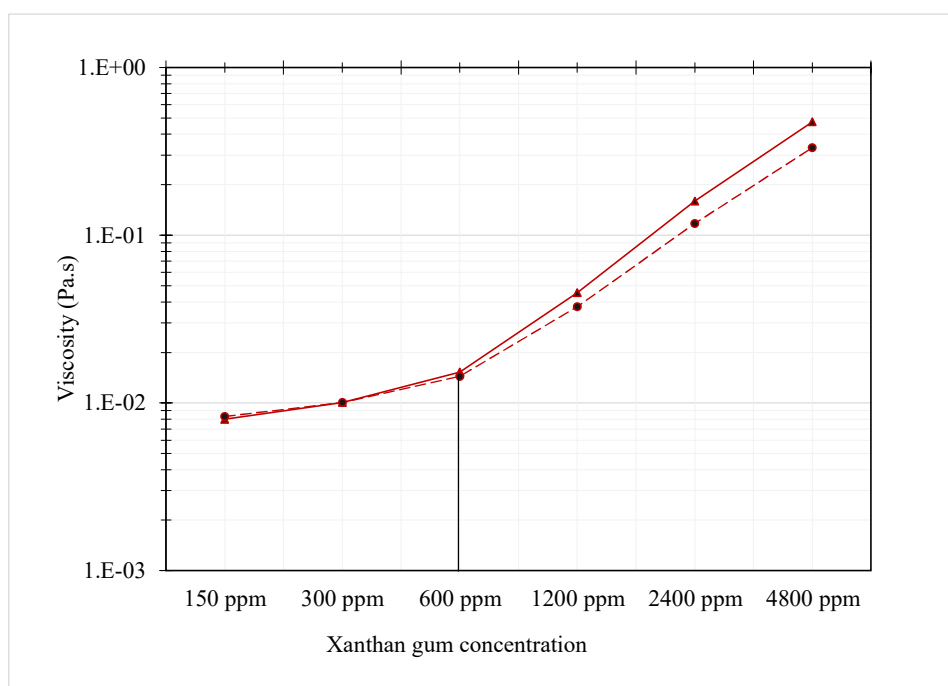
It has been suggested that, in the absence of ionic charges in the dilution medium, the XG chain is disordered and extended due to electrostatic repulsions between the charges within the polymer. (Stokke et al., 1992). This conformation provides relative flexibility to polymer chains and increases the viscous response of the solution. In the presence of  $\text{Na}^+$  and  $\text{Cl}^-$  ions, the XG backbone becomes stiffer and less stretched, while electrostatic repulsions affect the solubility of the polymer and therefore the viscosity of the solution.

However, higher viscosities were observed at a concentration of 0.5% than at 0.1%. This paradoxical effect can be explained by previous studies (Li et al., 2015), which reported that in XG solutions with low NaCl concentration, the polymer may rotate to a slightly messier and more extended conformation. In contrast, when NaCl ions are present in a solution with a higher salt concentration, the ordered conformation is favored. Charge screening causes the side chains to collapse down to the backbone, hence giving the xanthan molecule a rod-like shape, more compact, corresponding to a reduced hydrodynamic size of the molecule, leading to a reduced viscosity (Khouryieh, 2007; Li, 2015).

At a representative shear rate of  $7.3\text{ s}^{-1}$ , the viscosity decreases by 61% with a concentration of 3% NaCl. However, for EOR applications, working brines are estimated to have an average concentration of 30000 ppm (3%) NaCl. Therefore, this concentration value was fixed for the subsequent work. In particular, the polymer dilution curve was constructed for 3% NaCl for constant shear rates of  $7.3\text{ s}^{-1}$  (Figure I.9). The dilute zone corresponds to XG concentrations lower

than 600 ppm while the semi-dilute zone ranges between 600 ppm and 4800 ppm. The concentrated zone was not determined in the present work.

**Figure I.9** Dilution curve of xanthan gum with 3% NaCl.



*Note.* Measurement performed at a constant shear rate of:  $7.3 \text{ s}^{-1}$  (—▲);  $10 \text{ s}^{-1}$  (—●).

### ***Characterization of nanoparticle suspensions***

The viscosity behavior of NP-SiO<sub>2</sub> suspensions was analyzed to explore the degree of dispersion of the nanoparticles. Indeed, for a smaller agglomerate size or a better dispersion of the NP-SiO<sub>2</sub>, the suspensions tend to be more viscous and to adopt a Newtonian behavior (viscosity independent of the shear rate) (Mondragon et al., 2012).

However, the flow profiles obtained in the present study for 3 different Np-SiO<sub>2</sub> concentrations did not show a significant difference: there was no apparent viscosity change between suspensions of 100 ppm and 300 ppm Np-SiO<sub>2</sub> (Table I.2). This possibly due to the low and close concentrations evaluated.

**Table I.2.** *Viscosity of nanoparticles suspensions.*

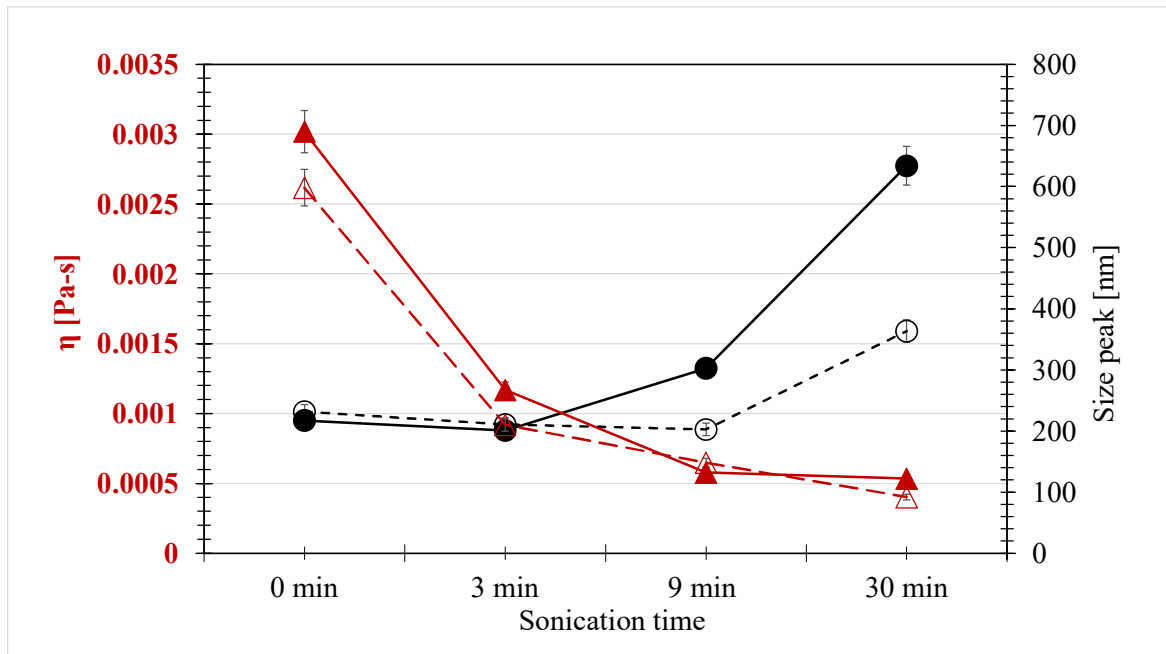
Fluid	Viscosity (Pa·s) <sup>1</sup>
Water	0.001000
100 ppm NP-SiO <sub>2</sub>	0.001012
200 ppm NP-SiO <sub>2</sub>	0.001140
300 ppm NP-SiO <sub>2</sub>	0.001167

*Note.* <sup>1</sup>Viscosity—Newtonian behavior.

The effect of salt on the NP-SiO<sub>2</sub> suspensions rheology was then investigated. No significant difference was observed in water or in brine. Particle size measurements showed initial agglomerates average size (before sonication) of 598 nm and 690 nm for 100 ppm and 300 ppm NP-SiO<sub>2</sub> concentrations respectively. During sonication, the agglomerates size decreased progressively due to their breakup.

For smaller agglomerates, the Np-SiO<sub>2</sub> dispersion displays a more isotropic distribution of the particles, thus increasing the viscosity. Therefore, a sonication time of 30 min was chosen to prepare the nanoparticle suspensions. Figure I.10 shows the decrease of the agglomerates size (dotted line) and the viscosity curves (solid line) at a shear rate of 10 s<sup>-1</sup>.

**Figure I.10** Viscosity and particle size of Np-SiO<sub>2</sub> suspensions as a function of sonication duration.



Note. Nanoparticles suspension at shear rates of  $10 \text{ s}^{-1}$ .

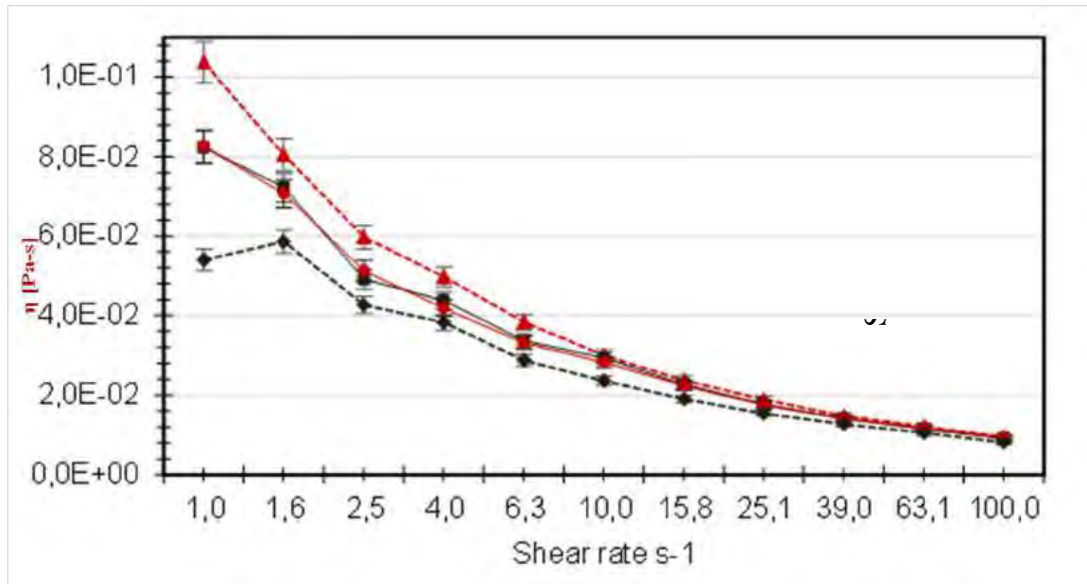
Left axis: viscosity  $\eta$  (red); Right axis: nanoparticles size DLS (black). Viscosity 300 ppm Np-SiO<sub>2</sub> (—▲); Viscosity 100 ppm Np-SiO<sub>2</sub> (---△); Size peak 300 ppm Np-SiO<sub>2</sub> (—●); Size peak 100 ppm Np-SiO<sub>2</sub> (---○).

### Nanofluids preparation

The four methods proposed for the preparation of nanofluids (Table I.1), ensured the same interaction time between the components (24 h). From the polymer dilution curve (Figure I.9), the intermediate concentration between the dilute and semi-dilute zone of 600 ppm of XG was selected and kept constant for the preparation of all nanofluids. Since the suspension rheology was little influenced by the Np-SiO<sub>2</sub> concentration, the Np-SiO<sub>2</sub> fraction was fixed to 300 ppm. In Figure I.11 are plotted the viscosity curves of the nanofluids prepared according to the 4 different

methods. No notable difference is observed in the rheological response. This indicates that the preparation process (addition order of the components, preliminary sonication of the nanoparticle suspensions) has little incidence on the final viscosity of the nanofluid.

**Figure I.11** Methods: Nanofluids viscosity as a function of the shear rate



*Note.* Preparation methods of nanofluids (600 ppm XG and 300 ppm Np-SiO<sub>2</sub> in 3% NaCl). Method 1 (--▲); Method 2 (—■); Method 3 (—●); Method 3 (--●).

Nevertheless, at low shear rates (less than 10 s<sup>-1</sup>), it is observed that with method 1 a higher viscosity is achieved in the fluid. In fact, using method 1, the viscosity of the nanofluid (XG + Np-SiO<sub>2</sub>) at 7.3 s<sup>-1</sup> was 30.1% higher than the XG solution without NP-SiO<sub>2</sub>. Therefore, method 1 was selected for the preparation process, since it yielded the highest viscosity profile with a minimum number of steps.

### ***Conclusions***

In this chapter, the potential of xanthan gum for EOR processes was evaluated and its improvement was sought through the addition of silica nanoparticles. The objective was to establish a method for preparing nanofluids composed of XG and Np-SiO<sub>2</sub>.

The research materials were supplied by different providers and the results of their characterization showed the expected specifications: Using infrared spectroscopy, the functional groups of XG were identified. XPS analyses corroborated the elemental composition of the surfaces of both the nanoparticles and the polymer. For the nanoparticles, the elemental surface was calculated with 55.24% oxygen and 44.76% silica, which would imply the presence of radicals of silanols and siloxanes on their surface. In this case, the silanols (Si–O–H) in dilution would have a negative charge on the nanoparticles. A spheric morphology of the nanoparticles was verified with SEM/EDX micrograph and a size between 7.21 – 10.15 nm in diameter.

The rheograms of the polymeric formulations presented Newtonian profiles for the concentrations of 150 ppm and 300 ppm, for the rest of the concentrations (600, 1200, 2400, and 4800 ppm) the determined profile was pseudoplastic with shear-thinning behavior.

The viscosity profiles of the polymer solutions did not show any changes in the maximum expansion of the polymer between 24 and 48 h. Therefore, complete hydration of the polymer was achieved by magnetic stirring for 24 h at room temperature in the range of concentrations studied.

The effect of NaCl on the formulation severely affects the fluid viscosity profile. A maximum reduction of 61% in the viscosity of the formulation was achieved at a concentration of 3% NaCl in the solution. However, for EOR application, a concentration of 3% in the formulation was established. In EOR processes, brine is commonly used as a preparation solvent for chemical treatments. Ideally, polymers should perform well at high salinity levels.

4 different methods (with varying ingredient incorporation order, sonication, polymer hydration time) were evaluated to prepare nanofluids composed of xanthan gum (XG), silica nanoparticles (Np-SiO<sub>2</sub>) and NaCl salt dispersed in water. Sonication, which produced deagglomeration of the particles, was shown to damage the polymer and was thus only applied to the nanoparticle suspensions (without XG). The properties of the final nanofluids were analyzed. It appears from rheological measurements that all 4 methods provided similar rheological behavior and viscosity values, showing little impact of the preparation method.

In conclusion, the simplest method, which also yielded the highest viscosities, was selected. In method 1, an increase in the viscosity of 30% of the nanofluid was achieved in comparison with the polymeric solution (without nanoparticles), at a shear rate of 7,3 s<sup>-1</sup>.

## Chapter II

### Evolution of Viscosity over Time

#### Abstract

This chapter aims to prove the efficient interactions between silica nanoparticles and xanthan gum structures in the formulations. Rheological tests were carried out at different aging times, showing the interaction between the components (XG - nanoparticles) and the effect of NP-SiO<sub>2</sub> on the nanofluids over time.

For the EOR processes, it is necessary to achieve appropriate viscosity values; however, these properties must be maintained over time during the application of the process. Therefore, evaluating the viscosity stability of formulations at different aging times is important.

Additionally, to test the effect of nanoparticles in the polymer formulation and their interaction with XG, intrinsic and relative viscosities were calculated using capillary viscometers. The electrostatic repulsion or attraction of the interactions was evaluated by means of the Zeta potential, and micrographs were taken visually using confocal microscopy. On the other hand, thermal tests of TGA and DSC were carried out in order to establish a check on the XG-nanoparticle interactions.

The effect of silica nanoparticles (NP-SiO<sub>2</sub>) in xanthan gum (XG) solutions was investigated by analyzing the viscosity profiles. First, nanofluids composed of XG and NP-SiO<sub>2</sub> dispersed in water and brine, were studied through two different aging tests. The addition of nanoparticles was shown to produce a slight effect on the viscosity of fresh fluids (initial time), while a more remarkable effect was observed over time. In particular, it appears that the presence of NP-SiO<sub>2</sub> stabilizes the polymer solution by maintaining its viscosity value over time owing to

a delay in the movement of the molecule. Finally, characterization techniques such as confocal microscopy, capillary rheometry, and zeta potential were implemented to analyze the XG/NP-SiO<sub>2</sub> interaction. The intrinsic and relative viscosities were calculated to understand the molecular interactions.

The presence of NP-SiO<sub>2</sub> increased the hydrodynamic radius of the polymer, indicating attractive forces between these two components. Furthermore, the dispersion of the nanoparticles in the polymeric solutions leads to aggregates with an average size smaller than 300 nm with good colloidal stability owing to the electrostatic attraction between XG and NP-SiO<sub>2</sub>. This chapter was published in the Journal of Nanomaterials: Buitrago Rincon D. et al. " Effect of Silica Nanoparticles in Xanthan Gum Solutions: Evolution of Viscosity over Time". Nanomaterials 2022, 12(11), 1906; <https://doi.org/10.3390/nano12111906>. (see appendix A.6).

## **Introduction**

Due to their practical significance, natural polymers, such as xanthan gum (XG) continue to attract the attention of researchers. Xanthan gum has been widely used for many applications in the food, pharmaceutical and petroleum industries among others. XG is of great interest for Enhanced Oil Recovery (EOR) processes used in the petroleum industry.

Water-soluble polymers, such as XG, are used in EOR to increase the viscosity of the water that is injected into the reservoirs in order to extract the oil. Indeed, this viscosity increase enhances the mobility ratio between the crude oil and the polymer solution, which impeaches viscous fingering and leads to a greater oil recovery (Seright,2009; Sheng,2011; Sveistrup,2015;

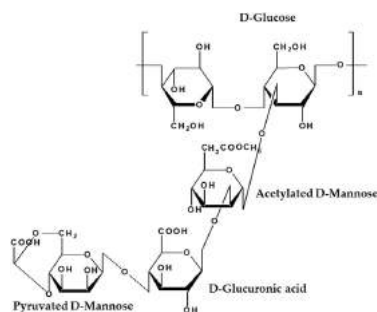
Swandvik,1977). Polymers such as xanthan gum induce high viscosities in aqueous solutions, even at low concentration.

However, EOR not only requires formulations with greater viscosity than oil, but also that this property remains stable in time against temperature conditions, ionic forces, and shear (Ecopetrol, 2019; Ghoumrassi-Barr, 2015).

Xanthan gum is an anionic heteropolysaccharide produced by the microorganism *Xanthomonas Campestris*. The primary structure of xanthan gum is a linear, linked  $\beta$ -D- glucose backbone with a trisaccharide side chain on every other glucose at C-3. The polymer chain consists of a D-glucuronic acid unit between two D mannose units. One-half of the terminal D-mannose unit contains a pyruvic acid residue linked via keto group to the 4 and 6 positions, with an unknown distribution. The D-mannose linked to the main chain contains an acetyl group at position O-6 (Figure II.1) (Jansson et al, 1975).

In aqueous solutions, the addition of polymer causes an increase of the viscosity, due to inter- and intramolecular forces within the polymer and with the surrounding solvent molecules. Furthermore, the presence of charged functional groups in its side chain (carboxyl groups (-COOH)) makes it an anionic polysaccharide (Camesano et al, 2001). These polymer solutions exhibit a shear-thinning rheological behavior (the viscosity decreases with increasing shear rate).

**Figure II.1** Chemical structure of xanthan gum



*Note.* Authors

Xanthan macromolecules may exhibit two different conformational structures: an ordered and a disordered (helical) conformation (Norton et al, 1984). The XG undergoes conformational changes in aqueous solutions when exposed to temperature, salinity, and deformation stress (Khouryieh, 2007; Pi, 2016). As a result, the molecule rotates its conformation and the intermolecular and intramolecular bonds existing in the system, tend to weaken and then break, causing a viscosity loss and/or polymer precipitation (Sheng, 2011).

In recent years, silica nanoparticles (NP-SiO<sub>2</sub>) have been used as an innovative technique to address different industrial challenges (Carmona, 2015; El-Diasty, 2015; Roustaei, 2013). Nanoparticles in general, and especially NP-SiO<sub>2</sub>, display exceptional properties owing to their small size and large surface area. The surface of NP-SiO<sub>2</sub> allows an interaction with the (-OH/H) functional groups present in the xanthan structure, leading the polymer chains to link with the NP-SiO<sub>2</sub>. Recent studies have suggested a limitation of the xanthan conformational transition due to the addition of NP-SiO<sub>2</sub> (Jordan et al, 2014). In these nanofluids, the interaction of the polymer with the NP-SiO<sub>2</sub> allows new cross-linked structures, which delay the conformational transition, improving the properties of XG solutions (Abidin,2012; Pi,2016). However, xanthan gum-silica nanoparticle interactions in dilute solutions have been little studied.

In a previous work, the polymeric dilution curve of xanthan gum was elaborated by sectorizing the regions of diluted zone and semi-diluted zone, and different methods to prepare the nanofluid (XG and NP-SiO<sub>2</sub> in water or brine) were evaluated (Buitrago-Rincon et al, 2021). This work is extended here, to describe the evolution of the viscosity of nanofluids and the effect of NP-SiO<sub>2</sub> over time. The objective of the present study is to investigate and understand the effect of NP-SiO<sub>2</sub> on xanthan gum solutions and to study the interactions in this colloidal system. Rheological and aging measurements are employed to characterize the viscosity and the stability

of the fluids in time. Intrinsic and relative viscosity, Zeta potential, and confocal microscopy measurements are used to characterize the synergistic interactions between the polymer and the nanoparticles.

## **Materials and methods**

### ***Materials***

The xanthan gum was purchased from Sukin Industries. The silica nanoparticles were fumed Aerosil 300 amorphous hydrophilic ( $300 \pm 30 \text{ m}^2/\text{g}$ ) from Evonik Industries. Sodium chloride was supplied by Sigma-Aldrich (purity  $\geq 99.5\%$ , 58.44 daltons). Deionized water was used as solvent and glutaraldehyde, provided by Sigma-Aldrich (50 wt.% in  $\text{H}_2\text{O}$ ), was added as a bactericidal agent.

### ***Nanofluids Preparation and Influence of Temperature during Preparation***

The polymer solutions were prepared by incorporating polymer powder in deionized water or NaCl brine (previously prepared at 3 wt%). The solutions were then left under magnetic stirring during 24 h. In Chapter I, various preparation methods of these nanofluids were evaluated (Buitrago-Rincon et al, 2021). The protocols differed in the polymer hydration time, the order of addition of the components, the sonication time applied to the NP-SiO<sub>2</sub> suspensions, and the interaction time between the components. The method yielding the highest viscosity profile (30.1% higher than the XG solution without NP-SiO<sub>2</sub>) with a minimum number of steps was retained. It consists in incorporating the XG and the NP-SiO<sub>2</sub> at the same time in the solvent, and to leave the resulting mixture under magnetic stirring during 24 h at room temperature. The

bactericide was added to the solvent at a fixed concentration (80 ppm) before incorporating the materials.

In the same chapter, the concentration regimes for XG solutions were determined: the dilute regime corresponds to 0–600 ppm XG, and the semi-dilute regime to 600–4800 ppm XG (Buitrago-Rincon et al, 2021). Therefore, to continue the investigation, it was decided to establish fixed concentrations of the polymer in each dilution zone, dilute regime (400 ppm XG) and semi-dilute regime (1000 ppm XG). The concentration of the solvent (NaCl brine) and silica nanoparticles were also fixed at 3 wt% and 300 ppm respectively.

In the present chapter, the effect of temperature applied during nanofluid preparation was evaluated. Using the previously selected preparation method, the operating temperature was set successively to 20 °C, 40 °C, 60 °C, and 80 °C.

### ***Rheological Characterization***

Two different apparatuses were used to measure the viscosity of the different fluids considered in this study: a rheometer and a capillary viscometer.

A strain imposed Rheometric Scientific RFS II rheometer was used, equipped with a rheoreactor geometry. This geometry consists of a rotating helical ribbon of 17.95 mm radius rotating in a tank of 27.5 mm internal radius and 42 mm inner height. It is adapted to low viscosity fluids since it generates higher torques than classical geometry, like plate/plate cells. Furthermore, the ribbon agitator ensures the homogeneity of the mixture. The accuracy of this system has been proven by previous studies (Aït-Kadi et al, 2002). The tests were executed at constant temperature of 25 °C or 60 °C. The shear rate was varied between 0.1 and 100 s<sup>-1</sup>, with sensitivities of 1 Pa.s for the viscosity and 0.002 N.m for the torque. Finally, the effect of NP-SiO<sub>2</sub> on the stability of the

viscous profile of the formulations under aging conditions was evaluated. All measurements were repeated at least twice for each formulation to confirm reproducibility. The particular shear rate of  $7.3 \text{ s}^{-1}$  was used to compare some results since it is a representative rate for the flow profile under well conditions for EOR applications (Ye et al, 2013).

Capillary viscometers measure a viscosity from the time it takes for a volume of polymer solution to flow through a thin capillary.

$$t_s \sim \frac{\mu_s}{\rho_s} \quad (1)$$

$$t \sim \frac{\mu}{\rho} \quad (2)$$

with  $t_s$  and  $t$  the flow times obtained for the solvent and the considered solution, respectively,  $\rho_s$  and  $\rho$  the solvent and solution densities, and  $\mu_s$  and  $\mu$  the solvent and solution viscosities. Considering equivalent densities (since the solutions are dilute), the relative viscosity can be obtained through

$$\mu_{rel} \sim \frac{t}{t_s} \quad (3)$$

In order to evaluate the hydrodynamic radius evolution of the polymer in time with and without nanoparticles, the intrinsic viscosity ( $\mu$ ) of the formulations was determined from rheological measurements. The intrinsic viscosity of fresh fluids (initial time) was obtained from capillary viscosimetry, while the evolution of the intrinsic viscosity over time was calculated from the rheograms obtained with the rheometer at a shear rate of  $7.3 \text{ s}^{-1}$ .

Intrinsic viscosity is related to the hydrodynamic volume occupied by isolated individual polymer molecules (Richardson et al, 2000). The relationship between dilute polymer solution

viscosity and concentration can be described by many empirical forms, the most common being the Huggins equation (Huggins, 1942).

$$\frac{\mu_{sp}}{C} = [\mu] + k' (\mu)^2 C \quad (4)$$

where  $k'$  is the Huggins constant and  $C$  is the polymer concentration. The specific viscosity  $\mu_{sp}$  is defined as the relative increase of viscosity.

$$\mu_{sp} = \frac{\mu - \mu_s}{\mu_s} = \mu_{rel} - 1 \quad (5)$$

with  $\mu$  and  $\mu_s$ , the apparent viscosities of the solution and the solvent, respectively, and  $\mu_{rel} = \mu/\mu_s$  the relative viscosity. The Huggins equation may be simplified by removing the second-order term for very dilute solutions. Combining the simplified Equations (4) and (5), the relative viscosity reads (Tanglertpaibul et al, 1987).

$$\mu_{rel} = 1 + [\mu]C \quad (6)$$

In this chapter,  $(\mu)$  was determined for all fluids of different ages by measuring the slope of the relative viscosity as a function of polymer concentration, within the range  $1.0 < \mu_{rel} < 2.0$ . The obtained intrinsic viscosities were then plotted as a function of aging time (Chou et al, 1987).

### ***Aging Tests***

In the context of EOR applications, it is important to consider the viscosity stability of XG solutions over time. Indeed, these fluids may remain several months in the reservoir rock and should keep their efficiency.

In order to study the evolution of the formulation viscosity over time, two aging tests were performed on the nanofluids. The first test was conducted for an aging time of 1 month. Fluids of different concentrations of NaCl (0% and 3wt%), NP-SiO<sub>2</sub> (0 ppm and 300 ppm) and a

fixed concentration of 1000 ppm XG (semi-diluted zone) were stored at a constant aging temperature (60 °C).

A second longer test was performed for an aging time of 7 months. The tested fluids contained NaCl (3 wt%), polymer at a dilute (400 ppm XG) or semi-diluted (1000 ppm XG) concentrations and nanoparticles of different concentrations (0 ppm and 300 ppm NP-SiO<sub>2</sub>). The viscous profile of the fluids was measured as a function of the shear rate at different times.

### ***Confocal Microscopy***

Confocal microscopy measurements were performed using a ZEISS LSM800 Confocal Laser Scanning Microscope. The microscope was equipped with four solid-state lasers, three GaAsP PMT detectors, and one T-PMT detector for transmission light detection. Images were obtained for nanoparticle suspensions (300 ppm), polymer solutions (1000 ppm), and nanofluids (XG: 1000 ppm; NP-SiO<sub>2</sub>: 300 ppm) in fresh conditions (initial time) and aged conditions (1 month). Confocal microscopy enables the creation of sharp images without any disturbing fluorescent light.

### ***Zeta-Potential Measurements***

Zeta potential measurements of polymer solutions in water and brine (3wt% NaCl), and nanofluid (400 ppm XG, 300 ppm NP-SiO<sub>2</sub> and 3wt% NaCl) were carried out with a Malvern nanosizer at 25 °C. The Zeta potential reflects the potential difference between the electric double layer of electrophoretically mobile particles and the layer of dispersant around them at the slipping plane. It provides an estimation of the surface charge of the particles.

### ***Thermal Analysis***

Thermal scans of polymer and nanofluids were determined by differential scanning calorimetry (DSC) and Thermogravimetric Analysis (TGA). For the DSC tests, a sample, and a reference (empty) were taken to study the thermal transitions of the polymer in a nanofluid and in a solution without nanoparticles. The DSC allows to see the glass transition temperature of the polymer ( $T_g$ ), the melting peak and the crystallization peak. The DSC device used was a Mettler Toledo STARe system, low-flow compressed air. The temperature ramp used for these analyzes ranged from  $-20$  to  $190^\circ\text{C}$ . Twelve nanofluid formulations were analyzed, with variable concentrations of polymer (400, 1000, and 3000 ppm XG), and nanoparticles (30, 100, and 300 ppm) prepared in brine (3% NaCl). Additionally, 3 polymer formulations (400, 1000, and 3000 ppm) without nanoparticles were scanned. The mass variation in polymeric solutions (1000 ppm XG) and nanofluids (1000 ppm XG + 300 ppm NP-SiO<sub>2</sub>) was measured by thermogravimetric analysis with temperature ramps between 25 and  $180^\circ\text{C}$ . The device used was a Mettler-Toledo TGA, low airflow.

## **Results and Discussion**

### ***Influence of Temperature during Nanofluids Preparation***

After choosing the preparation method from a previous chapter (Buitrago-Rincon et al, 2021), the effect of the temperature imposed during the preparation of nanofluids was evaluated at 20, 40, 60 and  $80^\circ\text{C}$ . The intermediate concentration of 600 ppm XG, separating the dilute and semi-dilute regimes, was selected and the NP-SiO<sub>2</sub> concentration was fixed to 300 ppm. All measurements were then performed at the same temperature  $60^\circ\text{C}$ .

The obtained viscosities are shown in Table II.1, for a shear rate of  $7.3 \text{ s}^{-1}$ , and compared to the viscosity of the polymer solution without nanoparticles. A viscosity increases ranging between 15.7% and 21% is obtained for tested temperatures between 20 to 60 °C. The highest viscosity is obtained for a preparation temperature of 20 °C. At higher temperatures (80 °C), however, the measured viscosity is almost that of the polymer solution, which indicates that the effect of the NP-SiO<sub>2</sub> is negligible.

**Table II.1.** *Relative viscosity increases due to preparation temperature.*

Fluid	Preparation Temperature	Viscosity Pa·s	Viscosity Increase <sup>1</sup>
Polymer solution	20 °C	0.030604	Control sample
Nanofluid	20 °C	0.037030	21.0%
Nanofluid	40 °C	0.035488	15.7%
Nanofluid	60 °C	0.035959	17.5%
Nanofluid	80 °C	0.031124	1.7%

*Note.* <sup>1</sup>Viscosity at a shear rate  $7.3 \text{ s}^{-1}$ .

This low effect of temperature could be related to the ionic strength. Indeed, the rheological behavior results from a balance of several factors. Hydrating the polymer at high preparation temperatures promotes thermal dissociation of the polymer structure. In aqueous solutions, the backbone of xanthan changes from a disordered (or partly ordered in the form of a randomly broken helix) to an ordered structure when increasing the temperature. The conformation of the polymer in the solution mainly affects the viscosity of the fluid in that a more disordered conformation will achieve a higher viscosity value. In this case, by increasing

the preparation temperature, the molecule is ordered and the interaction with the nanoparticles is promoted. However, the high ionic strength (3% NaCl) could inhibit the polymer chain extension/repulsion at high temperature due to charge screening effects and stabilize the ordered conformation, which leads to a lower fluid viscosity (Khouryieh et al, 2007).

### *Aging Tests—Stability*

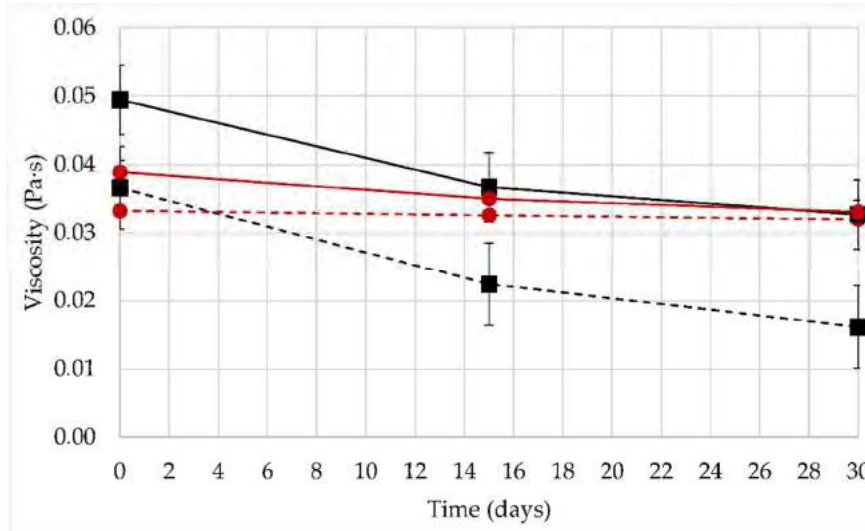
In order to evaluate the stability of the fluid viscosity in time, aging tests were carried out. Short aging tests (1 month) were applied to polymer solutions (1000 ppm XG) and nanofluids (1000 ppm XG and 300 ppm NP-SiO<sub>2</sub>), elaborated in water or brine (3wt% NaCl). The temperature used both for storage and for the viscosity measurements was 60°C (Figure II.2).

The formulations containing NP-SiO<sub>2</sub> present higher viscosities than polymer solutions without nanoparticles, at all times. Furthermore, the viscosity of all formulations is found to decrease in time, but the viscosity loss is limited in the presence of nanoparticles. In distilled water at 20 °C, the backbone of xanthan is disordered, and highly extended due to the electrostatic repulsions from the charged groups on the sidechains (Khouryieh et al, 2007). This disordered conformation of the polymer could promote a greater synergistic XG/NP-SiO<sub>2</sub> interaction.

Formulations prepared in a disordered conformation of the polymer (without NaCl) display a higher viscosity than salty solutions, due to the fact that the xanthan chains are more repelled from each other. A greater repulsion increases the hydrodynamic radius of the molecule, which then occupies a larger volume within the fluid, leading to a higher viscosity of the system. These results show the influence of nanoparticles on the conformation of XG,

and consequently, on the viscosity of polymer solution, showing a greater XG/NP-SiO<sub>2</sub> interaction.

**Figure II.2** Viscosity as a function of time – Short aging (30 days)



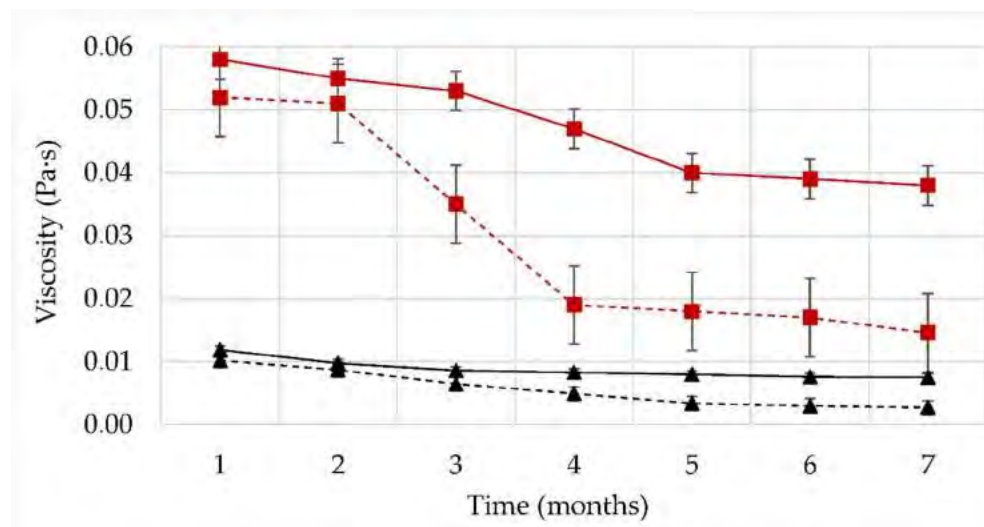
*Note.* Viscosity as a function of time. Viscosities were measured at a shear rate of  $7.3 \text{ s}^{-1}$ . Storage and measurements performed at  $T = 60 \text{ }^\circ\text{C}$ . Nanofluid in water (1000 ppm XG and 300 ppm NP-SiO<sub>2</sub>) (—■); Polymer solution in water (1000 ppm XG) (—■); Nanofluid in 3% NaCl brine (1000 ppm XG and 300 ppm NP-SiO<sub>2</sub>) (-●); Polymer solution in 3% NaCl brine (1000 ppm XG) (- -■).

The effect of the nanoparticles on the viscosity of the fluid is more remarkable in solutions with water solvent. At a shear rate of  $7.3 \text{ s}^{-1}$  for fresh fluids (time zero), the viscosity is increased by 35% with nanoparticles in water, compared to the 20% increase obtained in brine. The viscosity stability over time is also different in water and in brine. Solutions prepared in distilled water undergo a greater loss. After 30 days, a viscosity loss of 45% is

measured for polymeric solutions and only 30% for nanofluids. In brine (3wt% NaCl), the effect of nanoparticles on fluid viscosity is reduced: the viscosity hardly changed during the entire aging period. In the presence of NaCl, the polymer stabilizes to an ordered conformation. Xanthan gum chains are much more rigid and stable due to the collapse of the trisaccharide side chains onto the main backbone. This effect reduces the mobility of the molecule and hinders the degradation of the molecular chains with or without nanoparticles (Li, 2015; Stokke, 1992).

A second aging test was performed for a longer time (7 months) to further study the effect of the nanoparticles and their interaction with the polymer in solutions with high ionic strength (3wt% NaCl, Figure II.3). For these tests, two polymer concentrations were considered (dilute, 400 ppm XG and semi-dilute, 1000 ppm XG), and a single nanoparticle concentration (300 ppm NP-SiO<sub>2</sub>). The storage temperature of the fluids and the test measurement temperature were the same, 60 °C.

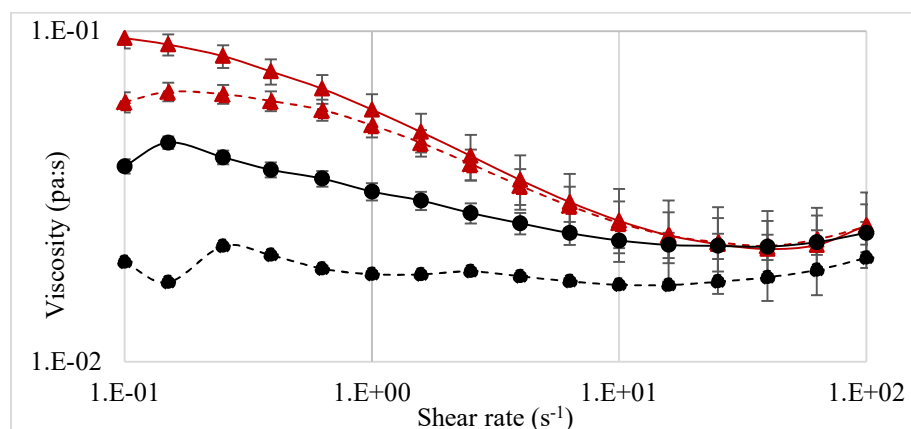
**Figure II.3** *Viscosity as a function of time – Long aging (7 months)*



*Note.* Viscosity as a function of time at a shear rate of  $7.3 \text{ s}^{-1}$ . Storage and measurement at  $T=60$  °C. Semi-dilute nanofluid (1000 ppm XG, 300 ppm NP-SiO<sub>2</sub> and 3% NaCl) (—■); Semi-dilute polymer solution (1000 ppm XG and 3% NaCl) (- -■); Dilute nanofluid (400 ppm XG, 300 ppm NP-SiO<sub>2</sub> and 3% NaCl) (—▲); Semi-dilute polymer solution (400 ppm XG and 3% NaCl) (- -▲).

After 7 months, all the polymer solutions showed a strong decrease in viscosity while the nanofluids displayed a moderate viscosity loss. The same behavior was observed for both dilute and semi-dilute polymer solutions. The semi-dilute polymer solution without nanoparticles underwent a 72% viscosity reduction, while the same formulation containing nanoparticles exhibited a viscosity drop of only 34%. For the dilute polymeric solution, a viscosity drop of 73.5% in time was found without nanoparticles, while the drop was halved (37%) in the presence of nanoparticles. These longer tests confirm that the presence of NP-SiO<sub>2</sub> promotes the stability of the fluid, maintaining the viscous profile.

**Figure II.4** *Viscosity nanofluid against polymer solution after 7 months*



*Note.* Viscosity as a function of shear rate. Storage and measurement at  $T=60$  °C.

Nanofluid fresh fluid (1000 ppm XG, 300 ppm NP-SiO<sub>2</sub> and 3% NaCl) (—▲); Nanofluid aged 7 months (1000 ppm XG, 300 ppm NP-SiO<sub>2</sub> and 3% NaCl) (- -▲); Polymer solution fresh fluid (1000 ppm XG and 3% NaCl) (—●); Polymer solution aged 7 months (1000 ppm XG and 3% NaCl) (- -●).

These rheological results could be attributed to weak physical attractive forces between the components, such as hydrogen bonds. The surface of silica nanoparticles exhibits silanol groups (Si-OH), while XG chains contain hydroxyl groups (-OH), which makes ( $-O-H^{\delta^+} \cdots O^{\delta^-}$ ) dipole–dipole interactions possible (Silverman et al, 2004). However, the nature of the interaction between xanthan gum and silica nanoparticles is still an open question. This aspect will be discussed in the following sections.

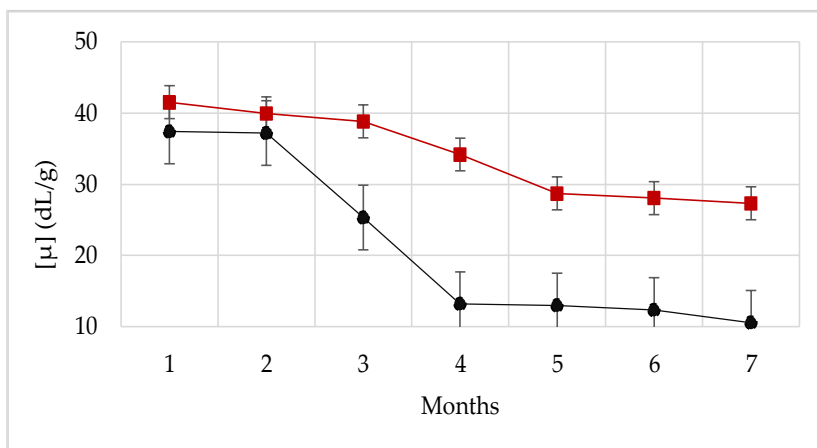
### ***Intrinsic and Relative Viscosity***

Intrinsic viscosity of xanthan gum solutions and nanofluids is shown in Figure II.5, as a function of aging time. The simplified Huggins equations (4)–(6), were applied for each month.

In dilute solutions, the polymer chains are separate, and the intrinsic viscosity of a polymer in solution depends only on the hydrodynamic dimensions of the polymer (hydrodynamic volume) (Rao et al, 2007). The intrinsic viscosity of XG solutions with and without NP-SiO<sub>2</sub> is shown in Figure II.5 as a function of aging time. The estimated intrinsic viscosity (41.52 dL/g) obtained for the nanofluid is much higher than that obtained from polymer solution (37.41 dL/g). These results suggest that the hydrodynamic radius of xanthan gum increases because of the nanoparticles, and this increase of the hydrodynamic

volume suggests an efficient interaction between the polymer and the nanoparticle. For both polymer solutions and nanofluids the intrinsic viscosity decreases over time. However, the reduction of the polymer dimensions is more remarkable in the absence of nanoparticles.

**Figure II.5** *Intrinsic viscosity ( $\mu$ ) as a function of time*

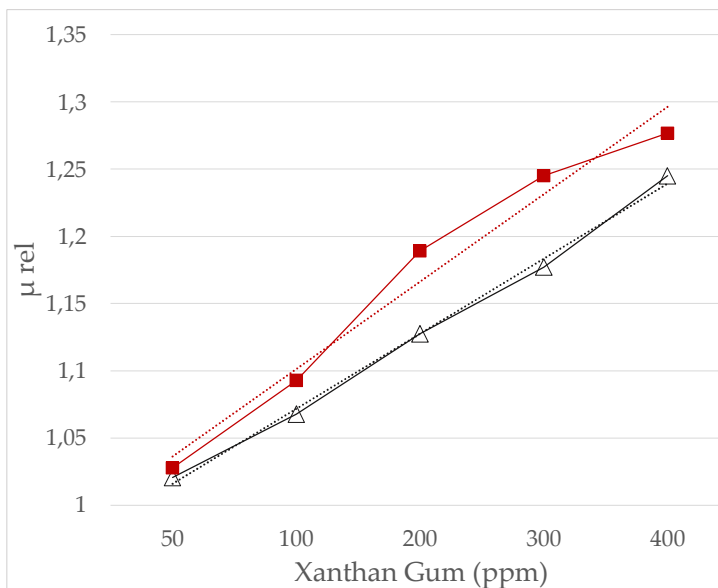


*Note.* Storage and tests performed at  $T = 60\text{ }^{\circ}\text{C}$ . Nanofluid (—■); Polymer solution (—●).

In order to evaluate the interaction between the xanthan gum and the silica nanoparticles, the relative viscosity  $\mu_{rel}$  is plotted as a function of xanthan concentration (Figure II.6). As expected, the relative viscosity  $\mu_{rel}$  of polymer solutions and nanofluid was found to increase with polymer concentration. The slope is higher for nanofluids than for polymer solutions, indicating a higher intrinsic viscosity and thus a higher polymer hydrodynamic radius in the presence of nanoparticles. Furthermore, a linear variation was found for the polymer solutions, which denotes a mass contribution of the xanthan gum without specific interactions (Khouryieh, 2007; Pi, 2016).

On the contrary, the relative viscosities of the nanofluids did not vary linearly, indicating that specific attractive forces were present between the xanthan molecules and the silica nanoparticles. The non-linear trend is due to another factor than the polymer concentration increase. Thus, the hypothesis of intermolecular binding between xanthan gum and silica nanoparticles is supported by the intrinsic viscosities and relative viscosities values obtained for the different formulations.

**Figure II.6** Relative viscosity  $\mu_{rel}$  as a XG concentration



*Note.* Relative viscosity  $\mu_{rel}$  against xanthan gum concentration.

Nanofluid (—■); Polymer solution (—Δ)

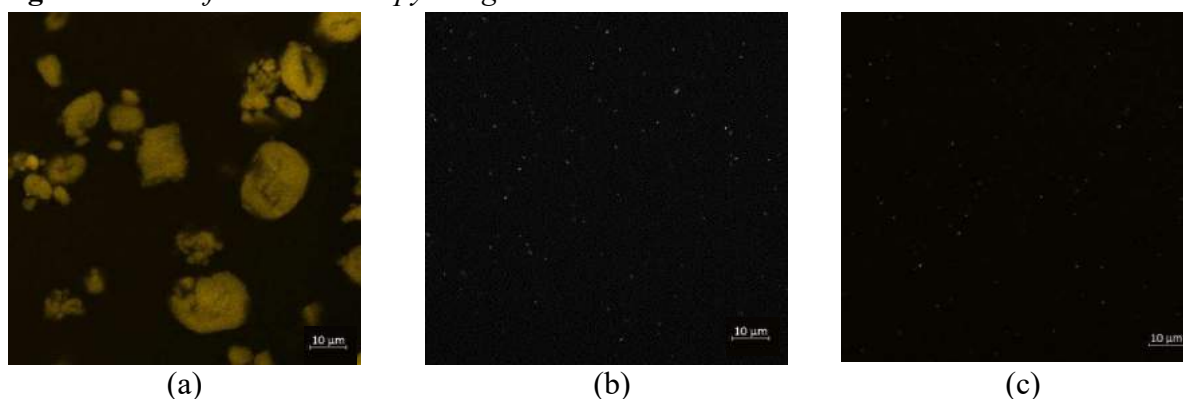
### **Confocal Microscopy**

The colloidal dispersion of the nanoparticles in the brine and the polymeric solution was observed through confocal microscopy tests, see Figure II.7. All images were unchanged for all formulations after 1 month aging. The sensitivity of the confocal microscope is around 300

nm, below this scale it is not possible to observe. The images of the nanoparticle suspensions, Figure II.7.a., showed microscopic agglomerates reaching sizes up to 20  $\mu\text{m}$ .

As expected, the polymer molecules were not visible on the images of polymer solutions, see Figure II.7.b. On nanofluid images, nanoparticle aggregates were not distinguishable, see Figure II.7.c. This means that the aggregation of the nanoparticles is affected by the polymer, decreasing the size of the NP-SiO<sub>2</sub> aggregates from 20  $\mu\text{m}$  to sizes less than 300 nm (the maximum resolution of the equipment).

**Figure II.7** *Confocal microscopy images*



*Note.* (a) Nanoparticle suspension: 300 ppm NP-SiO<sub>2</sub> and 3% NaCl in deionized water; (b) polymer solution: 1000 ppm XG and 3% NaCl in deionized water; (c) nanofluid: 1000 ppm XG, 300 ppm NP-SiO<sub>2</sub> and 3% NaCl in deionized water.

This indicates that an interaction between xanthan gum and silica nanoparticles exists, which leads to the breakup of micron-sized nanoparticles agglomerates.

***Zeta Potential***

Aqueous and saline solutions of xanthan gum, as well as nanofluids containing xanthan gum and NP-SiO<sub>2</sub> in brine, were also characterized by Zeta potential measurements (Table II.2). Xanthan gum is a polyelectrolyte that exhibits a negative surface charge in aqueous solution due to its anionic character provided by the carboxyl groups present in the trisaccharide side chain of its repeat unit (Camesano et al, 2001).

**Table II.2.** *Zeta potential*

Formulation	Solvent	Zeta potential (mV) <sup>1</sup>
Xanthan gum (400 ppm)	Water	-19.1
Xanthan gum (400 ppm)	Brine 3% NaCl	-14.8
Nanofluid: XG (400 ppm) and 300 ppm NP-SiO <sub>2</sub>	Brine 3% NaCl	-23.0

*Note.* Zeta potential of XG solution in water or brine and nanofluid (XG/NP-SiO<sub>2</sub>/NaCl).

<sup>1</sup>Temperature 25 °C.

Measurements show that the addition of nanoparticles in the polymer solution induces an increase of the absolute value of the Zeta potential. The Zeta potential of the nanofluids shows stronger interaction between the XG and NP-SiO<sub>2</sub>, indicating that improved dispersion stabilization has been achieved (Bhattacharjee et al, 2016). This higher negative value for the nanofluids contributes to explain the stability of the Xanthan/ NP-SiO<sub>2</sub> suspensions over time. Polymeric solutions of Xanthan gum in distilled water obtained  $\zeta$  of -19.1 mV, confirming the electrostatic repulsion between the polymer chains. By adding the NaCl ions to the polymer solution,  $\zeta$  increases to -14.4 mV due to the screening of the Na<sup>+</sup> and Cl<sup>-</sup> ions on the XG-charged

monomer units, resulting in a decrease in the surface charge density (Sultan et al, 2016). On the other hand, when NP-SiO<sub>2</sub> is added to xanthan gum solution in brine, the absolute surface electric charge raises to  $-23.0$  mV. This effect is probably related to the formation of hydrogen bonds between NP-SiO<sub>2</sub> and XG, which are responsible for the formation of stronger networks and structures. As a result of these physical interactions, the XG repeat units are less exposed to the undesired protective effects of salt ions.

### *Thermal Analysis*

DSC measurements in solution did not yield conclusive results. Indeed, it was not possible to determine the glass transition value ( $T_g$ ) of the polymer either in solution or in a nanofluid. The objective of these analyzes was to determine the influence of the presence of silica nanoparticles on the  $T_g$  value of xanthan in solution, due to the new interactions formed. Despite the numerous formulations and tests carried out, the results did not allow the identification of the thermal transition peaks of the polymer. Appendix 7 shows the scans obtained, where it was only possible to observe the heat exchanges related to water. It is possible to attribute these results to the low concentrations of polymer used in the research, therefore the high concentration of water in the formulation could mask the transition of the polymer in solution.

The mass variations obtained by TGA (Appendix 8), evidenced a shift in the gravimetric ramp of the polymeric formulations with and without nanoparticles. The nanofluids showed an increase of  $10^\circ\text{C}$  compared to the polymeric solutions (without nanoparticles) in the bottom temperature of the evaporation of water. However, this variation in reaction kinetics could also be found with the addition of more material in the formulation, and it was not a conclusive result.

Hence, these results did not prove interactions between the polymer and the nanoparticles, since the gravimetric variation would only indicate the presence of nanoparticles in the formulation.

## Conclusions

In the present work, the interaction between xanthan gum (XG) macromolecules and silica nanoparticles (NP-SiO<sub>2</sub>) in water or brine was investigated. Various polymer, nanoparticle and salt concentrations were considered. Different experimental techniques were used: rheometry, capillary viscosimetry, confocal microscopy and Zeta potential measurements. Aging tests were performed, during which the fluids were stored for several months at 60°C. Measurements were carried out just after fluid preparation and at successive aging times.

The individual components were first characterized in water and brine. XG molecules are satisfyingly dissolved after 24 h and the resulting solutions (without particles) exhibit a shear-thinning behavior. The addition of salt to these solutions causes a viscosity decrease while maintaining a shear-thinning behavior. Nanoparticle suspensions (without polymer) are Newtonian for the considered particle concentrations and their viscosity is not affected by the addition of salt.

The preparation temperature of the nanofluids (XG and NP-SiO<sub>2</sub> in brine) was varied, and a moderate effect was found on the resulting viscosities.

The viscosity of the XG solutions with and without NP-SiO<sub>2</sub> was characterized over time. The presence of nanoparticles led to higher viscosities. The viscosity of all fluids decreased in time, but the decrease was limited by the presence of nanoparticles, which demonstrates the

stabilization of xanthan gum solutions by the addition of nanoparticles. However, these positive effects of NP-SiO<sub>2</sub> are attenuated by the presence of salt.

The intrinsic viscosity of the polymer solutions with and without nanoparticles was calculated from the rheological measurements. The intrinsic viscosity is higher with NP-SiO<sub>2</sub> at every time. This indicates that the hydrodynamics radius of the polymer is larger when nanoparticles are present, which is a sign of polymer/particle interaction. Furthermore, the relative viscosity was found to vary nonlinearly with polymer concentration in the presence of NP-SiO<sub>2</sub>, which is another sign of polymer/particle interaction.

Confocal microscopy images show that the nanoparticles dispersed in water form large aggregates (20 μm), but that the aggregates are much smaller (under 300 nm) in the presence of xanthan gum, evidencing an action of polymer on particle dispersion. It was also shown experimentally that the presence of nanoparticles affects the Zeta potential of XG solutions.

The thermal analyzes performed (DSC and TGA) were inconclusive. Both nanofluids and polymer solutions present a majority percentage of water in their composition, compared to the low concentrations of polymer and nanoparticles. Under these conditions, the thermal variations of the water masked those of the polymer, making it impossible to find the glass transition point of the XG present in the liquid-vapor-liquid transition interval of water.

The nature of the interactions between the XG macromolecules and the silica nanoparticles remains an open question. It is suggested that they may result from weak interactions by hydrogen bonds.

### Chapter III

#### Oil Recovery Efficiency in Core Flooding Tests

##### Abstract

The objective of this chapter is to study the effect of the incorporation of silica nanoparticles (NP-SiO<sub>2</sub>) in xanthan gum (XG) solutions on the oil recovery improvement through the analysis of efficiency in core flooding tests.

This final chapter evaluates the XG polymer solutions and nanofluids under reservoir conditions through rock-fluid interaction (coreflooding) and fluid-fluid (interfacial tension) tests. The objective was to establish the performance conditions of the formulations when interacting with a prototype reservoir rock. Additionally, the previously selected formulations (XG solution and nanofluid) were compared with synthetic hydrolyzed polyacrylamide (HPAM) solutions. HPAM is currently the most popular and efficient polymer for chemical methods of EOR processes. The comparison was made using viscosity curves and displacement tests in a rock matrix under simulated reservoir conditions.

First, the viscosity profiles of two polymer solutions, XG biopolymer and synthetic hydrolyzed polyacrylamide (HPAM) polymer, were characterized individually through rheological measurements, with and without salt (NaCl). Both polymer solutions were found suitable for oil recovery at limited temperatures and salinities.

Then, nanofluids composed of XG and dispersed NP-SiO<sub>2</sub> were studied through rheological tests. The addition of nanoparticles was shown to produce a slight effect on the viscosity of the fluids, which was more remarkable over time. Interfacial tension tests were

measured in water-mineral oil systems, and no remarkable effects were observed on the interfacial properties with the addition of polymer or nanoparticles in the aqueous phase.

Finally, three core flooding experiments were conducted using sandstone core plugs and mineral oil. The polymers solutions (XG and HPAM) with 3% NaCl recovered 6.6% and 7.5% of the residual oil from the core, respectively. In contrast, the nanofluid formulation recovered about 13% of the residual oil, almost two times greater than the original XG solution. Therefore, this study provides a conclusive result: the nanofluid was more effective at boosting oil recovery in the sandstone core than the HPAM and XG solutions.

This chapter resulted in a publication in the Journal Nanomaterials: Buitrago Rincon D. et al. " Silica Nanoparticles in Xanthan Gum Solutions: Oil Recovery Efficiency in Core Flooding Tests". Nanomaterials 2023, 13(5), 925; <https://doi.org/10.3390/nano13050925>. (see appendix A.9)

## **Introduction**

The Enhanced oil recovery (EOR) processes, including polymer flooding, are employed to significantly improve the oil recovery factor (Sheng, 2011; Sveistrup, 2015). These chemical methods consist in injecting a displacing fluid in oil reservoirs to mobilize the crude oil trapped in the porous rocks. Typically, the displacing fluid contains a water-soluble polymer (polymer flooding) (Seright et al, 2009). Mobility ratio (M) determines the relative rate of one fluid to another and, the mechanism involved in polymer flooding is based on decreasing the water/oil mobility ratio: the mobility difference between displacing (polymer flooding) and displaced fluids (oil). The water/oil mobility ratio is inversely proportional to the viscosity, so that the higher the

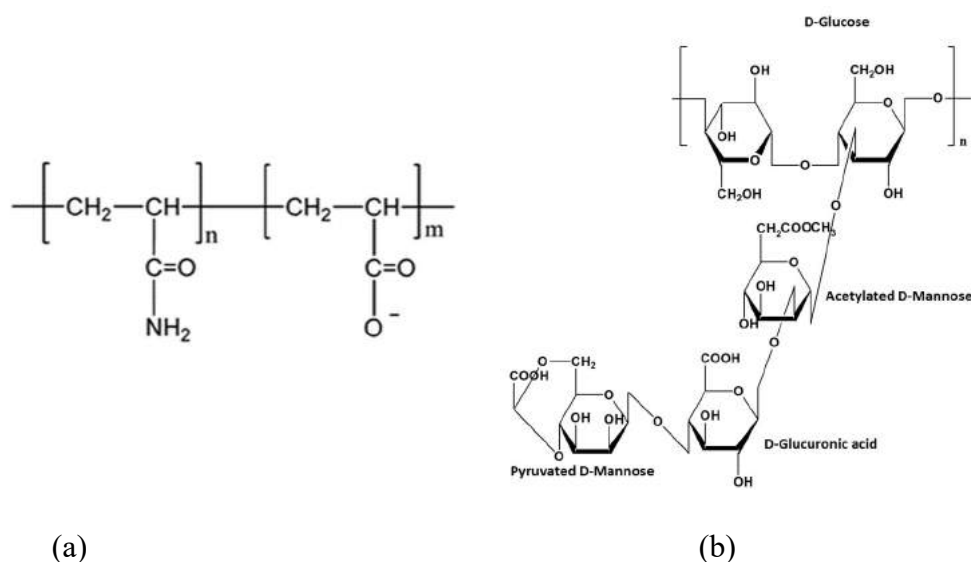
viscosity of the fluid, the lower the value of  $M$ . The displacement of the oil by fluid occurs in a piston-like flow, but with low viscosity, the waterflooding fingers through the oil causing formation damage and plugging (Ecopetrol, 2020; Ghoumrassi-Barr, 2015; Jansson, 1975).

The main criteria to choose EOR polymers are: very high molecular weight, inexpensive, thickener capacity, and complete solubility in water. Additionally, aqueous polymer solutions should be able to tolerate high salinity, high temperatures, and show resistance to viscosity degradation over time (Camesano et al, 2001). The rheological properties of a polymer solution are strongly dependent on the polymer structure, composition, conformation, and interactions between the polymer and the solvent. The most classic polymeric system employed for EOR is synthetic hydrolyzed polyacrylamide (HPAM), followed by natural xanthan gum (XG). XG polymer is a biosourced alternative to conventional flooding methods. However, XG alone has shown limitations in these processes due to its degradation over time, accelerated by temperature (Camesano, 2001; Norton, 1984; Sheng, 2011).

HPAM is a co-polymer of acrylamide and acrylic acid, see Figure III.1a. This polyelectrolyte exhibits negative charges on its chains. HPAM solutions significantly improve the microscopic oil displacement efficiency, thanks to their synthetic nature and adaptability (Carmona, 2015; Khouryieh, 2007; Pi, 2016). The molecular chains of HPAM adjust easily during flow under shear rate. Indeed, the backbone of HPAM is flexible. However, the HPAM carboxyl groups are extremely sensitive to salts, especially high valence salts. Inorganic salts can compress the double electrical layer of this polyelectrolyte, weakening the static repulsion between the HPAM lateral groups. The conformational transition becomes more constricted, and the viscosity of the polymer solution decreases sharply. The chemical modification of HPAM through the

addition of specific lateral groups decreases the sensitivity of the molecules to salt (Abidin, 2012; El-Diasty, 2015; Sheng, 2011).

**Figure III.1** *Polymers molecular structure*



*Note.* HPAM (a), Xanthan gum (b).

XG is an anionic heteropolysaccharide produced by the microorganism *Xanthomonas campestris*. XG is a relatively cheap biopolymer and is suitable for oil recovery at limited temperatures and salinities (El-Diasty et al, 2015). It is mainly composed of a linear  $\beta$ -D linked glucose backbone with a trisaccharide side chain on every other glucose at C-3. In aqueous solutions, xanthan macromolecules can exhibit a disordered conformational structure that tends to maximize the solution viscosity, see Figure III.1b (Jordan, 2014; Sheng, 2011). In its ordered conformation, it exhibits a rigid structure and a reduction in fluid viscosity. XG molecules may become rigid when an amount of electrolyte is present, which leads the side chains to collapse around the backbone. Nonetheless, the XG biopolymers have a wide range of applications in many

industries due to their thickener properties, high salinity tolerance (more than HPAM), thermal stability, affordability, safety (non-toxic), as well as its low environmental impact.

This leads to the motivation for this study. Green polymers such as XG have the potential for EOR processes. However, its main limitation has been its biodegradability in aqueous solutions under the adverse conditions of pressure, temperature, and ionic strength occurring in the field. To improve the efficiency of XG solutions, materials such as silica nanoparticles (Np-SiO<sub>2</sub>) are added, improving the rheological behavior, and maintaining its stability over time at high salinity and high-temperature conditions due to weak physical attractive forces (hydrogen bonds) between XG and Np-SiO<sub>2</sub>. The XG / Np-SiO<sub>2</sub> interactions change the conformation of the polymer, which can result in improved microscopic and macroscopic sweep efficiencies (Buitrago-Rincon, 2021, 2022; Roustaei, 2013).

In chapter I (Buitrago-Rincon et al, 2021), different methods were investigated for the preparation of nanofluids composed of hydrocolloid XG and hydrophilic silica nanoparticles (Np-SiO<sub>2</sub>) dispersed in water and brine. It was determined that the order of the addition of the components, the hydration time of the polymer XG, and the interaction time of the XG with the nanoparticles affected the resulting viscosity profile of the fluid. The method producing the highest viscosity at a shear rate of 7.3 s<sup>-1</sup> was selected. The presence of nanoparticles caused an increase of 30% of XG solution viscosity. In addition, the polymeric dilution curve of XG at high salinity concentrations, 3% NaCl, was determined. From this curve two different working zones for EOR processes were identified: the dilute zone (up to 600 ppm XG) and the semi-dilute zone (from 600 ppm to 4800 ppm XG). It was determined that the effect of the nanoparticles was more noticeable (on the rheological response) in the semi-dilute zone: higher viscosity and better stability were achieved in the presence of nanoparticles.

In chapter II (Buitrago-Rincon et al, 2022), the effect of silica nanoparticles (Np-SiO<sub>2</sub>) in XG solutions was investigated through the analysis of viscosity profiles and their stability over time. The nanofluids composed of XG and Np-SiO<sub>2</sub> dispersed in water and brine were studied through two different aging tests (1 month and 7 months), at a constant storage temperature (60 °C). The addition of nanoparticles was shown to produce a slight increase in the viscosity of the fresh fluids (initial time = 0), while a more remarkable effect was observed over time: the viscosity diminution in time is significantly limited by the Np-SiO<sub>2</sub>. The presence of Np-SiO<sub>2</sub> stabilizes the polymer solution, maintaining its viscosity over time, due to a delay in the movement of the molecule. This indicates delayed biodegradation of the molecule at high temperatures and high ionic strengths in the solution. In this previous study, the molecular interaction between the XG molecule and the Np-SiO<sub>2</sub> surface was demonstrated. The presence of Np-SiO<sub>2</sub> increases the hydrodynamic radius of the polymer, which indicates attractive forces between these two components, maintaining colloidal stability with average size aggregates lower than 300 nm.

In the current chapter, core flooding experiments are presented to further investigate the potential of nanofluids (XG + Np-SiO<sub>2</sub>) for enhanced oil recovery. First, the viscosity of XG polymeric solutions with and without nanoparticles was evaluated and compared to that of HPAM polymeric solutions (the most used polymer in EOR processes). Then, the effect of nanoparticles on interfacial tension (brine/polymer/mineral oil) was determined. Finally, the displacement efficiency of the nanofluids at reservoir conditions was evaluated and compared to the performance of XG and HPAM solutions without nanoparticles. This study aims to contribute to filling the knowledge gap in the nanofluid literature for EOR applications.

## **Materials and methods**

### ***Materials***

The xanthan gum was purchased from Sukin Industries. A commercial HPAM polymer, FLOPAAM 3230 S (hydrolysis degree: 30% at 25°C), was obtained from SNF Floerger. The silica nanoparticles were fumed Aerosil 300 amorphous hydrophilic ( $300 \pm 30 \text{ m}^2/\text{g}$ ) from Evonik Industries. Sodium chloride was supplied by Sigma-Aldrich (purity  $\geq 99.5\%$ , 58.44 daltons). Deionized water was used as a solvent. USP mineral oil was supplied by Elementos químicos LTDA ( $0.867 \text{ g/cm}^3 @ 25 \text{ }^\circ\text{C}$  and  $8.46 \text{ cP} @ 60 \text{ }^\circ\text{C}$ ).

### ***Fluids Preparation***

All formulations were prepared according to the same method. In a previous study (Buitrago-Rincon et al, 2021), the preparation method was selected and optimized for both polymeric solutions and nanofluids. Polymer solutions were prepared by incorporating polymer powder (XG or HPAM) in deionized water or 3% NaCl brine (previously prepared). A stirring time of 24 h was determined to ensure complete hydration of the polymers. For the nanofluids preparation, the polymer and the nanoparticles were introduced at the same time in brine (previously prepared). Then, the resulting fluid was mixed for 24 h (with a magnetic stirrer) to ensure complete polymer hydration and particle-polymer interaction. This method was the one yielding the best results, reaching the highest viscosity profile, with a complete interaction between the XG molecule and the silica nanoparticles (Buitrago-Rincon et al, 2021). In another previous study (Buitrago-Rincon et al, 2022), the rheological behavior and the stability of the fluids were evaluated. The best results were obtained for an XG concentration of 1000 ppm (semi-dilute regime), and a fixed concentration of 300 ppm for nanoparticles.

### ***Viscosity Behavior***

The viscosity behavior of the studied polymer solutions was determined using Anton Paar 302 rheometer with cone/plate geometry. The tests were executed at a constant temperature (60 °C) and for variable shear rates (0.1–100 ( $\text{s}^{-1}$ )), with sensitivities of 1 Pa. s for the viscosity.

### ***Interfacial Tension***

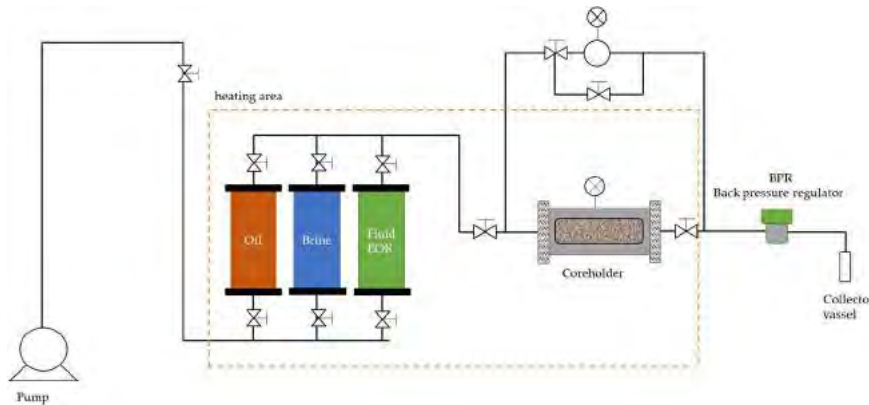
The effect of the Np-SiO<sub>2</sub> on the interfacial tension (IFT) between mineral oil and polymer solutions was evaluated. The Du Noüy ring method was used at a constant temperature (60 °C). The “weighting from below” practice was used in all the experiments since it proved to yield the most-probable reproducibility, equal to 0.002 mN/m. Three sets of measurements were conducted to determine oil-fluid interfacial tension alterations caused by nanoparticles: brine/mineral oil, XG solution/mineral oil, and nanofluid (XG + Np-SiO<sub>2</sub>)/ mineral oil. The fluids were previously heated up to 60°C and maintained at this condition during the tests.

### ***Core Flooding Experiments***

Three core flooding experiments were conducted to evaluate the displacement efficiency of the XG solutions, HPAM solutions and nanofluids (XG + Np-SiO<sub>2</sub>). They were performed on the STEAM LDE equipment (Martinez et al, 2021). Initially, petrophysical properties, such as effective porosity and absolute permeability, were determined by deionized water injection using mass balance and the Darcy equation. Subsequently, each porous medium was saturated with brine followed by a mineral oil injection process until irreducible water conditions were reached. Finally, the fluids being evaluated were injected into each porous medium and the recovery factor was

calculated using mass balances. These three stages are described as core preparation, brine flooding, and fluid flooding. Figure III.2 describes the experimental setup.

**Figure III.2** Core flooding experimental setup.



*Note.* STEAM LDE (Martinez et al, 2021).

**Core Preparation.** For the construction of the porous media, four core plugs of 3.86 cm internal diameter and 36.5 cm length were selected. The core plugs were packed with Ottawa sand using the same grain aggregation and ordering process, ensuring the reproducibility of the porous medium. The sand used was mainly composed of quartz with a density of  $2.65 \text{ g/cm}^3$ . After its construction, each core plug was assembled and confined within the core holder and mounted on the STEAM LDE equipment for the execution of the subsequent displacement tests. Once the core was installed, the outer surface was pressurized to simulate the same pressure as in the oil reservoir.

The volume and theoretical porosity of the porous medium was calculated from the mass of sand in each packing and the density of quartz. The effective porosity of the core was determined by means of the mass balance (eliminating dead volumes) of the injection of 5 porous volumes

(PV) of deionized water into the porous medium. The absolute permeability was calculated with Darcy's law, which models the flow of fluids through a porous medium.

$$Q = \frac{K_{abs} \Delta P A_T}{245 \mu L} \quad (1)$$

where  $Q$  is the flow rate ( $\text{cm}^3/\text{min}$ ),  $K_{abs}$  the permeability (mD),  $\Delta P$  the pressure loss (psi),  $A_T$  the flow cross-sectional area ( $\text{cm}^2$ ),  $\mu$  the fluid viscosity (cP),  $L$  the length of the medium (cm) and a conversion factor of 245. Equation (1) is reorganized into:

$$\frac{245 Q}{A_T} = K_{abs} \frac{\Delta P}{\mu L} \quad (2)$$

The absolute permeability of the core ( $K_{abs}$ ) was determined by measuring the slope of 245  $Q/A_T$  as a function of  $\Delta P/(\mu L)$  (Martinez, 2021; Ye, 2013).

**Reservoir Saturation Conditions.** In this study, each core is prepared under particular reservoir conditions: temperature of 60 °C, brine 3% NaCl (30,000 ppm), and mineral oil.

In the brine saturation stage, a 3% NaCl solution (prepared with deionized water) was applied to saturate each core (3 PV), and, thereafter, the cores were flooded with mineral oil until obtaining an irreducible water saturation ( $S_{wirr}$ ) of the cores and a maximum oil saturation in the core. When  $S_{wirr}$  conditions were reached, the effective permeability of the core to mineral oil was obtained with the measured pressure difference. Subsequently, the relative permeability ( $K_{ro}$ ) of the core under these conditions results from the ratio between the effective permeability of mineral oil ( $K_{eff}$ ) and the absolute permeability ( $K_{abs}$ ) (Martinez et al, 2021).

$$K_{ro} = \frac{K_{eff}}{K_{abs}} \quad (3)$$

Finally, the mineral oil saturated cores were aged at 1050 Psia pore pressure, for several hours.

***Flooding Process.*** In the final stage, the interaction of each fluid with the porous medium was estimated. Each fluid was evaluated successively in a different core under the same conditions: brine in Core 1, XG solution in Core 2, HPAM solution in Core 3, and nanofluid in Core 4. One PV of 3% NaCl brine was injected at a rate of 0.2 cm<sup>3</sup>/min, then each core was flooded with its own fluid. An injection rate of 0.2 cm<sup>3</sup>/min, 60°C temperature and 1050 psi pressure were applied. The displacement efficiency was calculated by dividing the displaced oil volume by the initial oil volume.

## Results and Discussion

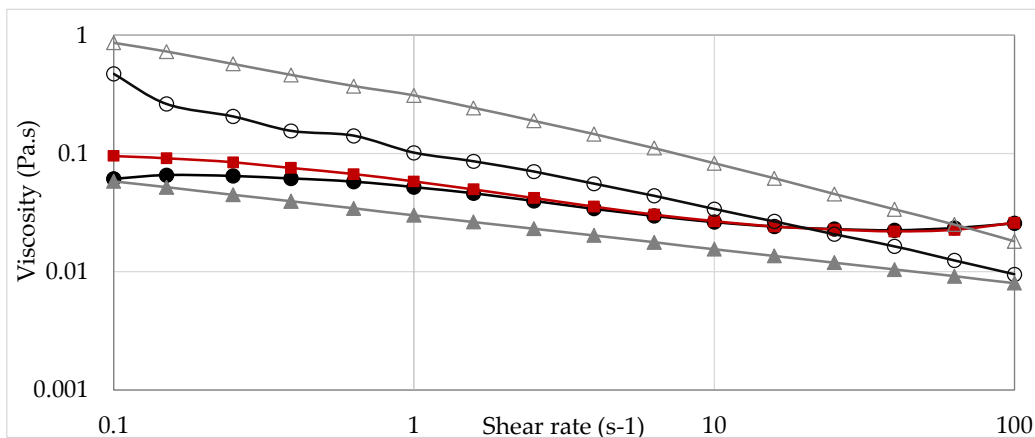
### *Viscosity Behavior*

The viscosity curves of XG solutions and HPAM solutions with and without NaCl (30000 ppm) are compared to that of nanofluid (XG + Np-SiO<sub>2</sub>) in brine.

All the viscosity curves obtained show a marked shear-thinning behavior at 1000 ppm polymer concentration, Figure III.3. The viscosities of the polymer solutions in deionized water are higher than those of solutions in brine. This is due to the fact that polymer chains are stretched in deionized water due to the repulsive forces between the negative charges (carboxylate groups) on the chain (Tanglertpaibul et al, 1987). A stronger viscosity decrease is observed in brine for HPAM formulations. At a representative shear rate of 7.3 s<sup>-1</sup>, the viscosity of XG solutions

decreases by 32.5% while the viscosity of HPAM solutions decreases by 50%. A possible explanation is the solvation and modification of the intermolecular hydrogen bonds of the polymers in saline solution. These macromolecular interactions change the polymer conformation, which can result in a viscosity reduction. For HPAM, the  $\text{Na}^+$  concentration in the aqueous solution prevents static repulsion effects on polyelectrolyte lateral groups, leading to electrostatic shielding and to a more contracted conformation. The hydrodynamic size of the polymer decreases, and the fluid viscosity is lower. On the other hand, in a saline medium, the transitional conformation of the XG changes into a more rigid structure. The electrostatic shielding effect of  $\text{Na}^+$  causes the lateral groups on the main chains to twine around the backbone and, due to this behavior, the conformation of XG converts into a rigid rod. The hydrophilic groups on the backbone are shielded and reduce the hydrodynamic size of the molecule, leading to a viscosity loss (Camesano, 2001; Carrington, 1996; Tanglertpaibul, 1987).

**Figure III.3** *Viscosity of solutions with and without NaCl as a function of shear rate.*



*Note.* HPAM solution in water (1000 ppm HPAM) ( $\Delta$ ); HPAM solution in brine (1000 ppm HPAM, 3 % NaCl) ( $\blacktriangle$ ); XG solution in water (1000 ppm XG) ( $\circ$ ); XG solution in brine (1000 ppm XG, 3 % NaCl) ( $\bullet$ ); Nanofluid (1000 ppm XG, 300 ppm Np-SiO<sub>2</sub>, 3 % NaCl) ( $\blacksquare$ ).

The same phenomenon was observed in previous works on the influence of NaCl on the preparation and performance of nanofluids. The presence of  $\text{Na}^+$  and  $\text{Cl}^-$  ions limits electrostatic repulsions between charges within the polymer XG, even in the presence of the nanoparticles, promoting a more rigid and less stretched backbone of the polymer/nanoparticle, resulting in a decrease in viscosity of the nanofluid (Buitrago-Rincon, 2022; Li, 2015; Silverman, 2004; Stokke, 1992; Rao, 2007).

### ***Interfacial Tension***

A correct knowledge of interfacial tension (IFT) and the viscosity of fluids used in EOR are necessary to efficiently manage the production process of field (Cheng et al, 2022).

The mechanism of EOR involved in polymer/nanofluids flooding is based on decreasing the mobility difference between displacing (polymer solutions) and displaced fluids (petroleum) in order to reduce lingering effects. When working with improved polymeric fluids, in this case XG, with the incorporation of silica nanoparticles, it is important to evaluate the effect of this system on the tension properties at the interface with oil prototypes. The polymer should act as an effective viscosifier for the aqueous phase, and its effect in IFT is usually less pronounced than for surfactant fluids (Avendano, 2012; Behera, 2021).

In this study, little effect was found on the interfacial properties when adding XG polymer in brine with or without silica nanoparticles. Table III.1 shows very high interfacial tension in all the fluids tested at these conditions. This lack of surface activity is usually explained by a very slow equilibration of polymeric micelles, which prevents the possibility of the macromolecules migrating to the interfaces and affecting the IFT. In conclusion, it could be difficult for both the

XG solution and the nanofluid (XG + Np-SiO<sub>2</sub>) to create stable emulsions with the oil under flow conditions (Avendano et al, 2012).

**Table III.1.** *Interfacial tension.*

Fluid	IFT with Paraffin (mN m <sup>-1</sup> ) *1	σ (mN m <sup>-1</sup> ) *2
Brine (3% NaCl)	24.2	0.91
Polymer solution	25.8	1.47
Nanofluid	24.7	1.06

*Note.* \*1. Measurements performed at T = 60 °C. Nanofluid (1000 ppm XG and 300 ppm Np-SiO<sub>2</sub>) in 3% NaCl brine. Polymer solution (1000 ppm XG) in 3% NaCl brine. Paraffin: model oil.

\*2. σ standard deviation.

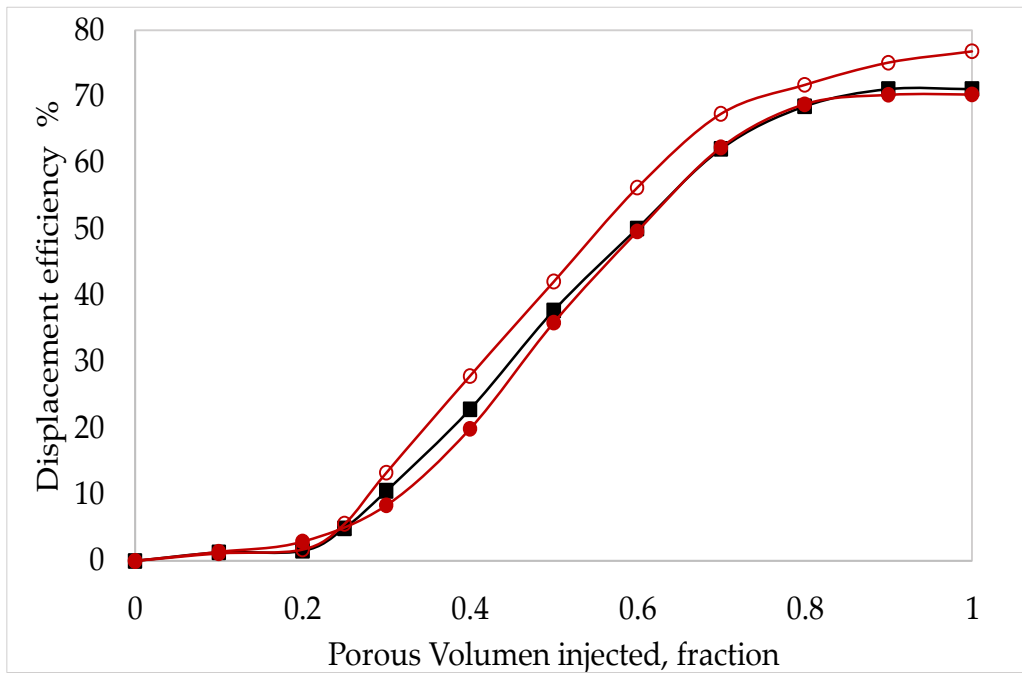
### ***Core Flooding Results***

Core flooding simulates reservoir conditions and, therefore, contributes to investigating the EOR performances of polymer systems. Table III.2 shows the obtained experimental data. The permeability was found to be similar in all the cores, between 2.3 and 2.7 D. Under waterflooding (3% NaCl brine), chosen as the reference case, 63.61% of the Initial Oil In Place (IOIP) was recovered. The displacement efficiency obtained under the flow of XG solution, HPAM solution, and nanofluid was, respectively, 70.27%, 71.11%, and 76.79% of IOIP, see Figure III.4.

These data evidence the addition of polymer molecules, such as HPAM and XG, in the initial stage allows for reaching larger oil recovery efficiencies compared to simple waterflooding. However, the oil recovery factor through nanofluid injection surpasses by far that obtained with

the polymer solutions. The incremental oil recovery (laboratory conditions) for the nanofluid was 13.18%, and only 7.5% and 6.6% for HPAM and XG solutions, respectively.

**Figure III.4** Displacement efficiency (%) as a function of porous volume injected.



*Note.* XG solution (1000 ppm XG, brine 3 % NaCl) (—●); HPAM solution (1000 ppm HPAM, brine 3 % NaCl) (—■); Nanofluid (1000 ppm XG, 300 ppm Np-SiO<sub>2</sub>, brine 3 %NaCl) (—○).

The viscosity profiles of nanofluids were higher than those of polymeric solutions (Figure III.3), therefore indicating higher displacement efficiency. In fact, the laboratory incremental percentages achieved by the nanofluid were almost twice those obtained by the two evaluated polymeric solutions (Table III.2).

**Table III.2.** *Core flood experiments.*

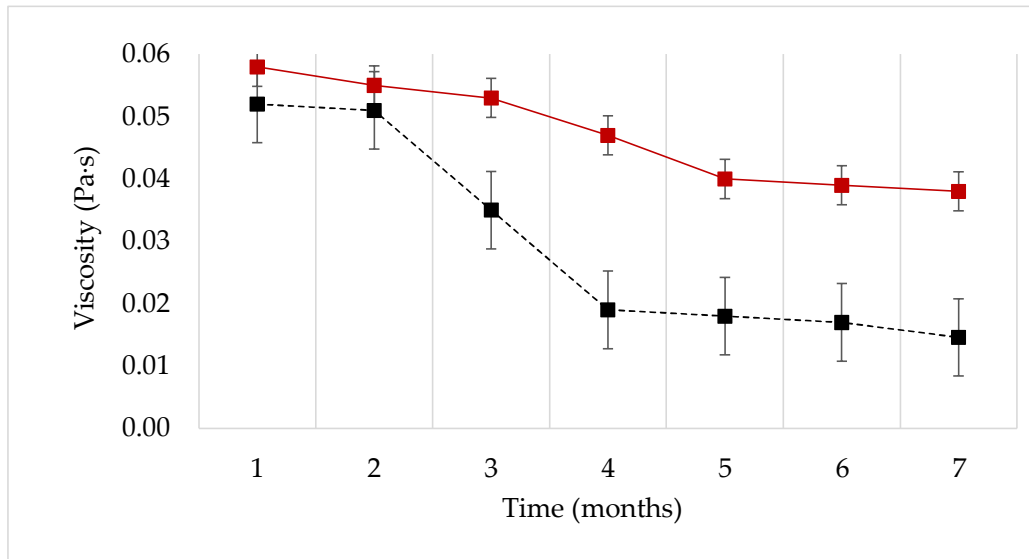
Parameter	Core 1	Core 2	Core 3	Core 4
	Brine (3 % NaCl)	XG Solution	HPAM Solution	Nanofluid
<b>Core conditions</b>				
Core length (inches)	29.7	29.18	29.18	29.49
Pore volume (cm <sup>3</sup> )	80.51	82.2	89.5	78.84
Effective porosity (%)	22.5	23.39	25.46	22.20
Pore volume (cm <sup>3</sup> )	80.51	82.2	89.5	78.84
<b>Saturations conditions</b>				
Absolute permeability (D)	3.1	2.7	2.3	2.7
Swirr (%)	17.5	26.33	25.59	25.76
Residual oil saturation (%)	26.0	22.0	15.0	21.5
<b>Flooding</b>				
Initial oil saturation (%)	82.5	73.67	74.41	74.24
Displacement efficiency (%)	63.61	70.27	71.11	76.79
Incremental laboratory EOR (%)	-	6.6	7.5	13.18

In a previous study (Buitrago-Rincon et al,2022), Figure III.5 was obtained. It was found that the effect of silica nanoparticles on XG solutions promotes fluid stability, by maintaining the viscosity profile: XG polymer solutions without nanoparticles and XG solutions with nanoparticles (nanofluids) were prepared and aged for this test. The fluids were stored for 7 months aging time at a constant temperature (60 °C), representative of the reservoir conditions.

After 7 months, all the polymer solutions showed a strong decrease in viscosity, while the nanofluids displayed a moderate viscosity loss. The XG polymer solution without nanoparticles underwent a 72% viscosity reduction, while the same formulation containing nanoparticles

exhibited a viscosity drop of only 34%. These results showed the potential of nanofluids (XG + Np-SiO<sub>2</sub>) for EOR processes (Buitrago-Rincon et al, 2022).

**Figure III.5** *Viscosity as a function of time at a shear rate of 7.3 s<sup>-1</sup>.*



*Note.* Storage and measurement at  $T = 60$  °C. Nanofluid (1000 ppm XG, 300 ppm Np-SiO<sub>2</sub> and 3% NaCl) (—■). Polymer solution (1000 ppm XG and 3% NaCl) (- - ■) (Buitrago-Rincon et al, 2022).

For the present study, aged fluids were not evaluated. All formulations (polymeric solutions and nanofluids) were fresh (aging time = 0). Under these conditions, the HPAM solution was found to perform better than the XG solution (without nanoparticles). This could be due to the fact that HPAM solutions are more elastic than XG solutions at low concentrations. Thus, in porous media at this concentration, the higher elasticity of HPAM promotes a slightly higher displacement efficiency than XG polymer (Huh, 2008; Sultan, 2016; Wang, 2000). But the nanofluids were found to perform better than HPAM and XG solutions. Indeed, both the displacement efficiency

and the laboratory incremental EOR for the nanofluid were higher than for the polymeric solutions. The incremental EOR performed by the nanofluids was 99.7% higher than that of XG solutions, and 75.7% higher than that of HPAM solution.

One possible explanation for the performance of the nanofluids is the effect of silica nanoparticles on the structure of XG. It is well known that the viscosity of polymeric solutions, both XG and HPAM, decrease with aging (time, temperature, pressure, etc.) due to transitional changes of the molecule and its subsequent polymeric degradation. In previous works (Buitrago-Rincon et al, 2022), it was shown that the presence of nanoparticles increases the viscosity of XG polymeric solutions, by increasing the hydrodynamic radius of the polymer, which is a sign of efficient polymer/nanoparticle interaction.

These rheological results could be attributed to weak physical attractive forces between the components, such as hydrogen bonds. The surface of silica nanoparticles exhibits silanol groups (Si-OH) while XG chains contain hydroxyl groups (-OH), which makes dipole–dipole interactions possible (Buitrago-Rincon, 2022; Rao, 2007).

In addition, it is reasonable to assume that a degradation of the polymers (XG and HPAM) occurs during the core flooding test due to the high pressures and high temperatures in the porous medium (such as an accelerated aging). In this case, as shown in Figure III.5, the nanoparticles limit the movement of the polymeric molecule, thus delaying its degradation. This implies maintaining the viscous properties of nanofluid for a longer time, and the resulting flow profile, could shut off high-permeability zones. Consequently, the viscous fingering effects are dampened, leading to a better volumetric sweep efficiency, so that oil is more effectively produced.

## Conclusions

EOR methods based on polymer flooding are well established, but new challenges always emerge, which give impulse to the search for new solutions. Polymeric nanofluids of xanthan gum and silica nanoparticles represent a very attractive alternative to these techniques because they can, simultaneously provide an increase in water viscosity and maintain this viscosity at aging conditions, both of which are beneficial to the efficiency of the process.

After evaluating the potential of nanofluids (XG + Np-SiO<sub>2</sub>) and comparing them with the most popular polymer flooding in the EOR industry (HPAM and XG), the present chapter leads to the following concluding remarks:

There are no variations in the brine-mineral oil interfacial tension due to the presence of XG polymer or silica nanoparticles. Therefore, stable emulsions between nanofluids and oil may not be promoted.

HPAM solutions tend to exhibit higher elasticity than XG solutions, especially at low concentrations. In porous media with this low concentration, the increased elasticity of HPAM contributed to a slightly higher displacement efficiency compared to the XG polymer.

The most significant finding of the study was that the nanofluids outperformed both the HPAM and XG solutions by a significant margin. Both displacement efficiency and incremental Enhanced Oil Recovery (EOR) for the nanofluid were notably higher than those for the polymeric solutions. Nanofluids displayed a substantial improvement in incremental EOR when compared to XG and HPAM solutions. Specifically, the nanofluids achieved an EOR that was 99.7% higher than that of XG solutions and 75.7% higher than that of HPAM solutions. This remarkable performance advantage suggests that nanofluids have the potential to greatly enhance oil recovery in porous reservoirs.

Thus, it was possible to modify the mobility ratio at lab conditions. The mobility ratio and viscosity of the flooding solution exhibit an inverse relationship. In other words, as the viscosity of the flooding solution increased, the mobility ratio in the porous medium decreased (under the same reservoir conditions), leading to enhanced displacement efficiency.

## Conclusions

The present study discusses the effect of silica nanoparticles on the viscosity of xanthan gum solutions for Enhanced Oil Recovery (EOR).

Chemical methods, including the use of water-soluble polymers, have been found to increase the recovery factor. Synthetic polymers of the partially hydrolyzed polyacrylamide (HPAM) type are the most popular, but they have disadvantages such as high costs associated with their synthesis or structural modifications, and high sensitivity to temperature, pressure, shearing, and ionic forces. Xanthan gum-type biopolymers are a promising alternative, but they require further development. Silica nanoparticles can be incorporated into fluid formulation to preserve the physicochemical properties of the fluid in longer working times. Various factors affect the evaluation and selection of polymers for EOR, including a range of viscosity that allows an efficient sweep of the crude, maintaining rheological profile during injection time, and against the transport conditions within the reservoir.

This study conducted a comprehensive characterization of both xanthan gum and silica nanoparticles and then explored various aspects related to their properties and behavior in the context of nanofluid development.

The used characterizations techniques like infrared spectroscopy, XPS, XRD, and SEM/EDX analysis provided valuable insights into the properties of xanthan gum and silica nanoparticles. Xanthan gum was found to contain functional groups such as carbonyl and OH groups, while silica nanoparticles exhibited an amorphous nature with a spherical geometry and an average diameter of 8 nm. The surface composition of both materials was determined, which is crucial for understanding their behavior in the application.

The effect of mixing time on xanthan gum (XG) solutions of different concentrations was then investigated. It was found that 24 hours of hydration with magnetic stirring at room temperature was sufficient to reach complete hydration of the polymer up to a maximum concentration of 4800 ppm. This finding is essential to optimize the preparation of XG solutions and generate the dilution curve of XG polymer.

The rheological behavior of XG solutions was studied for different polymer concentration. The results showed that XG solutions exhibited shear-thinning behavior for concentrations above 600 ppm but were Newtonian at lower concentrations (150 ppm and 300 ppm). Viscosity increased for increasing polymer concentration. The study also examined the effect of sonication on viscosity, revealing a significant viscosity reduction after ultrasound exposure, due to physicochemical effects. This is why sonication was not used during the treatment and preparation of polymeric fluids or nanofluids

The presence of NaCl in XG solutions was found to affect the conformation of the polymer chains. Increasing NaCl concentration led to a viscosity decrease, attributed to the stiffening of the XG backbone and collapse of side chains. However, at low NaCl concentrations, higher viscosities were observed due to a slightly messier and more extended XG chain conformation. This finding has implications for the behavior of XG solutions in reservoirs, which may exhibit different NaCl concentrations.

This investigation explored the rheological behavior of NP-SiO<sub>2</sub> suspensions, which depends on the degree of nanoparticle dispersion. Interestingly, no significant viscosity difference was observed between suspensions of 100 ppm and 300 ppm NP-SiO<sub>2</sub>. The influence of salt on the viscosity of these suspensions was also studied, with no significant difference observed in water or brine. Sonication was found to efficiently reduce agglomerate size and to improve

nanoparticle distribution, leading to an increased viscosity. However, the sonication steps were discarded when choosing the methodology for the preparation of the nanofluids, in order not to degrade the polymer molecules.

Four different methods to prepare nanofluids composed of NP-SiO<sub>2</sub> and XG were compared. Method 1, involving the simultaneous addition of NP-SiO<sub>2</sub> and XG without sonication, yielded the highest viscosity profile with the fewest steps. This method was thus chosen to prepare nanofluids with fixed XG and NP-SiO<sub>2</sub> in 3% NaCl.

Once the method for nanofluids preparation was selected, the influence of the preparation temperature on the viscosity curves was evaluated. The nanofluids were prepared at different temperatures of 20, 40, 60, and 80 °C. The obtained viscosities at a shear rate of 7.3 s<sup>-1</sup> were compared to the viscosity of the polymer solution without nanoparticles. The results showed that increasing the temperature led to a viscosity increase, ranging from 15.7% to 21% (20-60 °C). The highest viscosity was observed for preparation temperature of 20 °C. Furthermore, at higher temperatures (80 °C), the measured viscosity approached to that of the polymer solution without nanoparticles, indicating that the effect of NP-SiO<sub>2</sub> on viscosity is negligible.

The effect of temperature on viscosity could be attributed to the ionic strength of the solution. The rheological behavior of the nanofluids is influenced by multiple factors. At higher preparation temperatures, the thermal dissociation of the polymer structure occurs, leading to a more ordered conformation of xanthan gum. A disordered polymer conformation results in a higher fluid viscosity. Therefore, increasing the temperature, which promotes an ordered conformation and enhances the interaction between the polymer and nanoparticles, results in a lower viscosity. Furthermore, the high ionic strength of the solution (3% NaCl) may inhibit the extension and repulsion of polymer chains at high temperatures due to charge screening effects.

This stabilization of the ordered conformation by the ionic strength leads to an even lower fluid viscosity.

Overall, the effect of temperature during nanofluid preparation has a significant effect on viscosity, with lower temperatures leading to higher viscosities due to enhanced interactions between the polymer and nanoparticles. However, at higher temperatures, the effect becomes negligible due to the stabilizing influence of ionic strength.

In order to evaluate the stability of the fluid viscosity in time, aging tests were carried out. Nanofluids containing NP-SiO<sub>2</sub> consistently exhibited higher viscosities than polymer solutions without nanoparticles. While all formulations showed some viscosity decrease over time, the presence of nanoparticles limited this loss. The effect of the nanoparticles on the viscosity of the fluid is more remarkable in solutions with water solvent. At a shear rate of  $7.3 \text{ s}^{-1}$  for fresh fluids (time zero), the viscosity is increased by 35% with nanoparticles in water, compared to the 20% increase obtained in brine.

The viscosity stability over time is also different in water and in brine. After 30 days, a viscosity loss of 45% is measured for polymeric solutions, since only 30% for nanofluids in water. In brine (3wt% NaCl), the effect of nanoparticles on fluid viscosity is reduced: the viscosity hardly changed during the entire aging period. In the presence of NaCl, the polymer stabilizes to an ordered conformation. Xanthan gum chains are much more rigid and stable due to the collapse of the trisaccharide side chains onto the main backbone. This effect reduces the mobility of the molecule and hinders the degradation of the molecular chains with or without nanoparticles.

However, a second aging test was performed for a longer time (7 months) to further study the effect of the nanoparticles and their interaction with the polymer in solutions with high ionic strength (3wt% NaCl). For these tests, two polymer concentrations were considered (dilute and

semi-dilute) and a single nanoparticle concentration (storage temperature fixed to 60 °C). After 7 months, all the polymer solutions showed a strong decrease in viscosity while the nanofluids displayed a moderate viscosity loss. The same behavior was observed for both dilute and semi-dilute polymer solutions. The semi-dilute polymer solution without nanoparticles underwent a 72% viscosity reduction, while the same formulation containing nanoparticles exhibited a viscosity drop of only 34%. For the dilute polymeric solution, a viscosity drop of 73.5% in time was found without nanoparticles, while the drop was halved (37%) in the presence of nanoparticles. These longer tests confirm that the presence of NP-SiO<sub>2</sub> promotes the stability of the fluid, maintaining the viscous profile.

These rheological results could be attributed to weak physical attractive forces, such as hydrogen bonds, likely contributed to rheological results. Silanol groups (Si-OH) on silica nanoparticles' surfaces and hydroxyl groups (-OH) on XG chains allowed for dipole–dipole interactions ( $-O-H\delta^+\cdots O\delta^-$ ), promoting XG-NP-SiO<sub>2</sub> interactions. These interactions were more pronounced in water-based solutions than in brine.

To probe the influence of the nanoparticles on the fluid and their interaction with the polymer, the intrinsic viscosity of the fluids was measured. The behavior of relative viscosities in nanofluids exhibited a nonlinear trend, indicating specific attractive forces between XG and silica nanoparticles. The estimated intrinsic viscosity (41.52 dL/g) obtained for the nanofluid was much higher than that obtained from the polymer solution (37.41 dL/g). This increase suggests an efficient interaction between the xanthan gum polymer and nanoparticles, leading to an expanded hydrodynamic radius of the polymer. Over time, the presence of nanoparticles stabilizes the hydrodynamic dimensions of the polymer, which explains maintaining viscosity.

The interaction between xanthan gum and silica nanoparticles was further examined based on relative viscosity. The study found that the relative viscosity increases with the polymer concentration, and this increase is more significant in nanofluids than in polymer solutions. The steeper slope observed in the nanofluids indicates a higher intrinsic viscosity and thus a greater hydrodynamic radius of the polymer in the presence of nanoparticles. Furthermore, the behavior of relative viscosities in nanofluids exhibited a nonlinear trend, suggesting the presence of specific attractive forces between xanthan gum molecules and silica nanoparticles. This nonlinear behavior indicates interactions beyond the simple increase in the polymer concentration.

Taken together, these results support the hypothesis of intermolecular binding between xanthan gum and silica nanoparticles, as inferred from the intrinsic and relative viscosity values obtained across different formulations. These findings contribute to a deeper understanding of the complex interplay between polymers and nanoparticles in solution, which has implications for various fields, ranging from materials science to nanotechnology.

The interaction between the polymer and nanoparticles in solution is evident in confocal microscopy. Confocal microscopy analysis showed that XG disrupts the agglomeration of NP-SiO<sub>2</sub> nanoparticles, transforming micron-sized aggregates into aggregates smaller than 300 nm. This interaction stabilizes the dispersion of nanoparticles in fresh fluids and over time. Also, Zeta potential measurements confirmed the interaction between XG and NP-SiO<sub>2</sub>, leading to enhanced dispersion stabilization.

Zeta potential measurements further confirmed the existence of an intricate interaction between xanthan gum and NP-SiO<sub>2</sub> nanoparticles. The introduction of nanoparticles into the polymer solution led to an increase in the zeta potential, suggesting an enhanced dispersion stabilization. Notably, the strong negative zeta potential observed in the nanofluids explains the

stability of the Xanthan/NP-SiO<sub>2</sub> suspensions, providing valuable insights for their practical applications.

This study explored the complex interplay between xanthan gum (XG) and silica nanoparticles (NP-SiO<sub>2</sub>) in nanofluid preparation and stability. It investigated how temperature, aging, and ionic strength influence the viscosity and interaction between these components.

Finally, XG polymer solutions and nanofluids were evaluated under reservoir conditions, through coreflooding tests, in order to understand the rock-fluid interaction and interfacial tension. These formulations (XG solution and nanofluid) were compared with synthetic hydrolyzed polyacrylamide (HPAM), a widely used polymer in enhanced oil recovery (EOR) processes. This comparison was conducted using viscosity curves and displacement tests in a simulated reservoir environment.

Polymer solutions, specifically Xanthan Gum (XG) and Hydrolyzed Polyacrylamide (HPAM), exhibited shear-thinning behavior at a polymer concentration of 1000 ppm. Viscosity reduction was observed in both polymer solutions when dissolved in brine, with a more significant reduction observed in the HPAM solutions. At a representative shear rate (7.3 s<sup>-1</sup>), the viscosity of HPAM solutions in brine decreased by 50%, whereas XG solutions showed a viscosity reduction of 32.5%. The presence of Na<sup>+</sup> ions in brine alters the polymer conformation, causing the contraction of HPAM and the rigidity of XG, leading to a reduction in viscosity.

Interfacial tension (IFT) and fluid viscosity are crucial factors in Enhanced Oil Recovery (EOR) processes. Incorporating the XG polymer into brine, with or without silica nanoparticles, has a minimal impact on the interfacial properties and interfacial tension. The slow equilibration of polymeric agglomerates prevents polymer molecules from affecting the IFT, resulting in high

interfacial tensions across all tested fluids. This lack of surface activity makes it challenging for XG solutions and nanofluids to form stable emulsions with oil under flow conditions.

This study verified a direct link between fluid viscosity and mobility ratio in porous media: higher viscosity leads to higher mobility and an improved displacement efficiency. Also, core flooding experiments replicated the reservoir conditions for the EOR investigation. The permeability values were consistent across all cores, ensuring uniform experimental conditions, and water flooding with 3% NaCl brine served as a baseline, recovering 63.61% of the Initial Oil In Place (IOIP).

Polymer solutions (Xanthan Gum and Hydrolyzed Polyacrylamide) improved oil recovery: XG solution achieved 70.27% displacement efficiency, while HPAM solution achieved 71.11 %. In this case, HPAM solution outperformed Xanthan Gum (XG) because of its higher elasticity. Nonetheless, Nanofluids exhibit higher viscosity profiles than polymer solutions, achieving an oil recovery factor of 76.79 % for IOIP. In conclusion, incremental oil recovery under laboratory conditions was significantly higher (nearly double) for nanofluids (13.18%) than for HPAM (7.5%) and XG (6.6 %) solutions. Nanoparticles also appear to mitigate polymer degradation during core flooding, due to their interaction with polymer structure, preserving fluid properties, and enhancing sweep efficiency.

In conclusion, this research highlights nanofluids as a promising solution for optimizing EOR strategies, unveiling the intricate dynamics of fluid behavior and interactions that drive effective oil recovery.

The research on xanthan gum (XG) and silica nanoparticles (NP-SiO<sub>2</sub>) in the context of nanofluid development has opened up several promising perspectives and avenues for future exploration. The significant improvement in oil recovery observed with nanofluids in laboratory

conditions suggests their potential for real-world EOR applications. Future research could focus on scaling up these findings to field-scale applications, potentially revolutionizing EOR strategies and increasing hydrocarbon production.

Also, further optimization of nanofluid formulations, including the choice of nanoparticles, polymer concentration, and other additives, can be explored to fine-tune their performance in EOR. Understanding the influence of different types of nanoparticles on nanofluid behavior and oil recovery efficiency is an area ripe for investigation.

Consequently, research could investigate deeper into strategies to enhance the long-term stability of nanofluids. Stabilization methods such as surface modifications of nanoparticles or the introduction of stabilizing agents could be explored. In fact, investigating the impact of various environmental conditions, such as temperature and salinity, on nanofluid stability is essential for practical applications. As example, studies on the nature and strength of these interactions, potentially through computational modeling and simulation, can provide valuable insights for nanofluid design.

Extending the research to encompass a wider range of reservoir conditions, including different rock types, temperatures, and salinities, will provide a more accurate assessment of nanofluid performance in diverse oil reservoirs. Also, coreflooding experiments under varying conditions can help bridge the gap between laboratory findings and field applications.

Moreover, the environmental impact and economic feasibility of using nanofluids in EOR processes should be thoroughly assessed. This includes evaluating the environmental footprint of nanoparticle production and disposal. Cost-benefit analyses should be conducted to determine the viability of nanofluid-enhanced EOR on a larger scale.

Collaborative efforts between researchers from diverse fields, including materials science, fluid dynamics, petroleum engineering, and environmental science, can lead to a holistic understanding of nanofluids' potential and limitations. These collaborations can also foster innovation and interdisciplinary solutions to challenges in nanofluid development and EOR.

In summary, the research on nanofluids composed of xanthan gum and silica nanoparticles has laid a solid foundation for their application in Enhanced Oil Recovery and potentially other fields. The perspectives mentioned above represent exciting promises for future research and development, with the potential to revolutionize the energy industry and address challenges related to oil reservoir depletion and environmental sustainability.

### References

Abidin, A.Z., Puspasari, T., Nugroho, W.A. (2012). *Polymers for Enhanced Oil Recovery Technology*. Procedia Chemistry, v 4, p11-16.

Aït-Kadi, A., Marchal, P., Choplin, L., Chrissemant, A.S., Bousmina, M. (2002). *Quantitative analysis of mixer-type rheometers using the Couette analogy*. Chemical. Eng. 80, 1166–1174.

Avendano, J., Pannacci, N., Herzhaft, B., Gateau, P., Coussot, P. (2012). *Normal Stresses and Interface Displacement: Influence of Viscoelasticity on Enhanced Oil Recovery Efficiency*. Oil Gas Sci. Technol. Rev. IFP Energ. Nouv. 67, 921–930.

Behera, U. S., Sangwai, J. S. (2021). *Nanofluids of silica nanoparticles in low salinity water with surfactant and polymer (SMART LowSal) for enhanced oil recovery*. Journal Molecular Liq., 342, 117388

Bhattacharjee, S. (2016). *DLS and Zeta potential—What they are and what they are not?*. Control Release 235, 337–351.

Bracho-García, D. (2013). *Estudio del efecto del tamaño y funcionalidad superficial de nanopartículas de SiO<sub>2</sub> sobre las propiedades de nanocompositos de polipropileno*. [Master thesis]. Universidad de Chile, Chemical Eng. Department.

Buitrago-Rincon, D., Sadtler, V., Mercado Ojeda, R., Roques-Carnes, T., Marchal, P., Pedraza Avella, J., Lemaitre, C. (2021). *Effect of Silica Nanoparticles in Xanthan Gum Solutions: Rheological Behavior and Preparation Methods of Nanofluids*. Chem. Eng. Trans. 86, 1171–1176.

Buitrago-Rincon, D., Sadtler, V., Mercado Ojeda, R., Roques-Carnes, T., Marchal, P., Pedraza Avella, J., Lemaitre, C. (2022). *Effect of Silica Nanoparticles in Xanthan Gum Solutions: Evolution of Viscosity over Time*. Nanomaterials, 12, 1906.

Camesano, T.A., Wilkinson, K.J. (2001). *Single Molecule Study of Xanthan Conformation Using Atomic Force Microscopy*. *Biomacromolecules*, v 2, p 1184–1191.

Carmona, J.A., (2015). *Reología de Dispersiones Acuólicas de Goma Xantana de Prestaciones Avanzadas*. [Ph.D. Thesis]. Universidad de Sevilla, Department of Chemical.

Carrington, S.P., Odell, J.A., Fisher, L.R., Mitchell, J.; Hartley, L. (1996). *Polyelectrolyte behavior of dilute xanthan solutions—salt effects on extensional rheology*. *Polymer*, 37, 2871–2875.

Cheng, J., Xu, J., Yang, J., Wenjie L., Cheng L., Honglai L. (2022). *Enhanced oil recovery by sacrificing polyelectrolyte to reduce surfactant adsorption: A classical density functional theory study*. *Chem. Eng. Sci.*, 261, 117957.

Chou, T.D., Kokini, J.L. (1987). *Rheological Properties and Conformation of Tomato Paste Pectins, Citrus and Apple Pectins*. *Journal Food Sci.* , 52, 1658–1664.

Ecopetrol, S.A., Agencia Nacional de Hidrocarburos ANH Colombia. (2021). *Proyectos de Inversión en Investigación, Desarrollo e Innovación (I+D+I) Que Adelanta el Instituto Colombiano del Petróleo*. Agencia Nacional de Hidrocarburos, Bogotá, Colombia.

El-Diasty, A.I., Aly, A.M. (2015). *Understanding the mechanism of nanoparticles applications in enhanced oil recovery*. SPE , Technical Conference and Exhibition, Cairo, Egypt, 14–16 September 2015.

Ghoumrassi-Barr, S., Aliouche, D. (2015). *A Rheological Study of Xanthan Polymer for Enhanced Oil Recovery*. *Journal Macromol*, 55, 793–809.

Huggins, M.L. (1942). *The viscosity of dilute solutions of long-chain molecules. IV. Dependence on concentration*. *Journal Am. Chem. Soc.*, 64, 2716–2718.

Huh, C., Pope, G.A. (2008). *Residual Oil Saturation from Polymer Floods: Laboratory Measurements and Theoretical Interpretation*; OnePetro: Richardson, TX, USA.

Ibrahim, A., Aly, M. (2015). *Understanding the Mechanism of Nanoparticles Applications in Enhanced Oil Recovery*. Society of Petroleum Engineers SPE, 175806.

Irima, D., Eliamayri, C. (2014). *Determinación de formulaciones base/polímeros (bp), con potencial aplicación como método químico en la recuperación mejorada de crudo extrapesado de la faja petrolífera del orinoco*. [Master Thesis]. Universidad Central de Venezuela.

Jansson, P.E., Kenne, L., Lindberg, B. (1975). *Structure of extracellular polysaccharide from Xanthomonas campestris*. Journal Carbohydr., 45, 275–282.

Jimenez A.M. (2009). *Análisis e interpretación de yacimientos sometidos a inyección de químicos (surfactantes, polímeros y miscelares) mediante analogías*. [Master Thesis]. Universidad Industrial de Santander, Colombia.

Jordan, R., Kennedy, M., Katherine, E., Jennifer, K., Brown, R. (2014). *Rheology of dispersions of xanthan gum, locust bean gum and mixed biopolymer gel with silicon dioxide nanoparticles*. Materials Science and Engineering, 48, 347–353.

Khouryieh, H., Herald, T., Aramouni, F., Alavi, S. (2007). *Intrinsic viscosity and viscoelastic properties of xanthan/guar mixtures in dilute solutions: Effect of salt concentration on the polymer inter-actions*. Food Res. Int., 40, 883–893.

Li, R., Feke D.L. (2015). *Rheological and kinetic study of the ultrasonic degradation of xanthan gum in aqueous solutions*. Food Chem. 172, 808–813.

Martinez, H.J. (2021). *Construcción de prototipo multifuncional para reproducir procesos de recobro mejorado enfocado en inyección de vapor con flue gas a alta presión y temperatura*. [Master Thesis]. Universidad Industrial de Santander, Colombia.

Michael Khouryieh, H. A. (2006). *Rheological characterization of xanthan-guar mixtures in dilute solutions*. [Ph.D. Thesis, Kansas State University]. Food Science Graduate Program College of Agriculture.

Milas M., Rinaudo M., Tinland B., (1986). *Comparative depolymerization of xanthan gum by ultrasonic and enzymic treatments*. Rheological and structural properties, Carbohydr. Polymers . 6 95–107.

Min-Ho O., Jae-Hyun S., Seung Y. (1999). *Rheological Evidence for the Silica Mediated Gelation of Xanthan Gum*. Journal of Colloid and Interface Science., 216, 320–328.

Moorhouse R., Walkinshaw M.D, Arnott S. (1977). *Xanthan Gum—Molecular Conformation and Interactions*. Department of Biological Sciences, Purdue University, IN 47907

Norton, I.T., Goodall, D.M., Frangou, S.A., Morris, E.R., Rees, D.A. (1984). *Mechanism and dynamics of conformational ordering in xanthan polysaccharide*. Journal Molecule Biol, 175, 371–394.

Oh M-H., So J-H., Yang S. (1999). *Rheological Evidence for the Silica Mediated Gelation of Xanthan Gum*. Journal of Colloid and Interface Science, 216, 320–328.

Pi, G., Li, Y., Bao, M., Mao, L., Gong, H., Wang, Z. (2016). *Novel and Environmentally Friendly Oil Spill Dispersant Based on the Synergy of Biopolymer Xanthan Gum and Silica Nanoparticles*. ACS Sustainable Chemistry & Engineering, 4, 3095–3102.

Rao, M.A. (2007). *Introduction: Food Rheology and Structure*. In *Rheology of Fluid and Semisolid Foods*. Food Engineering Series.

Reyes, M.A. (2013). *Estudio del sistema PMMA-nanopartículas inorgánicas. Efecto del ZrO<sub>2</sub>, ZnO, CeO<sub>2</sub> sobre las propiedades del sistema*. [Ph. D thesis]. Instituto politécnico nacional, Altamira, México.

Richardson, R.K., Kasapis, S. (1998). *Rheological methods in the characterisation of food biopolymers*. Food Science, 39, pp. 1–48.

Rocheffort, W.E., Middleman, S. (1987). *Rheology of xanthan gum: Salt, temperature, and strain effects in oscillatory and steady shear experiments*. Journal Rheol., 31, 337–369.

Roustaei, A., Saffarzadeh, S., Mohammadi, M. (2013). *An evaluation of modified silica nanoparticles' efficiency in enhancing oil recovery of light and intermediate oil reservoirs*. Journal. Pet., 22, 427–433.

Saleh H.M., Annuar M.S.M., Simarani K. (2017). *Ultrasound degradation of xanthan polymer in aqueous solution: Its scission mechanism and the effect of NaCl incorporation*. Ultrasonics Sonochemistry, 39, 250-261

Sandvik, E.I., Maerker, J.M. (1977). *Application of Xanthan Gum for Enhanced Oil Recovery, Exxon Production Research. In Extracellular Microbial Polysaccharides*. American Chemical Society, 19, 242–264.

Seright, R.S. (2009). *Injectivity characteristics of EOR polymers*. PE Res Eval & Eng, 783–792.

Shahzad, M., Abdullah, K, Sultan, S, Al-Mubaiyedh A., Hussein, I. A. (2015). *Review on Polymer Flooding: Rheology, Adsorption, Stability, and Field Applications of Various Polymer Systems*. Polymer Reviews, 55:3, 491-530

Sheng, J.J. (2011). *Modern Chemical Enhanced Oil Recovery: Theory and Practice*. Elsevier Alpharetta, GA, USA.

Silverman, R.B. *The Organic Chemistry of Drug Design and Drug Action*, 2nd ed.; Receptors; Academic Press: Cambridge, MA, USA, 2004; Chapter 3, pp. 121–172.

SNF, Floerger. (n.d.). *Geología del petróleo sistemas petrolíferos EOR (101)*.  
<http://www.snf-group.com/es/>

Stokke B.T., Elgsaeter A., Bjørnstad E.Ø., Lund T. (1992). *Rheology of xanthan and scleroglucan in synthetic seawater*. Carbohydrate Polymers, 17, 3, 209-220.

Sultan, A., Kedir, J.G., Seland, A., Skauge, A., Skauge, T. (2016). *Reentrant transition of aluminum-crosslinked partially hydrolyzed polyacrylamide in a high salinity solvent by rheology and NMR*. Journal Appl. Polymers., 133, 231–237.

Sveistrup, M., Van Mastrigt, F., Norrman, J., Picchioni, F., Paso, K. (2015). *Viability of Biopolymers for Enhanced Oil Recovery*. J. Dispers. Sci. Technol., 37, 1160–1169.

Tanglertpaibul, T., Rao, M.A. (1987). *Intrinsic viscosity of tomato serum as affected by methods of determination and methods of processing concentrates*. Journal Food Sci., 52, 1642–1688.

Wang, D., Cheng, J., Yang, Q., Gong, W., Li, Q. (2000). *Viscous-Elastic Polymer Can Increase Microscale Displacement Efficiency in Cores*; OnePetro: Richardson, USA.

Wei, B. (2016). *Viscoelastic and Viscoplastic Materials*. Advances in Polymer Flooding, 1743.

Whitcomb, P. J., Ek, b. J., Macosko, W. (1977). *Rheology of Xanthan Gum Solutions*. General Mills Chemicals, Engineering and Material Science.

Ye, Z., Feng, M., Gou, S., Liu, M., Huang, Z., Liu, T. (2013). *Hydrophobically associating acrylamide-based copolymer for chemically enhanced oil recovery*. Journal Appl. Polymers. 130, 2901–2911.

Yousefvanda, H., Jafaria, A. (2015). *Enhanced Oil Recovery Using Polymer/nanosilica*. Materials Science 11, 565 – 570.

## Appendix

## Appendix A.1. Xanthan gum technical data sheet



FICHA TÉCNICA

GOMA  
XANTHAN

## IDENTIFICACIÓN DE LA EMPRESA

SUQUIN SAS

[www.suquin.com.co](http://www.suquin.com.co)

Bucaramanga/Santander

Calle 31 N° 20-43

Teléfonos: 6335068, 6978212

## DESCRIPCIÓN DEL PRODUCTO

La goma xanthan es un polisacárido de alto peso molecular producido por fermentación con *Xanthomonas campestris* en las condiciones de medio, pH, O<sub>2</sub> - purificado, secado y molido.

## ÁREAS DE APLICACIÓN

La goma xanthan puede ser ampliamente utilizada en más de veinte campos industriales, tales como alimentos, farmacéutica, química fina, agricultura, extracción de petróleo. Actúa como texturizador.

## ESPECIFICACIONES TÉCNICAS

PROPIEDAD	VALOR
Nombre químico	Goma xanthan
Apariencia	Polvo blanco
Color	Un poco amarillo
Tamaño de partícula (80 mallas)	100 %
Viscosidad	1000 cps min.
Propiedad de tensión superficial	6.0 min.
Perdida en seco	13 % máx.
Ceniza	13 % máx.
Nitrógeno	1.5 % máx.

**GOMA XANTAN**

<b>Sinónimos:</b>	Goma de xantano. E-415.
<b>INCI:</b>	Xanthan gum.
<b>Fórmula molecular:</b>	$(C_{35}H_{49}O_{29})_n$
<b>Peso molecular:</b>	> 1.000.000
<b>Descripción:</b>	Goma producida normalmente por fermentación y purificación de un carbohidrato en cultivo puro de <i>Xanthomonas campestris</i> y posterior purificación, que es la sal sódica, potásica, o cálcica de un polisacárido de alto peso molecular que contiene D-glucosa, D-manosa, ácido D-glucurónico, y ácido pirúvico.
<b>Datos Físico-Químicos:</b>	Polvo fluido, blanco o blanco-amarillento. Soluble en agua formando una disolución muy viscosa, prácticamente insoluble en disolventes orgánicos. Punto de fusión: carboniza a 270 °C.
<b>Propiedades y usos:</b>	<p>Es de naturaleza aniónica, con un pH de estabilidad de entre 4 y 11. Forma geles no transparentes, de color blanquecino y traslúcidos, de consistencia media, mayor o menor según la concentración de goma utilizada. La gelificación es instantánea y el aspecto del gel mejora al cabo de 24 horas. Los geles que forma son muy refrescantes y no adhesivos, soportan bastante bien los electrolitos, y admiten la incorporación de alcohol hasta un 30 %.</p> <p>La goma xantán se emplea en la industria farmacéutica como agente suspensor, estabilizante, espesante y emulsionante, así como para preparar la matriz de comprimidos de liberación sostenida, y para retrasar la absorción de los principios activos en colirios.</p> <p>También se utiliza en la industria alimentaria.</p>
<b>Dosificación:</b>	Al 0,1 – 1 %.
<b>Incompatibilidades:</b>	Tensioactivos, polímeros, conservantes, iones metálicos polivalentes (p. ej. el calcio), boratos, agentes oxidantes, algunos recubrimientos de comprimidos, carboximetilcelulosa sódica, gel desecado de hidróxido de aluminio, amitriptilina, tamoxifeno, y verapamilo.
<b>Conservación:</b>	En envases bien cerrados. PROTEGER DE LA LUZ Y DE LA HUMEDAD.

## Appendix A.2. Silica Nanoparticles technical data sheet

Silica-based rheology control additive  
**AEROSIL® 300**

**DESCRIPTION**

AEROSIL® 300 is a hydrophilic fumed silica with a specific surface area of 300 m<sup>2</sup>/g. It provides a very strong rheological effect.

**KEY BENEFITS**

- higher efficiency
- high transparency after good dispersion

**EFFECT**

**Anti-settling**

**Anti-sagging**

**Corrosion resistance**

**TYPICAL APPLICATIONS**

- Wood coatings
- Plastic coatings

**TECHNICAL DATA**

loss on drying	<1.5 %
pH-value	3.7 - 4.5
SiO <sub>2</sub> content	>99.8 %
specific surface area (BET)	270 - 330 m <sup>2</sup> /g
tamped density	Approx. 50 g/l

**RECOMMENDED ADDITION LEVEL**

As supplied calculated on total formulation: 1.0 - 2.0 %

**PROCESSING INSTRUCTIONS**

Addition to the coating as supplied or as a predilution is possible.

**HANDLING & STORAGE**

When stored in an original unopened packaging, the product has a shelf life of 24 months from the date of manufacture. We recommend to store the product in closed containers under dry conditions and to protect the material from volatile substances.

**SUITABILITY**

waterborne	solventborne
●	●
radiation-curing	1-pack coatings
●	●
2-pack coatings	
○	

○ not suitable ● partly suitable ● suitable

This information and all further technical advice are based on our present knowledge and experience. However, it implies no liability or other legal responsibility on our part, including with regard to existing third party intellectual property rights, especially patent rights. In particular, no warranty, whether express or implied, or guarantee of product properties in the legal sense is intended or implied. We reserve the right to make any changes according to technological progress or further developments. The customer is not released from the obligation to conduct careful inspection and testing of incoming goods. Performance of the product described herein should be verified by testing, which should be carried out only by qualified experts with the responsibility of a customer. Reference to trade names used by other companies is neither a recommendation, nor does it imply that similar products could not be used.

Evonik Operations GmbH | Goldschmidtstraße 300, 45127 Essen, Germany | Telefon +49 201 173-2222 Telefax +49 201 173-1929 | [www.coatings.additives.com](http://www.coatings.additives.com)

**Appendix A.3. Sodium chloride technical sheet.**

Sigma-Aldrich . Specification Sheet

<b>Product Name</b>	Sodium chloride puriss. p.a., $\geq 99.5\%$
<b>Product Number</b>	71380
<b>CAS Number</b>	7647-14-5
<b>Molecular Weight</b>	58.44
<b>APPEARANCE (COLOR)</b>	Colorless or White
<b>APPEARANCE (FORM)</b>	Powder or Crystals
<b>ARGENTOMETR. TITRATION</b>	99.5 - 101.0 %
<b>SOLUBILITY (COLOR)</b>	Colorless
<b>SOLUBILITY (TURBIDITY)</b>	Clear
<b>SOLUBILITY (METHOD)</b>	0.5G IN 10ML WATER
<b>PH</b>	5.0 - 8.0

**Appendix A.4. Mineral Oil.**

<b>Reference</b>	AMIN-5GAL
<b>Product description</b>	ACEITE MINERAL USP
<b>Product Brand</b>	CHEMI
<b>Supplier</b>	Elementos quimicos LTDA
<b>Density (g/cm<sup>3</sup>) @ 25 °C</b>	0.867
<b>Viscosity (Cps) @ 60 °C</b>	8.46

## Appendix A.5. Effect of Silica Nanoparticles in Xanthan Gum Solutions: Rheological Behavior and Preparation Methods of Nanofluids

Journal: Chemical Engineering Transactions



CHEMICAL ENGINEERING TRANSACTIONS

VOL. 86, 2021

Guest Editors: Sauro Pierucci, Jiří Jaromír Klemesš  
Copyright © 2021, AIDIC Servizi S.r.l.  
ISBN 978-88-95608-84-6; ISSN 2283-9216

1171



A publication of  
The Italian Association  
of Chemical Engineering  
Online at [www.cetjournal.it](http://www.cetjournal.it)

DOI: 10.3303/CET2186196

### Effect of Silica Nanoparticles in Xanthan Gum Solutions: Rheological Behavior and Preparation Methods of Nanofluids

Dayan L. Buitrago Rincon<sup>a,b\*</sup>, Véronique Sadtler<sup>a</sup>, Ronald A. Mercado O.<sup>b</sup>, Thibault Roques-Carmes<sup>a</sup>, Philippe Marchal<sup>a</sup>, Julio A. Pedraza A.<sup>b</sup>, Cécile Lemaitre<sup>a</sup>

<sup>a</sup>Laboratoire Réactions et Génie des Procédés (LRGP), Université de Lorraine, 1 Rue Grandville Nancy – France.

<sup>b</sup>Chemical engineering school, Universidad Industrial de Santander, Cll 9-27 Bucaramanga - Colombia  
[dayan.buitrago-rincon@univ-lorraine.fr](mailto:dayan.buitrago-rincon@univ-lorraine.fr)

## Appendix A.6. Effect of Silica Nanoparticles in Xanthan Gum Solutions: Evolution of Viscosity over Time

Journal: Nanomaterials

### Effect of Silica Nanoparticles in Xanthan Gum Solutions: Evolution of Viscosity over Time

by  Dayan L. Buitrago-Rincon <sup>1,2</sup> ,  Véronique Sadtler <sup>2</sup> ,  Ronald A. Mercado <sup>1</sup> ,  
 Thibault Roques-Carmes <sup>2</sup> ,  Lazhar Benyahia <sup>3</sup> ,  Alain Durand <sup>4</sup> ,  Khalid Ferji <sup>4</sup> ,  
 Philippe Marchal <sup>2</sup> ,  Julio A. Pedraza-Avella <sup>1,\*</sup>  and  Cécile Lemaitre <sup>2,\*</sup> 

<sup>1</sup> Grupo de Investigación en Fenómenos Interfaciales, Reología y Simulación de Transporte (FIRST), Universidad Industrial de Santander, Bucaramanga 680002, Colombia

<sup>2</sup> Laboratoire Réactions et Génie des Procédés, Université de Lorraine, CNRS, F-54000 Nancy, France

<sup>3</sup> Institut des Molécules et Matériaux du Mans, Le Mans Université, CNRS, F-72085 Le Mans, France

<sup>4</sup> Laboratoire de Chimie-Physique Macromoléculaire, Université de Lorraine, CNRS, F-54000 Nancy, France

\* Authors to whom correspondence should be addressed.

*Nanomaterials* **2022**, *12*(11), 1906; <https://doi.org/10.3390/nano12111906>

**Received: 24 March 2022 / Revised: 3 May 2022 / Accepted: 17 May 2022 / Published: 2 June 2022**

(This article belongs to the Special Issue Nanotechnology for Interfacial Rheology, Dispersed Systems and Colloid Chemistry)

**Appendix A.7. Differential Scanning Calorimetry (DSC) measurements**

Figure A.7.1. DSC curve of the XG solid. Temperature: 0 and 450°C at 15°C/min.

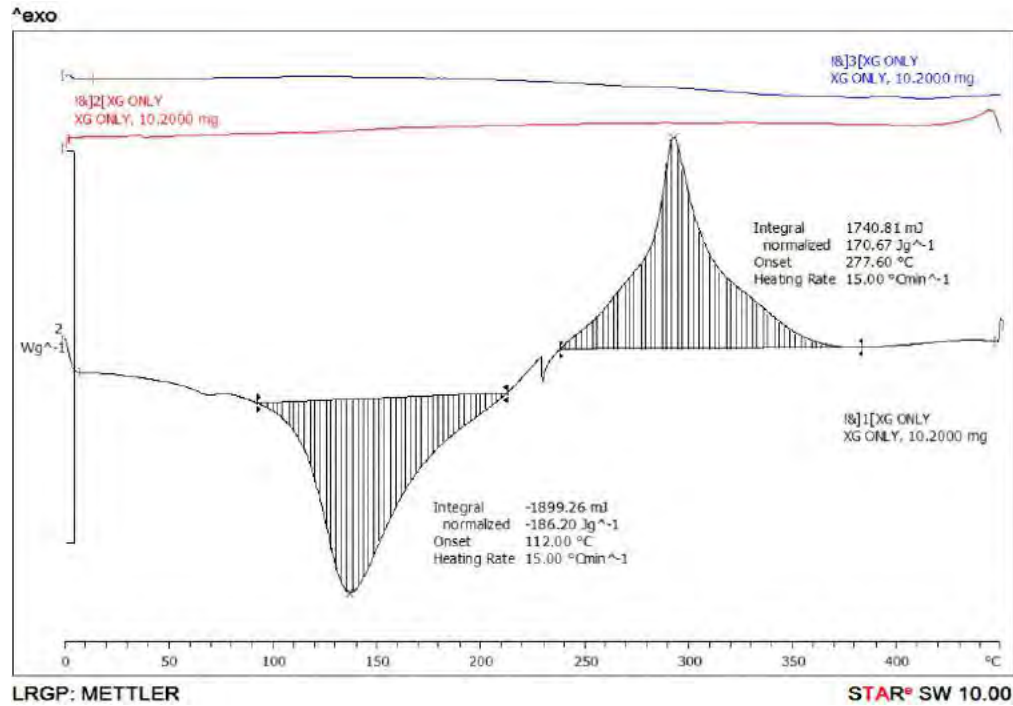
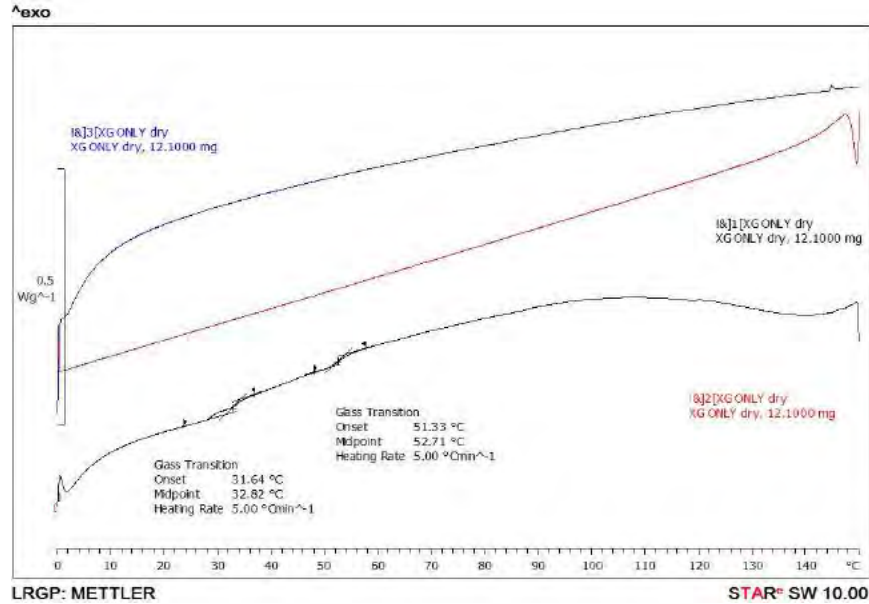


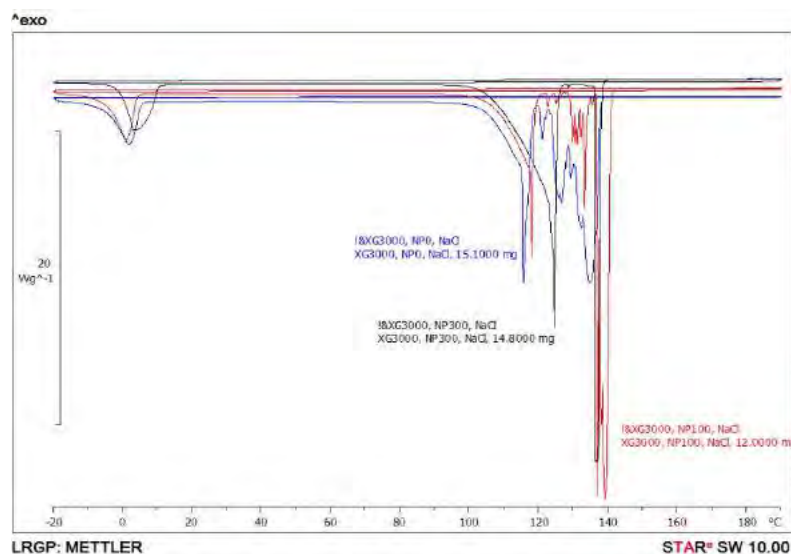
Figure A.7.2. DSC curve of dehydrated XG solid. Temperature: 0 and 150°C at 5°C/min.



In the initial DSC analysis spanning from 0 to 450°C, several important observations were made. First, there was an endothermic peak at approximately 110°C, which was attributed to the dehydration of the XG polymer, signifying the evaporation of water within the material. Additionally, there was an exothermic peak around 270°C, indicating the pyrolysis of the sample. In fact, the sample emerged from the analysis completely burned.

Subsequently, an analysis was conducted from 0 to 150°C with the intention of dehydrating the sample without causing combustion, enabling the determination of the glass transition temperature (T<sub>g</sub>) during a subsequent analysis. During this analysis, a minor signal alteration was noticed just before the endothermic peak, initially suggesting that this "signal variation" might correspond to the T<sub>g</sub>. To confirm this, the analysis was repeated, removing any uncertainty regarding this signal. However, it was conclusively determined that this signal was not the T<sub>g</sub> but rather an undesired artifact, likely originating from the device.

Figure A.7.3. DSC Nanofluid curves. XG=3000 ppm for NP=0 ppm, 100 ppm and 300ppm



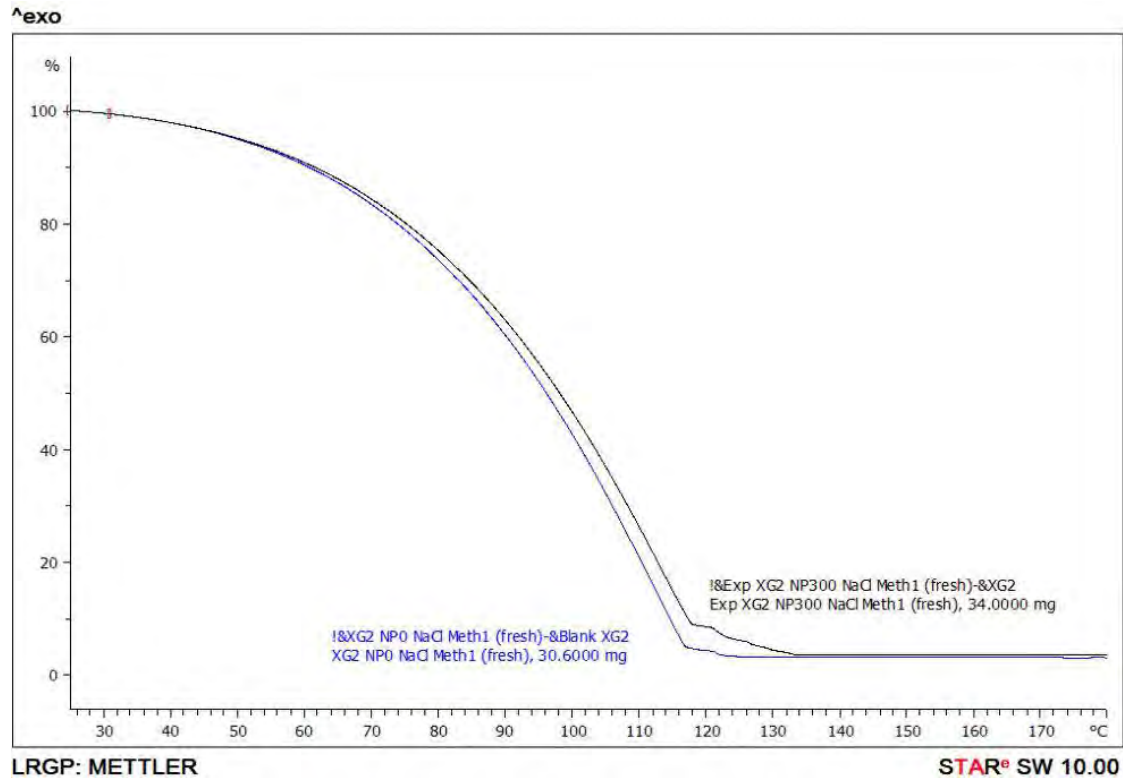
During the course of the analyses, it became evident that the melting peak originally thought to be a single entity actually displayed a split into two distinct peaks, resulting in the recording of two temperatures. The key question arose as to whether these observations truly represented two separate peaks or if they were, in fact, a single peak that appeared elongated, although this possibility seemed unlikely given the variations in heat flux values.

Upon closer examination, it was discerned that the DSC analysis performed was, in reality, an analysis of the water component rather than the XG polymer. This discrepancy arose because the water-to-XG ratio was excessively high, causing the XG to become almost submerged within the solution. As a result, the observable peaks were attributed to the evaporation of water, as evidenced by the endothermic nature of the peaks.

In total, more than 30 tests were performed, covering various conditions involving both solid polymer and polymer in solution, with and without nanoparticles. However, despite these great efforts, the results were inconclusive and did not yield a definitive result or solution. It was not possible to determine glass or transition temperatures in the samples.

### Appendix A.8. Thermogravimetric analysis

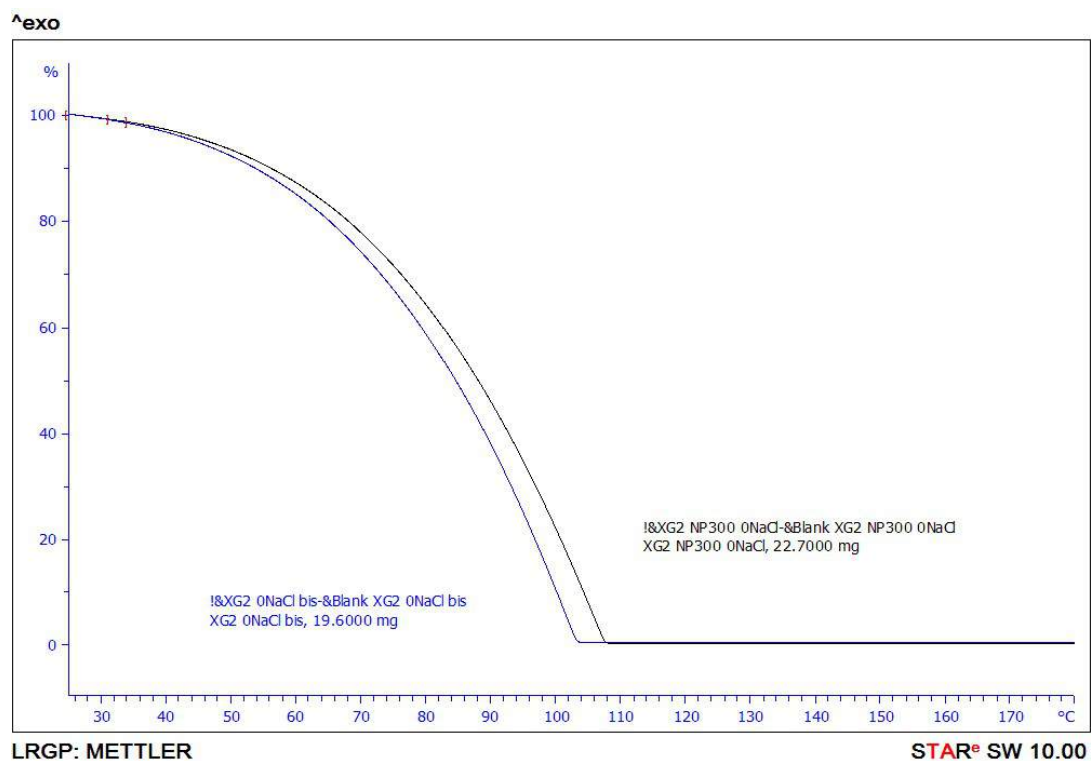
Figure A.8.1. TGA comparison fluids in brine: Nanofluid Vs. XG solution.



Note. Blue curve (400ppm XG, 3%NaCl, 300ppm of NP); Black curve (400ppm XG, 3%NaCl)

TGA measurements showed an impact of nanoparticles on the temperature at which water evaporates from the sample. Specifically, in solutions both with and without salt, but containing 300ppm of silica nanoparticles, there is a noticeable shift in the temperature at which the sample mass begins to decrease. This shift is approximately ten degrees higher than that observed in solutions without nanoparticles.

Figure A.8.2. TGA comparison fluids in water: Nanofluid Vs. XG solution.



*Note.* Blue curve (400ppm XG, 3%NaCl, 300ppm of NP); Black curve (400ppm XG, 3%NaCl)

The introduction of nanoparticles into the solution appears to slow down the reaction kinetics involved, primarily by delaying the evaporation of water. However, it's important to emphasize that these results do not conclusively demonstrate interactions between the polymer and the nanoparticles. They could suggest an influence of nanoparticles on the evaporation process, but this effect could be obtained with several additives.

## Appendix A.9. Silica Nanoparticles in Xanthan Gum Solutions: Oil Recovery Efficiency in Core Flooding Tests

Journal: Nanomaterials

### Silica Nanoparticles in Xanthan Gum Solutions: Oil Recovery Efficiency in Core Flooding Tests

by  Dayan L. Buitrago-Rincon <sup>1,2</sup>,  Véronique Sadtler <sup>2</sup>,  Ronald A. Mercado <sup>1</sup>,  
 Thibault Roques-Carmes <sup>2</sup>,  Philippe Marchal <sup>2</sup>,  Samuel F. Muñoz-Navarro <sup>3</sup>,  María Sandoval <sup>3</sup>   
 Julio A. Pedraza-Avella <sup>1,\*</sup>  and  Cécile Lemaitre <sup>2,\*</sup> 

<sup>1</sup> Grupo de Investigación en Fenómenos Interfaciales, Reología y Simulación de Transporte (FIRST), Universidad Industrial de Santander, Bucaramanga 680002, Colombia

<sup>2</sup> Laboratoire Réactions et Génie des Procédés, Université de Lorraine, CNRS, F-54000 Nancy, France

<sup>3</sup> Grupo de Investigación en Recobro Mejorado (GRM), Universidad Industrial de Santander, Bucaramanga 680002, Colombia

\* Authors to whom correspondence should be addressed.

*Nanomaterials* **2023**, *13*(5), 925; <https://doi.org/10.3390/nano13050925>

Received: 1 November 2022 / Revised: 2 February 2023 / Accepted: 3 February 2023 /

Published: 2 March 2023

(This article belongs to the Special Issue Nanotechnology and Nanomaterials for Interfacial Rheology, Dispersed Systems and Colloid Chemistry)